United States
Naval Postgraduate School

THESIS

THE EFFECTS OF OCEAN SURFACE ROUGHNESS ON THE TRANSMISSION OF SOUND FROM AN AIRBORNE SOURCE

by

Raymond Allan Helbig

December 1970

The Effects of Ocean Surface Roughness on the Transmission of Sound from an Airborne Source

by

Raymond Allan Helbig
Lieutenant Commander, United States Navy
B.S., Lehigh University, 1962

Submitted in partial fulfillment of the
requirements for the degree of

MASTER OF SCIENCE IN ENGINEERING ACOUSTICS

from the

NAVAL POSTGRADUATE SCHOOL
December 1970

ABSTRACT

Using the research platform "FLIP", experiments were conducted to determine the effect of measured ocean surface roughness on transmission of sound from an airborne source into the sea. Signal noise both at the air-water interface and at points in the underwater sound field were recorded using modified AN/SSQ-57 sonobuoys. Ocean wave spectra and rms wave height, σ , were determined from simultaneous recordings of ocean surface wave height variations. The results of analog data analysis compared well with theory developed by Hagy and Medwin: for $R < 1$, perpendicular incidence transmission loss increased approximately as $10 \log_{10} e^{R}$ where $R = k_2^2 \sigma^2 (c_2/c_1 \cos \theta_1 - \cos \theta_2)^2$. (Subscript 2 refers to propagation constant, speed, and angle of transmission in water; subscript 1 in air). For $1 < R < 4$ the transmission loss decreased with increasing roughness, presumably due to off-axis incoherent contributions.

TABLE OF CONTENTS

LIST OF FIGURES

TABLE OF SYMBOLS AND ABBREVIATIONS

c_1, c_2	Sound propagation speed in air and water respectively.
D	Depth of a point in the underwater sound field.
H	Helicopter altitude.
k_1, k_2	Sound propagation constants in air and water respectively.
$\vec{k}_1$	Vector propagation constant of the incident sound field in air.
$\vec{k}_2$	Vector propagation constant of the transmitted sound field in water.
$\vec{K}$	$\vec{k}_1 - \vec{k}_2$
K_x, K_y, K_z	The x, y, and z components of $\vec{K}$.
K_{xy}	$K_x^2 + K_y^2$
p_1	Rms incident pressure amplitude at the air-water interface.
p_2	Rms transmitted pressure amplitude at the air-water interface.
p_{1Z}	Rms incident pressure amplitude at a point on the air-water interface directly below the sound source.
p_{2t}	Rms transmitted pressure amplitude at a point in the underwater sound field.
p_{20}	Rms transmitted pressure amplitude at a point in the underwater sound field when the air-water interface is perfectly smooth.
R	Acoustical roughness parameter. $[R = k_2^2\sigma^2 (c_2/c_1 \cos\theta_1 - \cos\theta_2)^2]$
TL	Transmission loss. Defined as $20 \log (p_{1Z}/p_{2t})$
TL_s	Transmission loss for a perfectly smooth air-water interface. Consists of loss due to spreading from a point source as well as loss due to the impedance mismatch at the interface.

TL_R	Transmission loss due to roughness of air-sea interface only
ρ_1, ρ_2	Densities of air and water respectively.
θ_1	Angle of incidence in air. Measured with respect to a perpendicular from the source to the mean surface.
θ_2	Angle of transmission in water. Measured with respect to a perpendicular from the source to the mean surface.
σ	Rms surface wave height.
Σ	Rms surface wave slope.

ACKNOWLEDGEMENT

The continuing guidance of Dr. H. Medwin of the Naval Postgraduate School is particularly acknowledged. The author considers his association with Dr. Medwin throughout this project, to have been a most stimulating professional experience.

Lieutenant J. H. Hagy, Jr., USN participated in both ocean experiments and was actively involved in their planning. His engineering expertise is considered to have been invaluable in the experimental phase of the project.

Mr. William Smith's technical assistance in all areas of the project is greatly appreciated. The success of the ocean experiments in particular may be attributed largely to his efforts.

Thanks are also due to Mrs. Rosemary Lande whose skill in computer programming was instrumental in developing the multi-channel data analysis technique described herein and to Mrs. Patricia Auyong who is continuing this work.

A debt of gratitude is due to many people at Scripp's Institution of Oceanography. Included are: Dr. Fred Spiess, Director of the Marine Physical Laboratory, and Dr. Victor Anderson, Assistant Director, for their cooperation in making the services of "FLIP" available for this project, Mr. Earl Bronson, MPL Marine Coordinator, for his help in coordinating the details of "FLIP's" availability, Captain Richard A. Silva and the crew of "FLIP" for their complete cooperation and assistance during the ocean experiments, Dr. Russ Davis for his leading role in the collection of ocean surface data, Mr. Rick Ackerman and Mr. Joe Percy for their

assistance in obtaining equipment for the experiments, and to Mr. Lloyd Regier for his analysis of the ocean surface data.

The cooperation of Patrol Squadrons 46 and 50 at N.A.S. Moffet Field and Helicopter Antisubmarine Warfare Squadron 4 at N.A.S. Imperial Beach in providing aircraft for use as sound sources in the project is appreciated.

The support of ASW Systems Project Office, Code ASW 21 and Naval Ordnance Systems Command is acknowledged.

I. INTRODUCTION

This thesis describes the second phase of a study in progress at the Naval Postgraduate School (NPS) into the effects of a randomly rough air/water interface on transmission from a sound source in air. The first phase of the study was carried out by Lieutenant J. H. Hagy, Jr. and is reported in Ref. 1. Hagy developed the theory applicable to plane wave incidence on a rectangular area of a randomly rough interface and carried out tank model experiments to verify and to extrapolate the theory.

The second phase of the study reported herein involved the accumulation of sound transmission data at sea and subsequent analysis and comparison with theory. Data were taken during two 2 day periods at sea: 28-29 May 1970 (FLIPEX I) and 17-18 August 1970 (FLIPEX II). The data station in both cases was a point between San Clemente Island and the California coast at lat 33°-06' N, long 117°-51' W. The experimental platform used for obtaining both acoustic and oceanographic data was the Floating Instrumentation Platform (FLIP) operated by the Marine Physical Laboratory of Scripps Institution of Oceanography. The oceanographic study was conducted under the direction of Dr. Russ Davis of Scripps using Scripps instrumentation. The sound sources utilized for the various experiments were the Lockheed P-3B Orion patrol aircraft and the Sikorsky SH-3D helicopter. Data analyzed for this thesis was limited to that obtained using the SH-3D helicopter. The sensor used for obtaining noise levels at the ocean surface and at various points in the underwater sound field was the AN/SSQ-57 Sonobuoy manufactured by Sparton, Inc., modified as necessary for the experiment.

The objectives of this thesis were:

1) To compare the predicted smooth surface transmission loss, TL_s, with low frequency data corresponding to very low roughness; acoustical roughness is defined by:

$$R = k_2^2 \sigma^2 (c_2/c_1 \cos \theta_1 - \cos \theta_2)^2$$

2) To compare the predicted rough surface transmission loss $(0.1 < R < 4)$, for a point source in air, with experimental results.

II. THEORY

A. REVIEW OF EXISTING ROUGH SURFACE THEORY

A theory applicable to the transmission of sound from a distant source in air through a rectangular section of a randomly rough air-water interface was developed by Hagy at NPS [1]. His development was very similar to that used by Medwin [2] for scattering of sound from a rough surface. Approximations and assumptions employed in the theory were as follows:

1) The incident wave is plane and ensonifies a limited area of the interface.
2) The receiver is sufficiently far from the surface to regard the received waves as plane, i.e., the "far field approximation" is made.
3) Mutual interaction of the surface irregularities may be neglected.
4) The ensonified area is large compared to an acoustic wavelength.
5) The surface is considered perfectly rigid so that the reflection coefficient, R, equals unity at each point.
6) The Kirchhoff approximation is valid, i.e., the reflection coefficient for points of an extended rough interface area is the same as that for a perfectly smooth interface.
7) The surface correlation length is large compared with the acoustic wavelength.

Most of these assumptions are, at best, approximations of the situation sea experiments; that of a sound source located several hundred feet above the ocean surface. The source was not far enough from the surface for the incident wave to be plane. The area ensonified by the

incident wave front was, strictly speaking, infinite in extent. For a smooth surface, the area over which sound from a point source is transmitted into the half-space below the interface is the area subtended by a 13 degree cone with its apex at the source, i.e. the critical angle for air/water transmission is 13 degrees. Except for very rough seas which were not encountered in the sea experiments, assumption 3 is considered valid. The diameter of the 13° ensonified area as defined above is greater than the largest wave lengths considered in the analysis of the at sea experiments. However the dimensions which really should be used here are those of the annular Fresnel zones over which the incident wave can be considered plane. Because $(\rho c)_{water} >> (\rho c)_{air}$, approximation 5 is considered valid for the sea experiment. The criterion for application of the Kirchhoff assumption is considered by Beckmann to be that the minimum radius of curvature of the surface is large compared with the wavelength of the incident radiation. This is certainly not satisfied at 100 Hz for which the wavelengths in air and water are approximately 10.5 and 46.5 feet respectively.

B. SMOOTH SURFACE THEORY FOR A POINT SOURCE

The objective here is to derive an expression for the ratio of the acoustic pressure incident on the interface at a point directly beneath the source to the acoustic pressure at any point in the half-space below the interface. The interface is assumed to be perfectly smooth.

Assume that power P_1 is radiated into an infinitesmal angle, $d\theta_1$, by the spherically symmetric source, S.

Consider the cross-sectional area of the ray cone intercepted at the interface. Call it A.

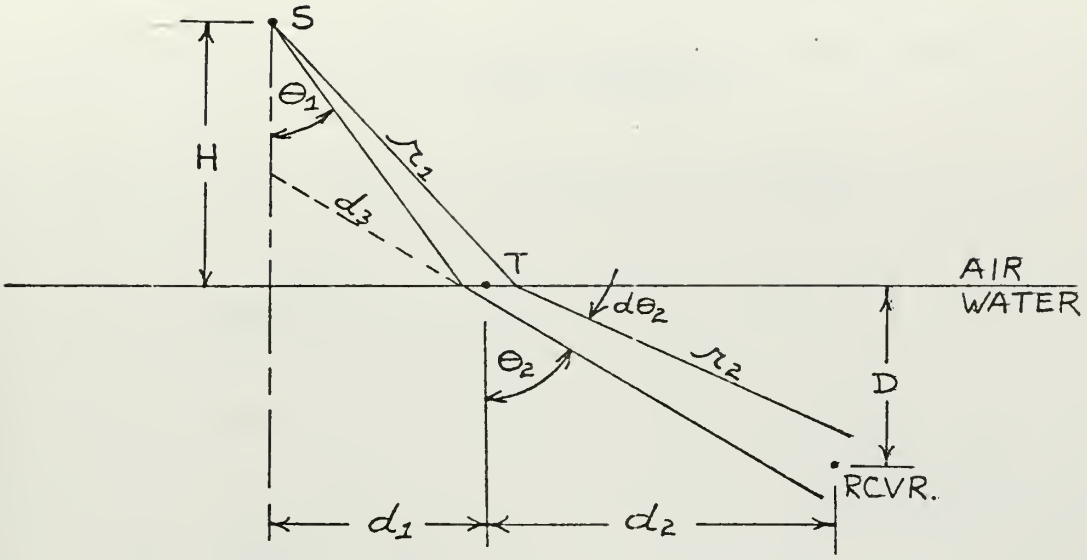

The incident intensity at point T at the interface is

$$I_1 = p_1^2/2\rho_1 c_1$$

Where: p_1 is the incident pressure amplitude

ρ_1 is the density of air

c_1 is the compressional wave speed in air

Then the incident power contained in the ray cone is:

$$(1)\quad P_1 = I_1 A \cos\theta_1 = \frac{p_1^2}{2\rho_1 c_1} A \cos\theta_1$$

Similarly the transmitted power is:

$$(2)\quad P_2 = I_2 A \cos\theta_2 = \frac{p_2^2}{2\rho_2 c_2} A \cos\theta_2$$

where: p_2 is the transmitted pressure amplitude at the interface

ρ_2 is the density of sea water

c_2 is the compressional wave speed in sea water at the interface

The intensity at point T at the interface is also given by:

$$I_1 = \frac{P_1}{(2\pi r_1 \sin \theta_1)\, r_1\, d\theta_1}$$

Now $r_1 = H/\cos \theta_1$

$$I_1 = \frac{P_1 \cos^2 \theta_1}{2\pi H^2 \sin \theta_1\, d\theta_1}$$

Similarly the intensity at the receiver is given by

$$I_{2t} = \frac{P_2}{2\pi(d_1 + d_2)(d_3 + D/\cos \theta_2)d\theta_2}$$

$$= \frac{P_2}{2\pi(r_1 \sin \theta_1 + D \tan \theta_2)(d_3 + D/\cos \theta_2)d\theta_2}$$

$$= \frac{P_2}{2\pi(H \tan \theta_1 + D \tan \theta_2)(d_1/\sin \theta_2 + D/\cos \theta_2)d\theta_2}$$

$$= \frac{P_2}{2\pi(H \tan \theta_1 + D \tan \theta_2)(H \tan \theta_1/\sin \theta_2 + D/\cos \theta_2)d\theta_2}$$

By Snell's Law: $\frac{c_1}{c_2} = \frac{\sin \theta_1}{\sin \theta_2}$

Then $c_2 \cos \theta_1\, d\theta_1 = c_1 \cos \theta_2\, d\theta_2$

and $\frac{d\theta_2}{d\theta_1} = \frac{c_2 \cos \theta_1}{c_1 \cos \theta_2} = \frac{\sin \theta_2}{\sin \theta_1} \cdot \frac{\cos \theta_1}{\cos \theta_2} = \frac{\tan \theta_2}{\tan \theta_1}$

Then:

$$\frac{I_1}{I_{2t}} = \frac{\cos^2\theta_1}{2\pi H^2 \sin\theta_1} \cdot 2\pi(H\tan\theta_1 + D\tan\theta_2)\left(H\frac{\tan\theta_1}{\sin\theta_2} + \frac{D}{\cos\theta_2}\right) \cdot \frac{d\theta_2}{d\theta_1} \cdot \frac{P_1}{P_2}$$

$$= \frac{\cos^2\theta_1}{H^2 \sin\theta_1} (H\tan\theta_1 + D\tan\theta_2)\left(\frac{\tan\theta_2}{\tan\theta_1}\right)\left(H\frac{\tan\theta_1}{\sin\theta_2} + \frac{D}{\cos\theta_2}\right) \cdot \frac{P_1}{P_2}$$

$$= \frac{\cos^2\theta_1}{H^2 \sin\theta_1} (H\tan\theta_1 + D\tan\theta_2)\left(\frac{H}{\cos\theta_2} + \frac{D\tan\theta_2}{\tan\theta_1\cos\theta_2}\right) \cdot \frac{P_1}{P_2}$$

$$= \frac{\cos^2\theta_1}{H^2 \sin\theta_1} (H\tan\theta_1 + D\tan\theta_2)\left(\frac{H\tan\theta_1 + D\tan\theta_2}{\tan\theta_1\cos\theta_2}\right) \cdot \frac{P_1}{P_2}$$

$$= \frac{\cos^2\theta_1}{H^2 \sin\theta_1} \cdot \frac{(H\tan\theta_1 + D\tan\theta_2)^2}{\tan\theta_1\cos\theta_2} \cdot \frac{P_1}{P_2}$$

Now find the intensity, I_{1Z}, at some point Z directly below the source:

$$I_1 = \frac{I_s}{r_1^2} \quad ; \quad I_{1Z} = \frac{I_s}{H^2}$$

where I_s is the intensity at unit distance from the source s.

$$\frac{I_{1Z}}{I_1} = \frac{r_1^2}{H^2} = \frac{1}{\cos^2\theta_1}$$

Then $$\frac{I_{1Z}}{I_1} = \frac{I_1}{I_{2t}} \cdot \frac{I_{10}}{I_1} = \frac{I_1}{I_{2t}} \cdot \frac{1}{\cos^2\theta_1}$$

$$\frac{I_{1Z}}{I_{2t}} = \frac{(H \tan \theta_1 + D \tan \theta_2)^2}{H^2 \sin \theta_1 \tan \theta_1 \cos \theta_2} \cdot \frac{P_1}{P_2}$$

Returning to equations (1) and (2) for P_1 and P_2 and substituting them into the above expression:

$$\frac{I_{1Z}}{I_{2t}} = \frac{(H \tan \theta_1 + D \tan \theta_2)^2}{H^2 \sin \theta_1 \tan \theta_1 \cos \theta_2} \cdot \frac{\rho_2 c_2 p_1^2 \cos \theta_1}{\rho_1 c_1 p_2^2 \cos \theta_2}$$

Now $$I_{1Z} = \frac{p_{10}^2}{2\rho_1 c_1} \quad ; \quad I_2 = \frac{p_{2t}^2}{2\rho_2 c_2}$$

Then

$$\frac{p_{1Z}^2}{p_{2t}^2} = \frac{(H \tan \theta_1 + D \tan \theta_2)^2}{H^2 \sin \theta_1 \tan \theta_1 \cos \theta_2} \cdot \frac{\cos \theta_1}{\cos \theta_2} \cdot \frac{p_1^2}{p_2^2}$$

$$\frac{p_{1Z}}{p_{2t}} = \frac{H \tan \theta_1 + D \tan \theta_2}{H (\sin \theta_1 \tan \theta_1 \cos \theta_1)^{1/2}} \left(\frac{\cos \theta_1}{\cos \theta_2} \right)^{1/2} \cdot \frac{p_1}{p_2}$$

Dividing both sides by $H \tan \theta_1$,

$$\frac{p_{1Z}}{p_{2t}} = \frac{1 + \frac{D}{H} \frac{\tan \theta_2}{\tan \theta_1}}{\left(\frac{\sin \theta_1 \tan \theta_1 \cos \theta_2}{\tan^2 \theta_1} \right)^{1/2}} \cdot \left(\frac{\cos \theta_1}{\cos \theta_2} \right)^{1/2} \cdot \frac{p_1}{p_2}$$

$$= \frac{1 + \frac{D}{H} \frac{c_2 \cos \theta_1}{c_1 \cos \theta_2}}{(\cos \theta_1 \cos \theta_2)^{1/2}} \cdot \left(\frac{\cos \theta_1}{\cos \theta_2} \right)^{1/2} \cdot \frac{p_1}{p_2}$$

$$\frac{p_{1Z}}{p_{2t}} = \left(1 + \frac{D}{H}\,\frac{c_2 \cos\theta_1}{c_1 \cos\theta_2}\right) \cdot \frac{1}{\cos\theta_2} \cdot \frac{p_1}{p_2}$$

Now
$$\frac{p_2}{p_1} = 1 + \frac{\rho_2 c_2 \cos\theta_1 - \rho_1 c_1 \cos\theta_2}{\rho_2 c_2 \cos\theta_1 + \rho_1 c_1 \cos\theta_2}$$

$$= 1 + \frac{\cos\theta_1 - \frac{\rho_1 c_1}{\rho_2 c_2}\cos\theta_2}{\cos\theta_1 + \frac{\rho_1 c_1}{\rho_2 c_2}\cos\theta_2}$$

For air to water transmission,

$$\frac{\rho_1 c_1}{\rho_2 c_2} \simeq \frac{1}{3700}$$

Then
$$\frac{p_2}{p_1} \simeq 2 \quad \text{for any incidence angle.}$$

Hence a general expression for the ratio of pressure at point 0 to pressure at the receiver for air to water transmission is:

$$\frac{p_{1Z}}{p_{2t}} = \left[1 + \frac{D}{H}\,\frac{c_2 \cos\theta_1}{c_1 \cos\theta_2}\right] \cdot \frac{1}{2\cos\theta_2}$$

Define transmission loss, TL_s:

$$TL_s \triangleq 20 \log \frac{p_{1Z}}{p_{2t}} = 20 \log \left[\left(1 + \frac{D}{H}\,\frac{c_1}{c_1}\,\frac{\cos\theta_1}{\cos\theta_2}\right)\frac{1}{2\cos\theta_2}\right]$$

For the receiver directly below point O, this reduces to:

$$TL_s = 20 \log \left[\left(1 + \frac{D}{H} \frac{c_2}{c_1}\right) \frac{1}{2} \right]$$

Note that at $D = 0$, $TL = 20 \log \frac{1}{2} = -6$ dB, i.e., there is a 6 dB <u>increase</u> in SPL. This is consistent with the boundary condition that pressure is continuous across the interface, i.e.,

$$p_s = p_{1Z} + p_r = p_{1Z} + Rp_{1Z} = 2p_{1Z}$$

where p_s is pressure amplitude at the surface

p_r is amplitude of the reflected pressure wave

$p_{2t} = p_s$ by the boundary condition

$$\left.\frac{p_{1Z}}{p_{2t}}\right|_{D=0} = \frac{1}{2}$$

A plot of TL_s vs. D/H is shown in Fig. 2-1.

C. ROUGH SURFACE THEORY FOR A POINT SOURCE

Hagy's theory [1] for rough surface transmission of a plane wave through a limited area concludes with his equation (29); using p_{2t} vice his p_2:

$$\left\langle p_{2t} p_{2t}^* \right\rangle = p_{20}^2 F^2 e^{-R} \left[(\text{sinc } K_x X \text{ sinc } K_y Y)^2 + \frac{\pi L^2}{A} \sum_{n=1}^{\infty} \frac{R^n}{nn!} \exp(-K_{xy}^2 L^2/4n) \right]$$

Fig. 2-1

PLOT OF TL_s vs. D/H:

$$TL_s = 20 \log \left[\left(1 + \frac{D}{H} \frac{c_2}{c_1}\right) \frac{1}{2} \right]$$

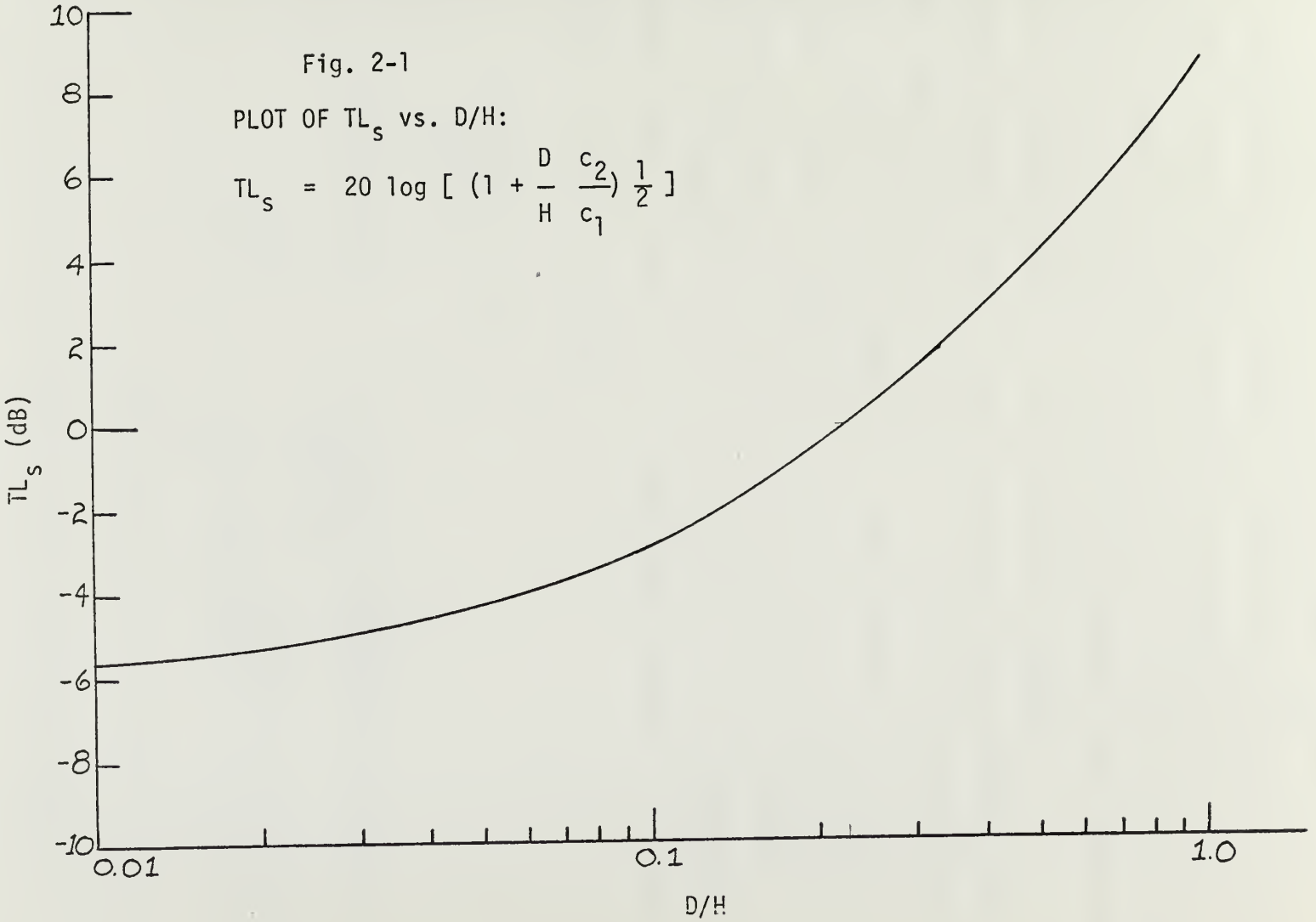

A rough surface theory applicable to transmission of sound for the case of a point source in air has not been developed to date, and will not be undertaken herein. In general it appears that an approach to the development would be based on approximating the spherical wave front by a series of annular wave fronts. The manner in which these annular zones contribute to the intensity at a point in the underwater sound field would then have to be determined for various degrees of roughness.

It seems certain that the coherent component of the intensity (first term of Hagy's equation (29) above) will be dominant in its contribution to total intensity at low roughness for a point source as it is for a plane wave. Further, it seems likely that for a point source above a low roughness surface, $R < 1$, this coherent contribution will again exhibit an e^{-R} dependence for the Snell direction, i.e. the refraction direction predicted by Snell's Law. Under these conditions $F = 1$ and $\text{sinc } K_x X = \text{sinc } K_y Y = 1$, so that

$$\frac{\langle p_{2t} p_{2t}^* \rangle}{\langle p_{20}^2 \rangle} = e^{-R}$$

where: $\langle p_{2t} p_{2t}^* \rangle$ = mean square transmitted pressure amplitude at a point in the underwater sound field

$\langle p_{20}^2 \rangle$ = mean square transmitted pressure amplitude at the same point for a smooth surface

$$R = K_2^2 \sigma^2 (c_2/c_1 \cos \theta_1 - \cos \theta_2)^2$$

In view of the above the following can be postulated for low roughness; $R < 1$:

$$TL = TL_S + TL_R$$

$$= 20 \log \left[\left(1 + \frac{D}{H} \frac{c_2}{c_1}\right) \frac{1}{2} \right] + 10 \log e^R$$

Preliminary analytical work by Dr. Medwin at NPS has suggested that for a point source, the incoherent contribution to intensity increases monotonically with frequency for $R > 1$ reaching a peak at $R \simeq 3$ and then falling off monotonically for higher frequencies.

III. EXPERIMENTAL EQUIPMENT FOR ACOUSTICAL MEASUREMENTS

A. GENERAL

It was determined in the early planning stages of FLIPEX I that the use of both fixed wing aircraft and helicopters as airborne sound sources was desirable. Because of their operational availability and their primary role as ASW aircraft, the Lockheed P-3B Orion patrol plane and the Sikorsky SH-3D helicopter were selected.

At the time, AN/SSQ-57 calibrated sonobuoys appeared to be very well suited for use as sensors with which to detect aircraft noise both at and below the surface. Accordingly, since P-3 aircraft routinely operate with sonobuoys of this type, it appeared very advantageous to utilize the P-3's on-board signal processing equipment for the purpose of recording both its own noise signal and that of the helicopter. However, an ensuing feasibility study of this scheme indicated the following problems:

a) Calibration of the P-3 equipment to enable the taped signal level for each sonobuoy to be converted to acoustic pressure level at the sonobuoy hydrophone is a difficult task not ordinarily undertaken. Added to the inherent difficulty of the task was the problem of frequent traveling to and from N.A.S. Moffett Field as well as the uncertainty as to which aircraft would actually be used.

b) The proximity of the experimental site to the California coastline introduced the problem of radio interference from commercial short wave transmissions (police, taxicabs, etc.). This was shown to be a serious problem during a trial run off Monterey.

The possibility of using P-3 VHF receivers and multi-channel tape recorders on board FLIP was also considered since at low altitude it was

suspected that commercial interference would be minimal. However the problems involved in procuring the equipment and assembling it as a system on board FLIP rendered this plan also not feasible.

The remaining possibility involved hard wiring the sonobuoys to FLIP and recording the signals on an NPS acoustic research multi-channel tape recorder installed on board FLIP. The decision was made to use this method for the experiment. In the remainder of this section, the modifications made to the AN/SSQ-57 sonobuoys, the design of the sensor unit, signal line and signal line/tape recorder interfaces will be discussed.

B. SONOBUOY MODIFICATION

A block diagram of the AN/SSQ-57 sonobuoy in its normal configuration appears in Fig. 3-1 below:

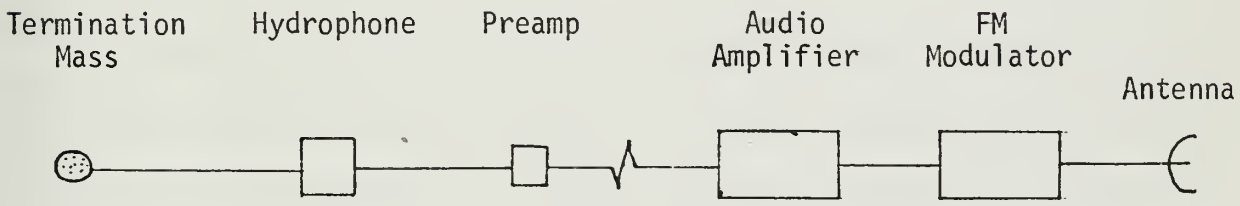

Fig. 3-1
BLOCK DIAGRAM OF AN/SSQ-57 SONOBUOY

The audio amplifier and FM modulator are circuit board solid state units and are enclosed within the watertight portion of the buoy cannister. The antenna extends approximately two feet above the top of the buoy. The buoy is slightly buoyant; its top rides a few inches above the water surface. The hydrophone, preamplifier, and termination mass are suspended from a compliant length of rubber at a dept of 95 ±15 feet [3]. The compliant rubber, hereafter referred to as the "bungee", has a length of approximately 35 feet when supporting the hydrophone, pre-amplifier, and

termination mass in water. Its purpose is to isolate the hydrophone from wave induced vertical motion of the sonobuoy cannister. If such vertical motion were not isolated, the resulting changes in hydrostatic pressure at the hydrophone would cause limiting in the audio amplifier.

The decision to hardwire the sonobuoys to FLIP meant that the RF modulator section in the buoy would be disabled and the output of the audio amplifier connected directly to the long line to FLIP. It was found that by disconnecting the RF modulator section from the 10.1 volt salt water battery power supply, the current drawn from the power supply was reduced by a factor of over 10. The implication was that with the sonobuoys hard wired, their normal eight-hour operating period [3], would be extended to a period of over eighty hours. This was very desirable since it meant that buoy replacement would not have to be undertaken during the two day experimental period.

The AN/SSQ-57 sonobuoy has an electric test plug built into its top. This plug facilitated the above battery life test and many which followed. It enabled the experimenters to energize the buoy by means of an external 10.1 volt power supply, to uncouple the preamplifier electrically from the audio amplifier, and to introduce a low level signal to the input of the audio amplifier. The use of this test plug is discussed in detail in Appendix A which deals with calibration.

In order to predict signal levels at the output of the audio amplifier, the Wenz curves [4] were consulted to predict a likely ambient noise level based on the prevailing wind speed range in Southern California coastal areas. Using this value and a typical hydrophone sensitivity and audio amplifier gain, the output level of the audio amplifier was predicted. This level was considerably higher than the noise level expected to be

introduced in the shielded signal line. Hence additional amplification of the higher level helicopter signal was not considered necessary.

Modifications made to the AN/SSQ-57 sonobuoy were as follows:

a) The dissolvable plug in the buoy cannister was removed and an aluminum disk epoxied in its place.

b) Where hydrophone depths greater than 95 feet were desired, the AN/SSQ-57 hydrophone assembly was replaced with an AN/SSQ-41A sonobuoy hydrophone assembly. Depths were set according to the requirements of the experiment.

c) The 1.5 volt DC power supply line was cut inside the watertight section of the buoy. Under normal ASW operation this voltage provides a means of limiting the buoy's operational life to approximately 1 hour. An externally operated switch controls this option.

d) The node at which the 10.5 volt DC is supplied to the audio amplifier and the RF modulator was bypassed so as to provide 10.5 volt to the audio amplifier only.

e) Through the top plate of the buoy a hole was drilled and tapped with a 3/8" pipe thread. A brass 3/8" swagelock water tight fitting was inserted.

f) A two-terminal terminal board was affixed to the buoy center shaft a few inches below the top plate. A length of coaxial cable (utilizing the discarded antenna cable) was inserted connecting the output of the audio amplifier to the terminal board.

g) A Marsh-Marine RM-2-MP 2 connector male pigtail was inserted through the swagelock fitting and soldered to the terminal board. The fitting was then tightened down.

h) The aluminum cannister enclosing the hydrophone assembly was removed and discarded. With the buoy assembled, this permitted the bottom

retaining plate to be easily inserted in the bottom against the hydrophone assembly and locked in place with the retainer ring. This provided a quick release means of deploying the hydrophone assembly.

C. SURFACE MICROPHONE

One of the essential requirements of the experiment was that there be a means of measuring either incident acoustic pressure or surface acoustic pressure at the air water interface. Because of the continuity of pressure at the boundary, the surface acoustic pressure could be obtained by locating the sensor either just above the surface or just below it. To avoid turbulent water noise beneath the surface it was elected to have the sensor above the surface. Two problems had to be considered at this point. First, there surely would be a certain amount of shock pulsing of the sensor due to surface splash. Secondly, a standing wave pattern above the surface would be present which could have significant effect for frequencies $\geq$ 500 Hz with the sensor a few inches above the surface. To reduce the splash noise by raising the sensor would mean that the sensor would be in the standing wave pattern. To move the sensor very close to the doubled pressure anti-node would mean much more splash effect. For FLIPEX I, the decision was made to use two surface sensors; one 2 inches above the surface, one 6 inches above the surface. For FLIPEX II, a single sensor was used which was designed to ride just at the surface. This latter choice was based on the observation from FLIPEX I data that a standing wave pattern <u>did</u> exist which was seriously affecting the spectrum of the recorded helicopter noise.

The requirement that the surface sensor be compact, rugged, and water tight suggested the use of a sonobuoy hydrophone. An AN/SSQ-57 hydrophone was tested in air in the NPS anechoic chamber and found to be completely

satisfactory in its operation. For FLIPEX I, two AN/SSQ-57 hydrophones were affixed on top of discarded AN/SSQ-41 sonobuoy cannisters. A styrofoam collar was fitted around the top of each cannister to cause the assembly to respond rapidly to all wave frequencies. (There was concern that without the collar the cannister would bob slowly with the longer period waves, thus allowing the short period waves to break over its top.) Lead weights were inserted in the bottom of the cannister to add stability about an axis perpendicular to the surface. The drawback of this design was found during FLIPEX I to be that considerable noise at the surface microphone was generated by bumping of the support cannister against other floating components of the system. To eliminate this problem, an integral surface microphone/sonobuoy unit was designed for use during FLIPEX II. This unit consisted of a thick aluminum cap fitted into the top of a sonobuoy with the sonobuoy hydrophone cemented to a water repellent foam rubber pad sandwiched between the hydrophone and the cap. It was intended that this unit be streamed at the end of its own cable at such a distance that there would be no contact between it and the other floating units.

D. CONSTRUCTION OF SONOBUOY CLUSTERS

The objectives of the experiment indicated the use of as many underwater sensors as possible for sampling the underwater sound field. Available for use in the experiment was a Precision Instrument Inc. eight channel FM/AM tape recorder. For FLIPEX I, one channel was reserved for voice annotation; another channel for insertion of a tone to be eventually utilized as an on-off signal for analog to digital conversion of the data. Of the remaining six channels, two were to be used for recording the signal from the two surface microphones already described. Four underwater signal

channels remained. In order to provide flexibility in sampling various positions in the udnerwater sound field, it was decided that two clusters of three sonobuoys each would be employed. Each cluster would be individually tethered to FLIP. The three signals from the three individual sonobuoys would be conveyed to FLIP via a single Belden 8777 plastic covered cable, hereafter referred to as the "signal line", containing three pairs of twisted "Beldfoil" shielded pairs of 22AWG wire. Each pair will be referred to hereafter as line 1, 2, or 3. The clusters will be referred to hereafter as Clusters I and II. The constructional details of each cluster were as follows:

a) Two triangular aluminum frameworks were fabricated. Attached to each apex was a ring clamp having a diameter slightly larger than the sonobuoy. One frame was clamped to the uppermost portion of the buoy cannisters. The other frame was clamped about six inches below the first. The upper frame included a bracket for attaching the tether to FLIP.

b) Sandwiched between the frames was a triangular piece of styrofoam sufficient in size to provide the additional buoyancy needed. Inserted through a hole in the styrofoam was a watertight cannister containing the three transformers used to match the impedance of the sonobuoys to that of the lines.

c) Stretched between the antenna posts of two buoys was a white cloth marker bearing the number of the cluster for identification purposes.

A sketch of a fully assembled cluster appears in Fig. 3-2. Tethered to each cluster was a brightly colored 4 foot diameter "kiddy pool" used as a visual reference point by the helicopter pilots.

E. SIGNAL LINE

In order to provide some flotation for the signal lines, one inch polypropylene line was selected for use in tethering the clusters

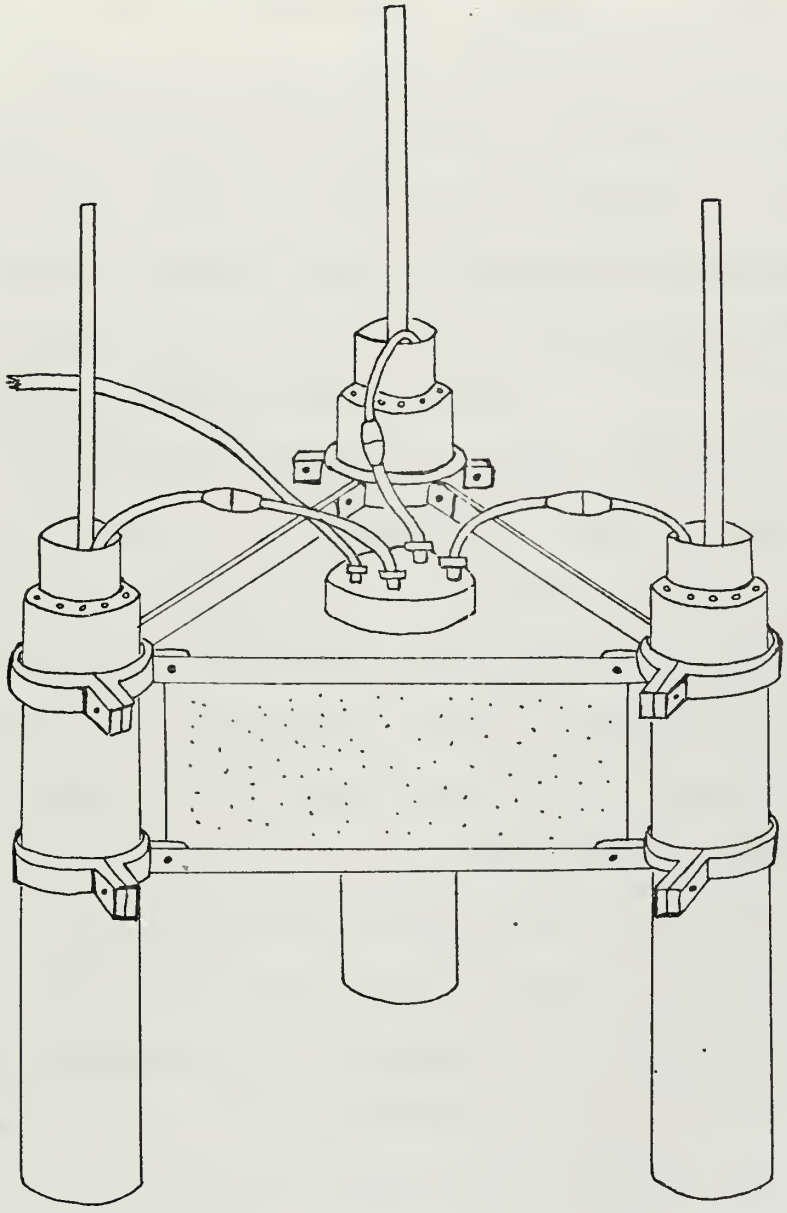

Fig. 3-2

FULLY ASSEMBLED SONOBUOY CLUSTER

to FLIP. A 300 foot length was available for Cluster I, 900 feet for Cluster II. The tether line was coiled on rotating drums to facilitate the movement of Cluster II with respect to Cluster I. Taped to the tether line was the 3 conductor shielded pair Belden Cable used for the signal line. To ensure flotation of the tether/cable combination, three inch fishing floats were secured at intervals along the line. In order that there be sufficient tension to keep the line stretched out downwind from FLIP, several thirty inch weather balloons inflated with a mixture of helium and air were attached to each cluster.

The use of transformers at both the outboard and inboard end of the signal lines was required for the purpose of impedance matching as well as to "float" the three data lines so as to prevent common grounding. The output impedance of the sonobuoy audio amplifier was found to be on the order of several hundred ohms. The input impedance of the tape recorder was found to vary between 10 and 50 kilohms depending on the input gain selection. Because of the loading effect on sonobuoy gain of such a large variation in load resistance, 100 k resistors were inserted in series with the tape recorder inputs. Triad TA-38 and TA-24 audio transformers were selected for the outboard and inboard ends respectively of the signal line . This selection resulted in a line impedance of approximately 1800 ohms and a voltage gain in the line varying from 14 dB at 20 Hz to 17 dB at 1 kHz.

F. INSTRUMENTATION ON BOARD FLIP

Instrumentation on board FLIP was all rack mounted in a large frame consisting of three nineteen inch wide bays. The frame was provided by Marine Physical Laboratory of Scripp's Institution of Oceanography and was designed specifically for use on board FLIP. Equipment mounted in the frame was as follows:

Input patch panels
Eight channel tape recorder
Four channel tape recorder
Decade oscillator
Output patch panel
Two loudspeakers
Audio amplifier
B & K microphone power supply
Two-trace oscilloscope
One-trace oscilloscope
VTVM
UHF radio transceiver

The use and, where applicable, the design of this equipment was as follows:

1. Input Patch Panels

As mentioned in the preceding paragraph, a 100 kilohm resistor was inserted in series with the input impedance of each tape recorder module. Some provision for measuring voltage attenuation across the resulting voltage divider was required. Accordingly an input patch panel having two BNC fittings with the 100 kilohm resistor in series between them was fabricated. The line output was connected to one BNC, the tape recorder input to the other BNC. The TA-24 transformer was also incorporated into the patch panel.

Schematically, the arrangement was as shown below in Fig. 3-3.

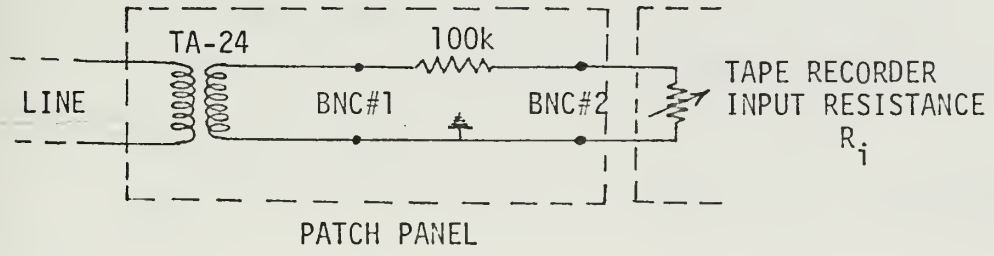

Fig. 3-3
SCHEMATIC OF TAPE RECORDER INPUT PATCH PANEL

Each patch panel consisted of three TA-24 transformers and three BNC pairs. There were two such panels for FLIPEX I, one to handle the input signals from each sonobuoy cluster. For FLIPEX II, a third panel was added for the surface microphone channel. Prior to each experiment each tape recorder channel was calibrated. This calibration included varying the tape recorder input gain, R_i, so that a certain input voltage level produced an output voltage of 1.0 volt. (One volt was the limit for distortion-free recording.) The calibration voltage was inserted at BNC #2. It was made larger than the largest signal level anticipated. Changing R_i meant a change in the input voltage divider attenuation. Hence, once R_i was set, a known signal level was inserted into BNC #1. Then the voltage level at BNC #2 was measured and the attenuation computed. The foregoing procedures were carried out with the line disconnected from the sonobuoys.

2. Eight-Channel Tape Recorder

For FLIPEX I, channels 1 through 6 were used for sonobuoy signal recording. Channel 7 was used for voice annotation and channel 8 for insertion of a tone to be used later in controlling analog to digital conversion. For FLIPEX II, channels 1 through 7 were intended for sonobuoy signal recording; channel 8 for both voice annotation and tone insertion.

3. Four-Channel Tape Recorder

Included as a back-up only for the eight-channel tape recorder.

4. Decade Oscillator

Used to provide the calibrating signal for calibration of the tape recorder.

5. Output Patch Panel

Consisted of an eight position barrel switch connected to the outputs of the eight recording/playback modules in the tape recorder. This permitted rapid selection of data channels for audio and visual signal monitoring.

6. Loudspeakers

One loudspeaker was connected through a universal audio transformer to the headset output of the UHF transceiver. The other loudspeaker was driven by either the output of the audio amplifier when being used for audio monitoring of the sonobuoy signals or driven by the output of the B & K microphone power supply when being used for a one-way intercom.

7. Audio Amplifier

Connected to the output patch panel. Was used to drive one loudspeaker for audio monitoring of sonobuoy signals.

8. B & K Microphone Power Supply

Used to drive a loudspeaker when a microphone was used for one way communication between FLIP's observation platform and the instrumentation space within FLIP.

9. UHF Radio Transceiver

Used for communications with aircraft involved in experiment. FLIP had no permanently installed UHF radio equipment on board.

10. Oscilloscopes

Used for visual monitoring of tape recorder input signals as well as actual recorded signal.

11. VTVM

Used for setting level of tape recorder calibration signal and for measuring attenuation across input voltage divider. Also used for ensuring that signal level being recorded did not exceed 1 volt rms which was the upper limit for distortion free recording.

IV. CONDUCT OF EXPERIMENTS

A. GENERAL

To achieve the objectives set forth in Section I, the ocean experiments were designed to obtain the following data:

1. Helicopter noise levels at the air water interface and at several points in the underwater sound field separated both horizontally and vertically.
2. Root mean square ocean surface waveheight.

This section is devoted to a description of the manner in which these data were obtained.

B. HELICOPTER NOISE LEVEL MEASUREMENT

Section III contains the details of the design and construction of the system components used in recording helicopter noise levels. A plan view showing the positioning of the two sonobuoy clusters with respect to FLIP is shown in Fig. 4-1 below.

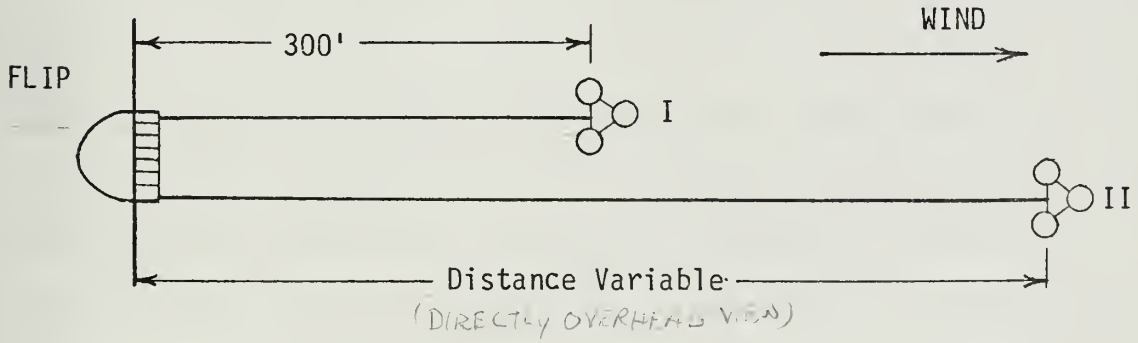

Fig. 4-1
PLAN VIEW OF EXPERIMENT ARRANGEMENT

The position of Cluster I was maintained at a distance of approximately 300 ft. from FLIP throughout all experiments. It was intended that the

position of Cluster II be varied from one experiment to another so that transmission at various grazing angles[1] could be obtained. This was done quite effectively during FLIPEX I. It was prevented during FLIPEX II by tangling of the cables in the water. Fig. 4-2 shows the surface microphone positions and hydrophone depths for both FLIPEX I and FLIPEX II.

As discussed in Section III, the surface microphone unit designed for FLIPEX II was to be streamed at the end of its own cable. This unit failed immediately upon immersion in the water due to a leaky connection in the signal line. As a substitute surface microphone, the 10 feet deep hydrophone, shown as a dashed line in Fig. 4-2, was retrieved and placed in the kiddy pool. This arrangement provided a microphone at the air-water interface and, except for surface wave noise, functioned very effectively.

The compilation in Fig. 4-3 shows the sonobuoys by serial number which were used, the cluster in which they were located, the line to which they were connected and the tape recorder channel used for recording their signals.

At the outset of FLIPEX I it was intended that all data be collected during helicopter hovers. However, two factors prevented this from being done. First the helicopter pilogs experienced considerable difficulty in maintaining the position of their aircraft directly overhead a visual reference point particularly at higher altitudes (e.g., 600 feet). Secondly, due to safety considerations, the helicopter could not hover at altitudes between 50 feet and 500 feet. A hover at an altitude below 50 feet resulted in a great amount of sea surface disturbance which was

---

[1]Grazing angle refers to the angle shown in the first sketch of Fig. 4-2.

FLIPEX I

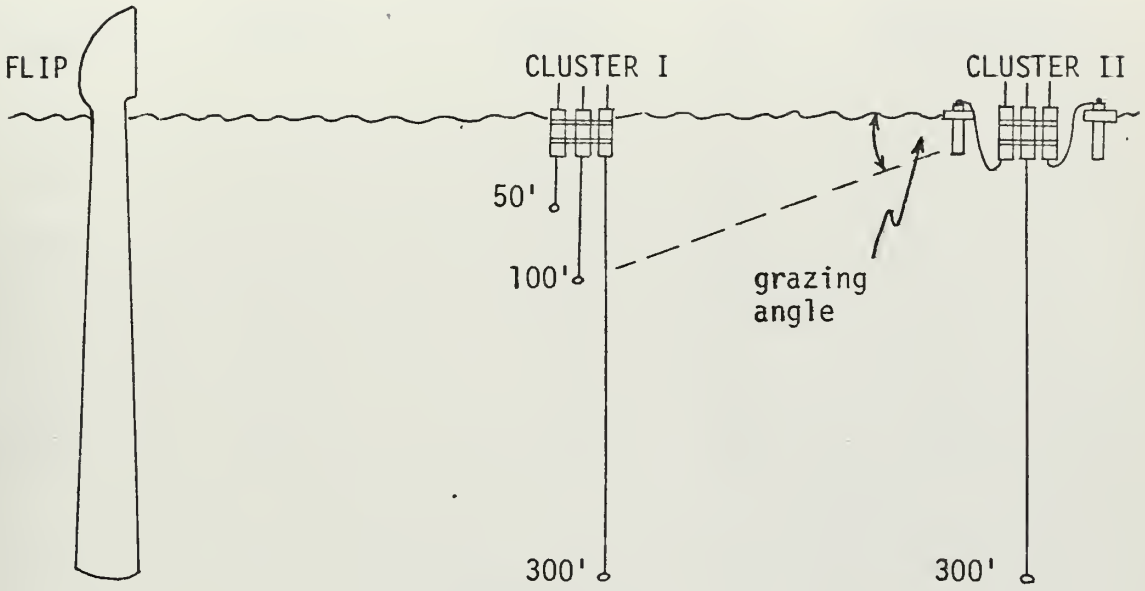

FLIPEX II

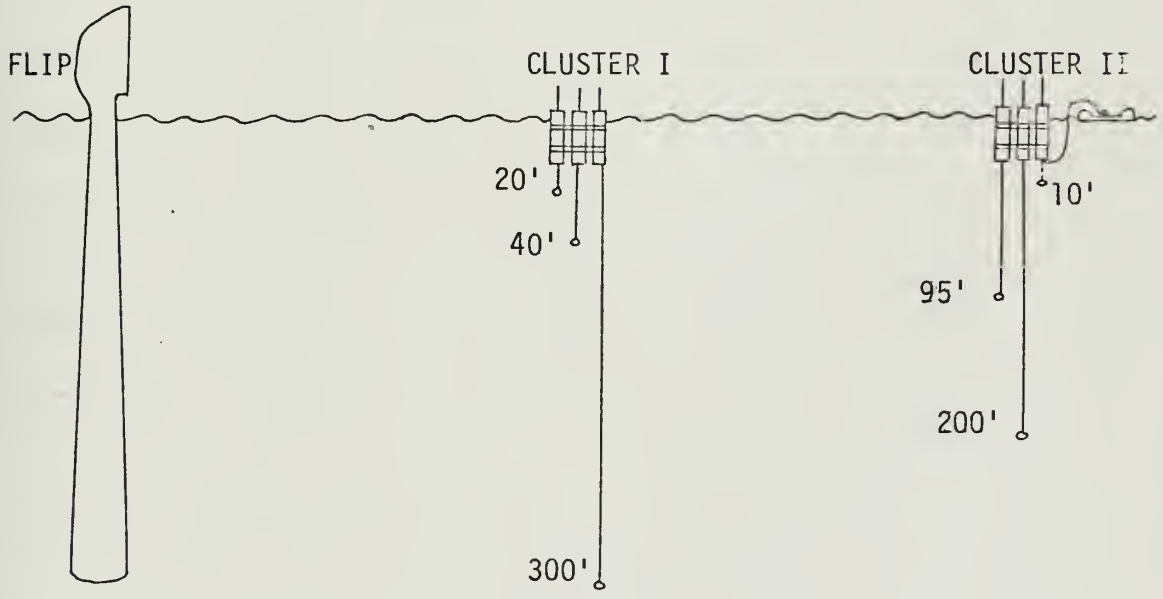

Fig. 4-2
SIDE VIEW OF EXPERIMENT ARRANGEMENT

FLIPEX I

Hydrophone Depth	Sonobuoy Ser. No.	Cluster No.	Line	Tape Recorder Channel
50'	6	I	1	1
100'	5	I	2	3
300'	2	I	3	5
2" sfc. mic.	14	II	1	2
6" sfc. mic.	12	II	2	4
300'	30	II	3	6

FLIPEX II

Hydrophone Depth	Sonobuoy Ser. No.	Cluster No.	Line	Tape Recorder Channel
20'	16	I	1	1
50'	7	I	2	3
300'	10	I	3	5
10' sfc. mic.	14	II	1	2
100'	31	II	2	4
200'	6	II	3	6

Fig. 4-3
COMPILATION OF HYDROPHONE/SONOBUOY/CLUSTER/
LINE/TAPE RECORDER CHANNEL CORRESPONDENCE

unacceptable for this experiment. Consequently it was decided to have the helicopter make slow (approximately 5 knot) passes over the sonobuoy clusters. Position accuracy was excellent using slow passes and the passes could be conducted at any altitude.

Figure 4-1 shows the sonobuoy clusters streaming downwind. This was generally the case since FLIP's drift direction is determined by subsurface currents which were usually in a direction opposite to that of the wind. The only exception to this was during a shift in wind direction on the morning of 18 August. The clusters streamed upwind during Experiment 11, and generally crosswind during Experiments 12 through 14.

In Appendix B each experiment conducted during FLIPEX I and FLIPEX II is described in detail. Included in each description are:

1) Specific purpose of experiment
2) Date and time of experiment
3) Helicopter altitude
4) Type of run (hover or pass)
5) Duration of hover or number of passes
6) Position of run with respect to clusters
7) Cluster separation
8) Remarks

C. SURFACE WAVE MEASUREMENT

Under the direction of Dr. Russ Davis of Scripps, time series wave height variations were recorded during both FLIPEX I and FLIPEX II. Whenever possible, such data were taken simultaneously with helicopter noise data. During FLIPEX I, wave data were recorded using four wave probes and a Vibrotron pressure transducer. During FLIPEX II, four wave

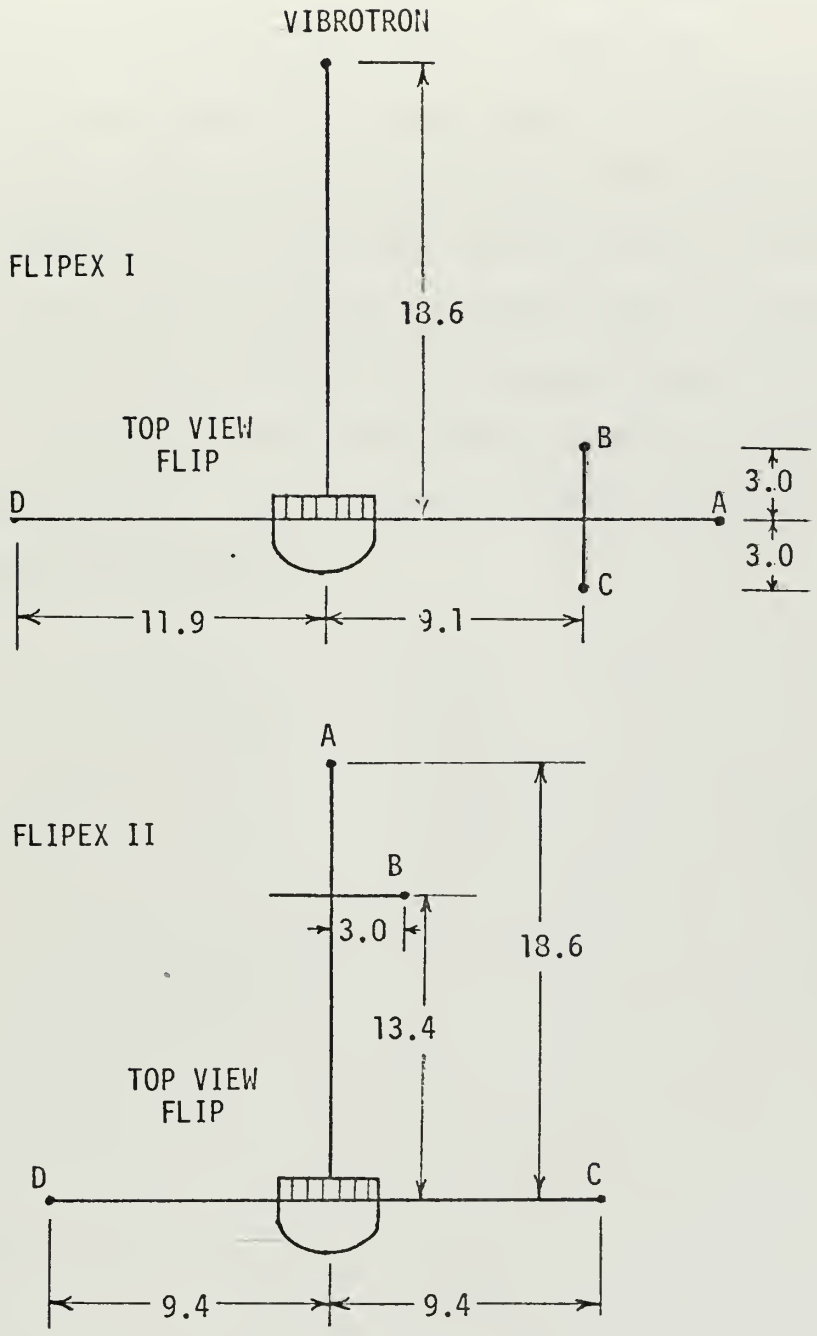

Note: All dimensions in meters

Fig. 4-4
POSITIONING OF WAVE PROBES

probes were used. The positioning of these devices is shown in Fig. 4-4. Wave probe positions are shown by their letter designations.

Surface wave frequency spectra were generated by transforming the wave height variation time records for each device. Then mean square wave heights for several wave period ranges were obtained by integration of the frequency spectra over appropriate frequency ranges. This processing was carried out at Scripps. Difficulty with the wave probes was experienced during FLIPEX I. Hence mean square wave heights provided by the Vibrotron, only, were considered valid. Mean square wave heights for FLIPEX I and FLIPEX II are compiled in Appendix D.

V. DATA ANALYSIS

A. GENERAL

The helicopter noise spectrum is characterized by discrete frequency components, due to rotor passage rates, embedded in or protruding above the broad band spectrum of engine and aerodynamic noise. The entire noise output is time-variable, principally because of the turbulent medium through which it propagates.

Three techniques were considered for analysis of the helicopter noise data. They were as follows:

1) Correlation analysis utilizing the several discrete frequency components known to exist below 120 Hz [5].
2) Analog analysis in which the taped signal would be narrow band filtered and integrated in a wave analyzer, the output being plotted to determine average mean square noise level.
3) Conversion of analog information to digital form followed by digital processing to obtain high frequency resolution power spectral densities for each recorded signal.

B. CORRELATION ANALYSIS

Correlation analysis using the several discrete low frequency components identified in Ref. 5 was attempted using a Princeton Applied Research Inc. Model 101 Correlation Function Computer. The first step of the procedure was to cross-correlate the surface microphone signal, A_1, with the hydrophone signal, A_2, at some depth. Both inputs to the correlator were narrow band filtered by General Radio Type 1564A Sound and Vibration Analyzers about the discrete frequency of interest. It was found that

considerable long term (of order 10 sec) time variation existed in the amplitudes, A_1 and A_2 of these discrete components. It is assumed that this was due to drift in helicopter hover position. This meant that the amplitude of the sinusoidal cross-correlation function, $C_{I2}(\tau)$, was also time varying and at any point in time was equal to $\langle A_1 A_2 \rangle / 2$ where $\langle A_1 A_2 \rangle$ is the time weighted average of the product $A_1 A_2$ taken over the 20 second integration time of the correlator. By plotting the rms value of the sinusoidal cross-correlation function over a long period of time as could be done with a hover, a reliable average value of $\langle A_1 A_2 \rangle$ could have been obtained. However it was determined that position keeping problems with the hovers at altitudes greater than 500 feet precluded their use except over the short periods of time during which they were actually directly overhead the surface microphone. In the course of this study, an experiment was conducted in which the short term variation of the 1/10 th octave filtered surface microphone and hydrophone signals were plotted side by side on a strip chart. There was no visual correlation between the short term variations shown by the two graphs.

If a reliable average of $\langle A_1 A_2 \rangle$ could have been obtained, a second step in the analysis might have been to auto-correlate the narrow band filtered surface microphone signal and obtain C(0) which is the value of the auto-correlation function with zero time delay. Assuming a signal to noise ratio of at least 10 dB, C(0) equals the mean square signal voltage (or power) in the signal (where averaging is done over the integration time of the correlator). However in the frequency range where the discrete frequency components exist, the signal to noise ratio was so poor for the surface microphone as well as the submerged hydrophones that C(0) did not represent helicopter noise power.

An alternative correlation technique suggested by the above problem was to examine the auto-correlation function which has the following form for a discrete frequency embedded in narrow band random noise:

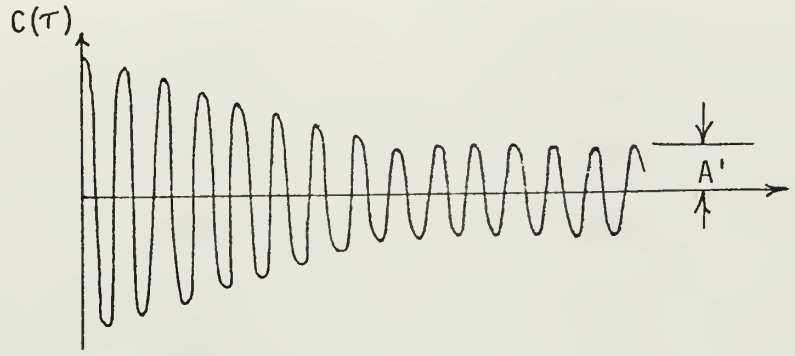

A' in this case is the helicopter noise power in the band. This type function was indeed observed. The problem was the time variation of A' which could be observed on the oscilloscope. No simple means was available for picking off A' and plotting it over a period of time to obtain an average.

Faced with the foregoing problems, a correlation analysis using analog inputs was abandoned. If a correlation analysis had been conducted successfully, the results would have had application limited to only a very narrow range of very low roughness ($R < 0.1$).

C. ANALOG NOISE ANALYSIS

Preliminary analysis of the recorded data indicated that the signal to noise ratio of helicopter noise over ambient noise was in excess of 5 dB for the noise spectrum between 100 Hz and 1000 Hz.

The frequency range 100 Hz to 1000 Hz corresponded to a roughness range of approximately 0.05 to 4.0 for the typical sea surface encountered during the experiment. Hence it appeared that this frequency range was entirely adequate for investigating the effect of a broad range of surface roughness on transmission and for comparison with theory. To obtain a

good distribution of roughness values, the following frequencies were selected for analysis:

105 Hz	464 Hz
150 Hz	500 Hz
200 Hz	597 Hz
256 Hz	700 Hz
300 Hz	802 Hz
345 Hz	900 Hz
387 Hz	950 Hz
425 Hz	975 Hz

Because of the rather steep frequency response of the sonobuoy audio amplifier/signal line combination (approximately 5 dB per octave), a narrow bandwidth of 10 Hz was selected for the analysis.

The analysis utilized a Hewlett Packard Model 3590A Wave Analyzer with a Model 3594A Sweeping Local Oscillator Plug-In. To expedite frequency band center changes, a General Radio Type 1163A frequency synthesizer was used as an external local oscillator for the wave analyzer. The logarithmic output of the wave analyzer was used as the vertical input to a Varian Model F-100 X-Y Recorder. A block diagram of the system is shown in Fig. 5-1.

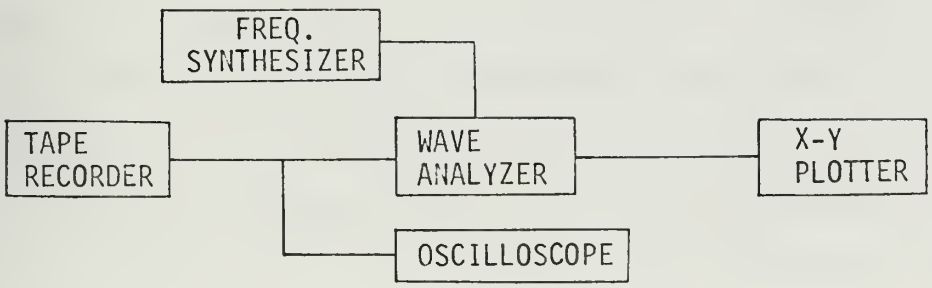

Fig. 5-1
BLOCK DIAGRAM FOR ANALOG ANALYSIS

Equipment settings were as follows:

Tape Recorder
- Tape Speed: 3.75 ips
- Output Cut-off: 1 kc

Wave Analyzer
- Max. Input voltage: 1
- Absolute/Relative Switch: ABSOLUTE
- Meter: LIN DB
- Mode: RESTORED
- Auto/Manual Selector: AUTO
- Bandwidth: 10
- Response Time: SLOW
- Frequency Range: EXT L.O.

Frequency Synthesizer
- Frequency set to 1280 kHz plus desired frequency band center

X-Y Recorder
- Horizontal Range: 50 sec/in
- Vertical Range: 1 v/in

This arrangement was particularly useful for analyzing and displaying the helicopter passes since the resulting plot showed the ambient noise levels before and after each pass as well as the total noise during each pass. A series of plots made for several frequencies using a typical helicopter pass appears in Fig. 5-2. The large time variation in rms level even with the slow response time of the wave analyzer is evident. Considerable smoothing of the presentation would have been possible by playing the tapes back at 37.5 ips and translating the band center frequencies up by a factor of 10. However when this was done, the wave analyzer's response time was too slow for the helicopter passes and the rms output levels were too low.

Signal levels for the helicopter passes were determined by taking an eyeball average of the time variations across the peak of the pass.

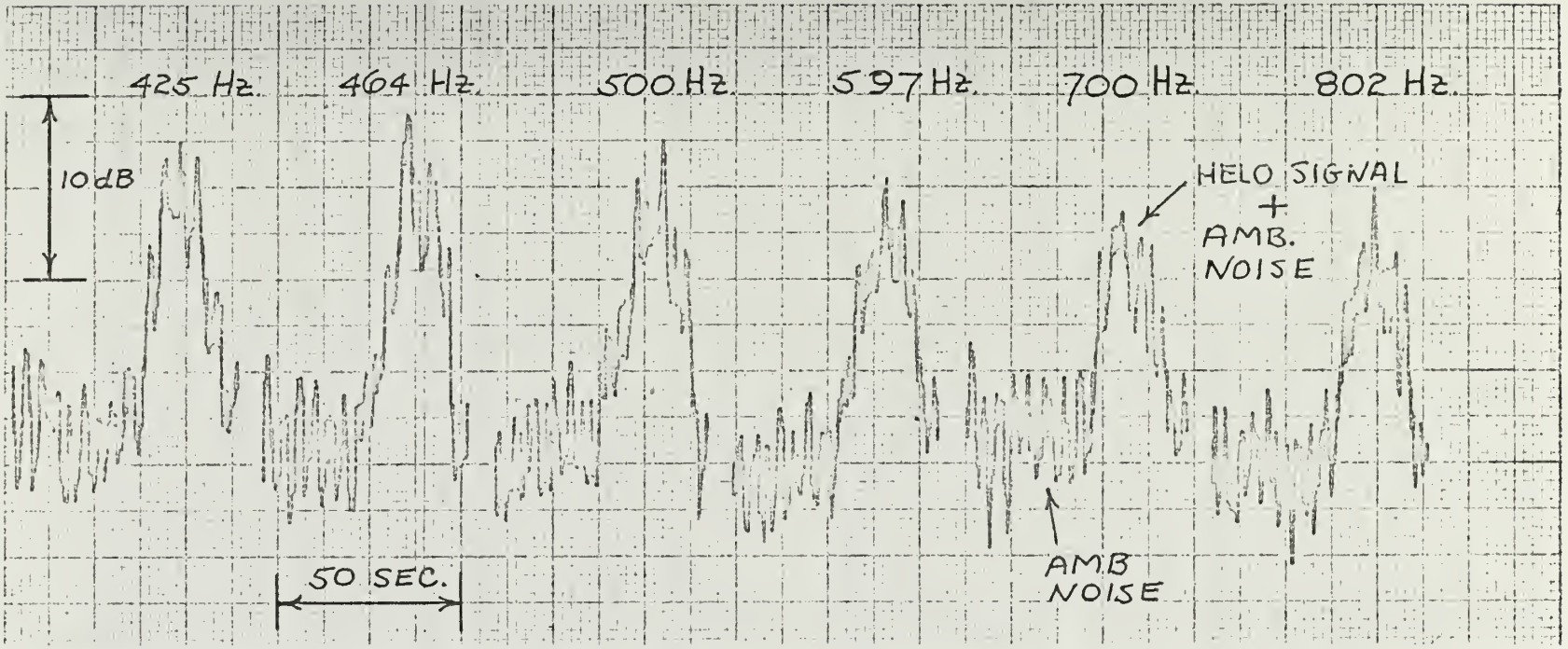

Fig. 5-2

SAMPLE PLOTS OF ONE HELICOPTER PASS RECORDED AT 40 FOOT HYDROPHONE

Note: Frequencies shown are center frequencies of 10 Hz analysis bands.

Ambient noise levels between passes were determined in the same way. Since the plots represented rms levels in dB, this eyeball average of dB levels was something less than the true average rms voltage level. The error here was on the order of 0.5 dB. Since the time variation was about the same for the surface microphone as it was for the submerged hydrophones, this error canceled itself out when computing transmission loss. Sound levels for each frequency for each pass for each hydrophone read as above corresponded to helicopter plus ambient noise voltage levels. To obtain helicopter signal levels, the ambient noise levels were subtracted off using Appendix II of Reference 6.

Signal levels at the hydrophone were than determined using the calibration conversion curves shown in Appendix A for converting analog voltage levels in dB (re 1 volt) to actual acoustic levels in dB (re 1 μbar).

Signal levels for the surface microphone were, assuming the validity of the Kirchhoff assumption, 6 dB higher than actual incident signal level. Transmission loss has been defined as 20 times the logarithm of the ratio of incident pressure to pressure at a point in the underwater field. Accordingly surface microphone signal levels obtained from the plots were reduced by 6 dB before transmission loss from the surface to each hydrophone was computed. It was not surprising, then, to find that transmission loss in dB was usually negative for the hydrophones at depths shallower than 50 feet. It should be pointed out that the fact that pressure doubling occurs at a smooth surface has been obscured in some textbooks by the emphasis on the sound intensity which decreases at the interface.

D. COMPUTER ANALYSIS

A computer analysis of the data was deemed very desirable because of the high frequency resolution available, the capability for correlation using low frequency discrete components, and the great time savings when compared with the analog analysis techniques. This analysis has proceeded in parallel with the analog study, but unfortunately has lagged to the point that no digital information is available at the time of this report.

The sequence of operations involved in the computer analysis is as follows:

1) Multi-channel Analog to Digital Conversion of samples of ambient noise as well as helicopter signal in presence of ambient noise.
2) Interface conversion of digital tapes to format compatible with IBM 360 digital computer.
3) Fast-Fourier Transform of data to obtain power spectral densities of helicopter noise plus ambient noise, and ambient noise.
4) Subtraction of ambient noise power from helicopter noise in presence of ambient noise power to obtain helicopter noise power.
5) Division of surface microphone helicopter noise power by helicopter noise power at each hydrophone to determine transmission loss between the surface and the hydrophone at all frequencies.

The analog to digital conversion was carried out using the COMCOR Ci-5000 Analog Computer and SDS-9300 Digital Computer in the hybrid computer facility operated by the Electrical Engineering Department (Spanagel 500) at NPS. Four data channels were sampled simultaneously at a sampling rate of 2000 samples/sec. To ensure against aliasing, low pass filters with cut-off set at 800 Hz were used at the outputs of the

tape recorder channels. The frequency response of the tape recorder/ filter combination is shown in Fig. 5-3.

Interface conversion of digital tapes involved taking the BCD format tapes which are produced by the SDS-9300 digital computer and rewriting in EBCDIC format for use on the NPS Computer Center's IBM 360/67 digital computer (Ingersoll Hall, NPS). The decision to us the IBM 360 for the Fast Fourier Transform analysis instead of the SDS-9300 was based on the greater memory capacity and tape handling ability of the IBM 360.

The program which was written for Fast Fourier transforming of the four data channels was a direct adaptation of that developed by Wilson, Boston, and Denner of NPS [7]. It involves the determination of Fourier coefficients for contiguous blocks of data. The block length selected was 1.024 sec resulting in frequency resolution of 1/1.024 Hz.

Ambient noise power spectral densities are averaged over all blocks. These averaged densities are then subtracted from the power spectral densities for each block of helicopter noise plus ambient noise. The result is the helicopter noise power spectral density for each block.

The ratio of surface microphone helicopter noise power and hydrophone helicopter noise power is taken for each block and the ratios averaged over all blocks. These averaged ratios are then adjusted using the hydrophone sensitivities, and sonobuoy signal line frequency response to obtain transmission loss for each frequency.

The foregoing described the programming involved in the continuing computer analysis. At the time of this writing, first analyses appear to be consistent with the analog analysis and analog to digital conversion of additional data is in progress.

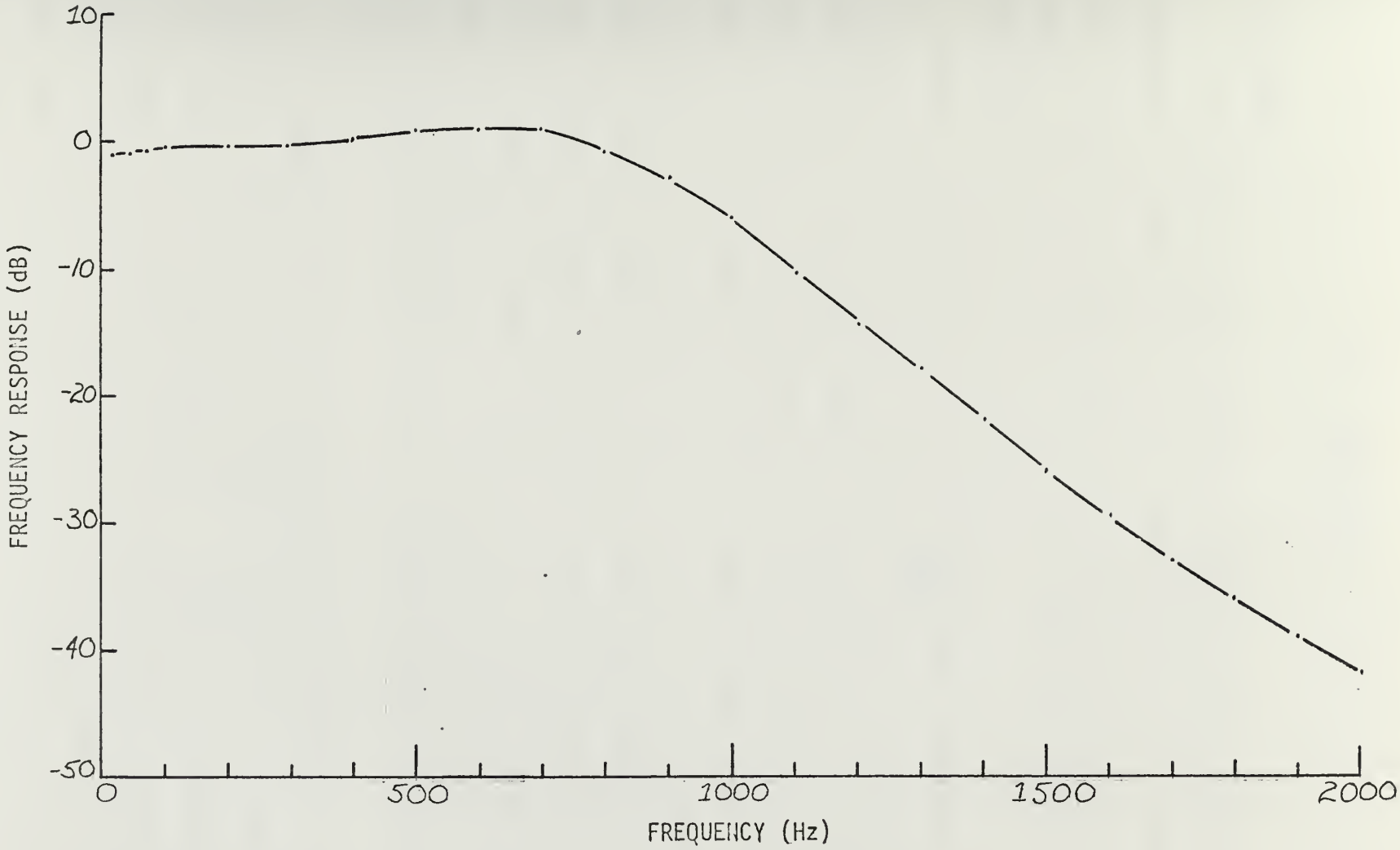

Fig. 5-3

TAPE RECORDER/LOW PASS FILTER FREQUENCY RESPONSE

VI. DISCUSSION

A. GENERAL

Although there was ample information recorded on the experiment tapes to determine transmission loss for off-normal points in the underwater sound field, it was decided that, due to time considerations, only transmission loss to points directly beneath the sound source would be determined for inclusion in this thesis.

Using 10 Hz bandwidth samples of helicopter noise centered at the frequencies listed in Chapter V, Section C, frequency spectra were determined for the incident signal at the surface as well as for the signal recorded at each underwater hydrophone for Experiments 11, 16, and 17. For broad band noise the 10 Hz bandwidth noise samples were converted to pressure spectrum levels in dB (re 1 μbar) by subtracting 10 dB. Using the results of the limiting experiment (Appendix G), a small correction factor was applied to compensate for occasional limiting of the sonobuoy audio amplifier which occurred during the experiments. The incident signal spectrum was obtained by subtracting 6 dB from levels recorded by the surface microphone, i.e., the Kirchhoff approximation was invoked.

The underwater data selected for analysis were provided by the three hydrophones of Cluster I. The helicopter either hovered or made passes over Cluster I in all three experiments. Since the surface microphone was adjacent to Cluster II, it was not directly beneath the helicopter for these experiments. However, study of surface microphone levels during Experiment 20 showed that this additional propagation range did not result in any measurable decrease in signal level at any frequency.

Helicopter noise spectra (relative to an arbitrary level in dB) appear in Appendix E. A smooth curve has been faired through the data points which exhibited some scatter largely due to error in "eyeballing" the mean noise levels from the plots. The absolute helicopter noise spectra are on file with Dr. H. Medwin, Physics Department, Naval Postgraduate School.

Transmission loss for a point in the underwater sound field has been defined as follows:

$$TL = 20 \log \frac{p_{1Z}}{p_{2t}}$$

Where p_{1Z} = incident rms pressure amplitude at the surface below the source

p_{2t} = transmitted rms pressure amplitude at a point in the underwater sound field

As discussed in Chapters I and II, TL is the sum of two losses: TL_S which is transmission loss due to spreading attenuation and impedance mismatch at the interface, and TL_R which is transmission loss due to the rough surface effect. The dominant contribution to transmitted intensity at a point in the underwater sound field at low roughness, $R < 1$, is from the coherent component of transmitted pressure. For this region of roughness, theory predicts $TL_R = 20 \log e^R$. At higher roughness, the incoherent component of transmitted pressure is expected to dominate. From preliminary theoretical work done by Medwin at NPS, it is expected that TL_R will be a decreasing function of frequency for $1 < R < 4$, increasing again for $R \geq 4$.

B. RESULTS AND CONCLUSIONS

Transmission loss for the Cluster I hydrophone positions for Experiments 11, 16 and 17 (See Figs. 6-2, 6-3, 6-4) was obtained for each analysis frequency by taking the difference between the incident pressure spectrum and the transmitted underwater pressure spectrum. Transmission loss in dB is plotted against R on linear paper. Theory predicts that for $R < 1$ this plot will be a straight line of slope $R\ (10 \log_{10} e)$. A line having this slope is shown for comparison on the plots.

The transmission loss plots show that as roughness increases there is an increase in transmission loss for $R < 1$ and a general decrease in transmission loss for $1 < R < 4$. These results are entirely consistent with predictions from existing rough surface theory. The slopes for that portion of the plots corresponding to $R < 1$ show a roughness dependency varying from $e^{0.26R}$ to $e^{2.0R}$ with a mean dependency for all plots of $e^{1.15R}$. The maximum transmission loss point which for most plots occurs at $R \approx 1$ is consistent with theory and shows the value of roughness for which the incoherent contribution of transmitted intensity begins to dominate in its contribution to mean square transmitted pressure. It may be noted in several plots that at roughness approaching 4.0 there appears to be a leveling off and in some cases an increase of transmission loss (downswing on the plots). This may be accounted for by reference to the scattering function S(g) evaluated by Medwin [2] which appears as S(R) in the plane wave transmission theory of Hagy [1]. This function displays a rapidly changing slope in the region $2 < R < 4$. It is likely that S(R) will appear in the incoherent term of the expression for mean square pressure when the theory is developed for a point source.

C. VALIDITY OF COMPARISON OF EXPERIMENTAL RESULTS WITH THEORY

There is considerable apparently random variation in the slopes of the plots as well as the value of roughness corresponding to maximum transmission loss. This is not surprising for two reasons: 1) Rotor induced turbulence under the helicopter caused the sound field at the air-water interface to vary with time and position, i.e. the field was non-stationary and inhomogeneous; 2) the interface itself was a statistically rough surface. It should be expected, then, that the transmission loss obtained for one pass of approximately ten seconds duration would differ from that of another similar pass. Also to be considered is the error generated by "eyeballing" the plots of time-varying rms band levels as well as the inherent difficulty in taking the difference between two plots particularly in regions where the slopes are steep. The importance of the data, however, is that the trends in transmission loss as a function of roughness predicted by theory are unmistakably confirmed.

In the processing of data, the Kirchhoff assumption was invoked when 6 dB was subtracted from surface microphone spectrum levels to obtain incidence spectrum levels. The criterion for application of the Kirchhoff assumption in terms of the surface correlation length, L, is that L must be greater than the acoustic wavelength, λ. In Appendix E, the roughness corresponding to $L/\lambda_2 = 1$ (where λ_2 is the wave length in water) was calculated. The result suggests that the Kirchhoff approximation was violated for most of the experimental data. However it must be kept in mind that the use of λ_2 instead of λ_1 here may not be appropriate. Furthermore the correlation length, L, utilized here is based on the decay of a Gaussian form correlation function and is thus smaller than that which would be obtained using the decay of the real correlation function

envelope. L based on the latter is quite possibly more valid. Hence the test in Appendix E represents the "worst case" and may be far too stringent. It does however certainly suggest that pressure may not have doubled at the interface and that incident pressure level may have been greater than that obtained by subtracting 6 dB from the measured pressure level at the surface. This may partially account for the discrepancy at very low roughness between observed transmission loss and that predicted by the smooth surface point source theory of Section II.

The smooth surface theory of Section II assumed a point source and, accordingly, spherical spreading in air. The difference between surface microphone noise levels for Experiment 16 (helo altitude 300 feet) and Experiment 17 (helo altitude 600 feet) was taken for several analysis frequencies. The results compiled below are far from the simple 6 dB difference that might have been expected and suggest that the effective "point source" of the sound was at some height above the helicopter.

Band Center Frequency (Hz)					
150	200	300	500	700	900
1.3	0	1.4	1.0	2.3	3.1

Fig. 6-1
DB DIFFERENCE IN SURFACE SPL FOR SOURCE AT 300 FT. COMPARED WITH 600 FT.

This implies that in order to use the derived expression for TL_s, a virtual altitude H' corresponding to observed spreading must be used in place of H. Since $H' > H$, predicted smooth surface transmission loss would be decreased. This may also partially account for the discrepancy at very low roughness between observed transmission loss and that predicted by smooth surface point source theory.

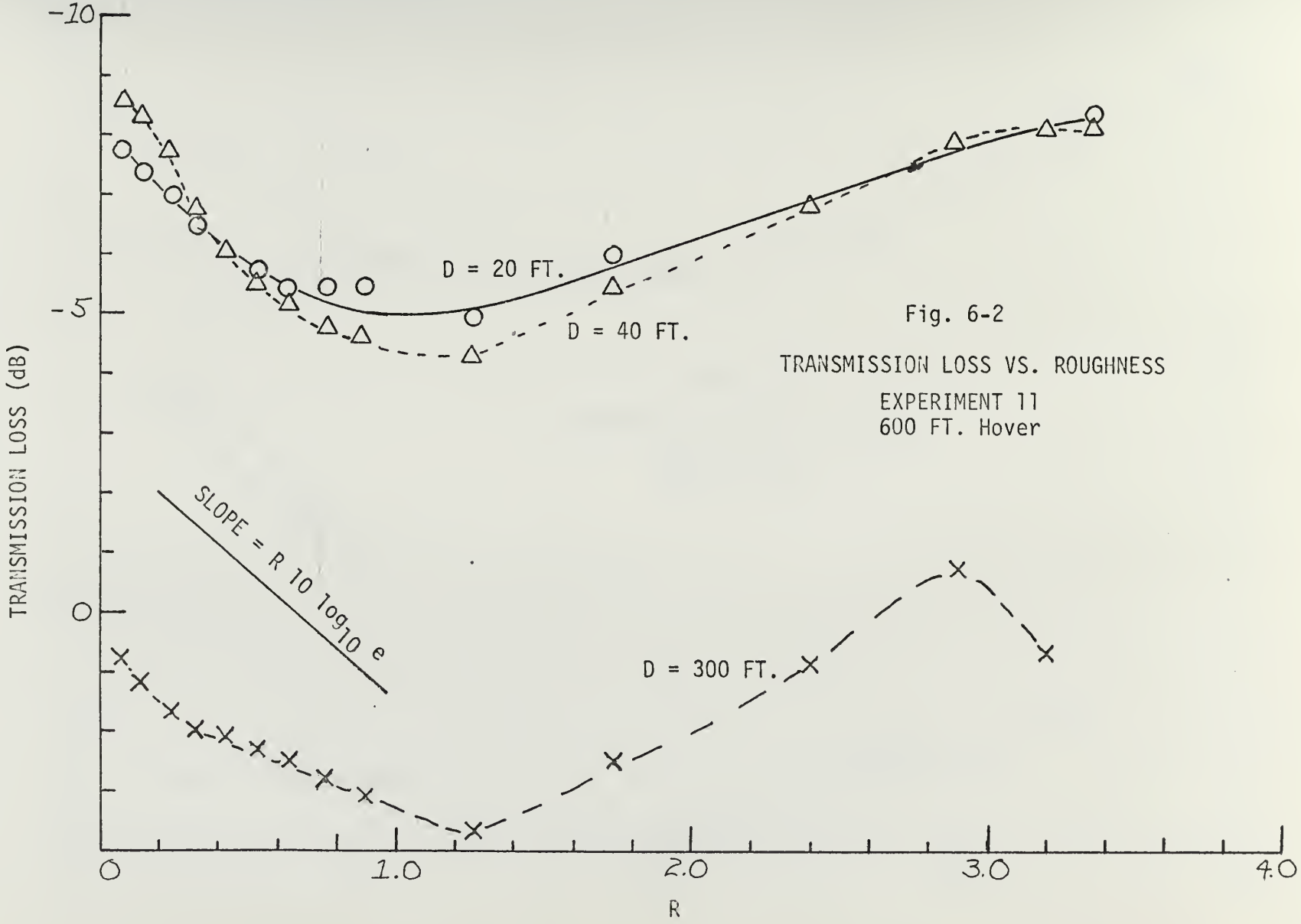

Fig. 6-2

TRANSMISSION LOSS VS. ROUGHNESS

EXPERIMENT 11
600 FT. Hover

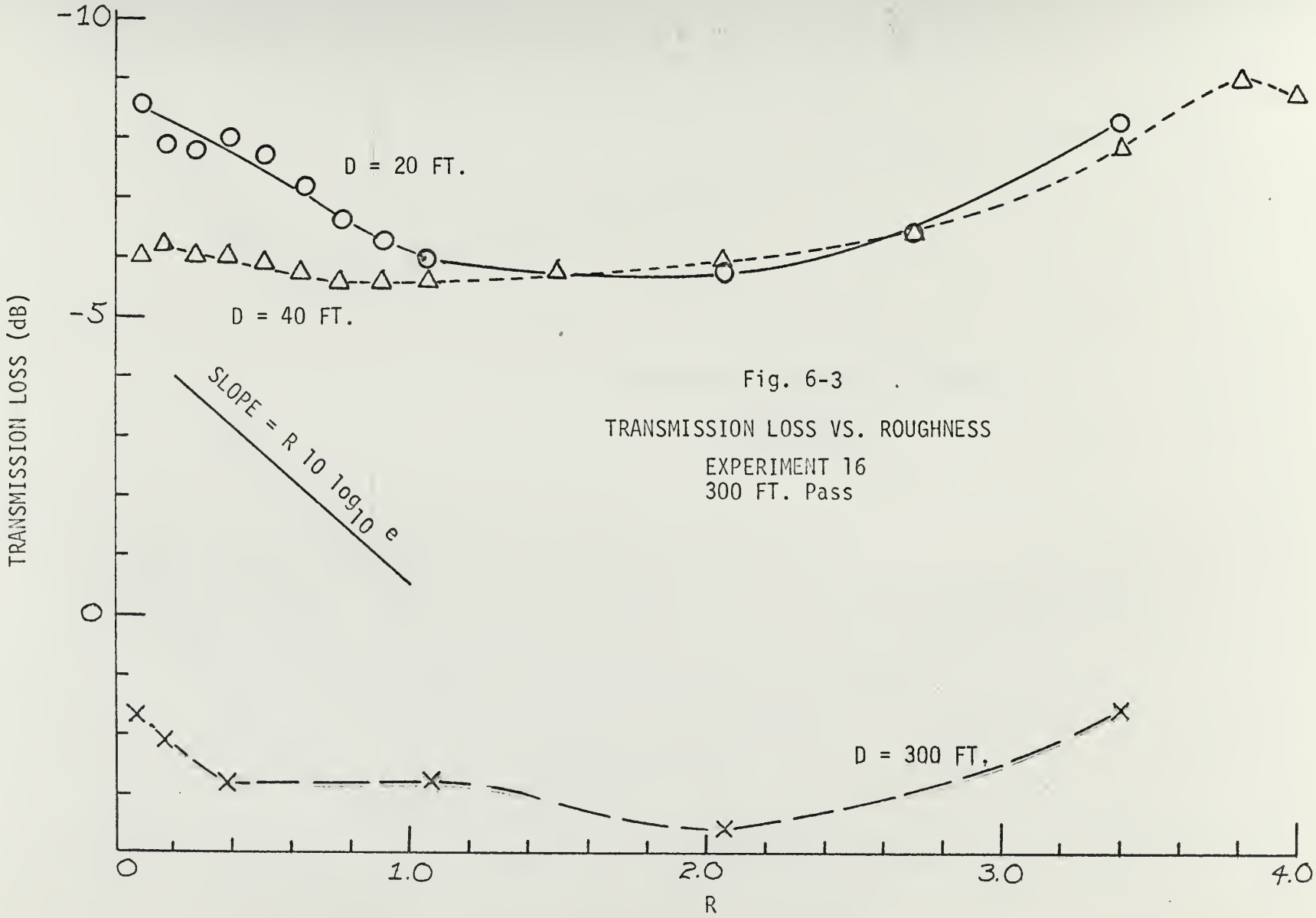

Fig. 6-3

TRANSMISSION LOSS VS. ROUGHNESS

EXPERIMENT 16
300 FT. Pass

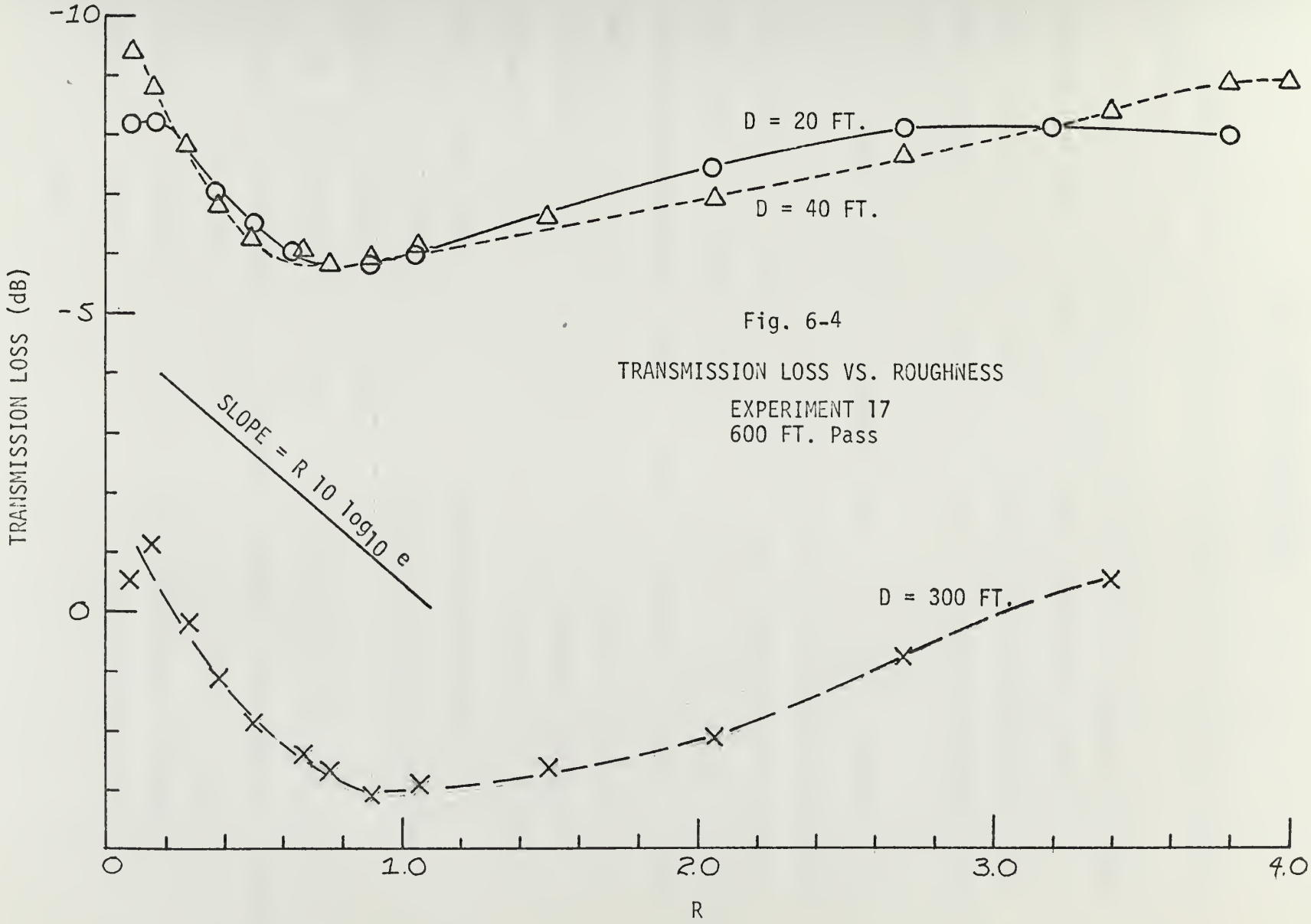

Fig. 6-4

TRANSMISSION LOSS VS. ROUGHNESS

EXPERIMENT 17
600 FT. Pass

VII. RECOMMENDATIONS

Recommendations for continued work in this area for accomplishment at NPS are as follows:

1) Analysis of surface microphone noise for all sections of FLIPEX II tape for which distance from the surface microphone to helicopter is known. Such data could be used to determine the radiation pattern of the helicopter in air in particular so as to establish a virtual altitude H' for use in the TL_s expression derived in Section II.

2) Continuation of the computer analysis described in Section D of Section V. In addition to providing accurate high frequency resolution transmission loss values for all points in the underwater field using the technique outlined in Section V, the computer should also be utilized for cross-correlation of the low frequency components of surface microphone and hydrophone noise. The low signal to noise ratio which exists at frequencies below 100 Hz suggests that this technique coupled with autocorrelation of the surface microphone noise may be the only method for getting at transmission loss for frequencies below 100 Hz.

3) Continued analog analysis of other data using the technique described in Section C of Section V.

4) Experimentation utilizing a laboratory model similar to that used by Hagy [1], but employing a point source having a good frequency response over the range 1 kHz to 100 kHz. With such a model, the validity of the Kirchhoff approximation could be thoroughly investigated, the smooth surface theory developed in Section II verified, and transmission loss due to surface roughness accurately determined.

5) Development of a rough surface theory adequate for predicting transmission loss associated with transmission from a point source in air.

6) Development of a rough surface theory that will predict transmission loss for the case $L < \lambda$.

APPENDIX A CALIBRATION

1. GENERAL

In order to accurately determine transmission loss at the air sea interface as well as to determine absolute intensity levels at points in the underwater sound field of the helicopter, calibration of the sonobuoys, signal lines, tape recorder and analysis equipment was required. In this section, calibration procedures for system components utilized during the experiments will be presented. Calibration of analysis equipment will be discussed in the section on data analysis.

2. HYDROPHONE CALIBRATION

For each of the AN/SSQ-57 sonobuoys used in the experiments, hydrophone/preamplifier sensitivity and frequency response of the hydrophone/preamplifier/audio amplifier combination were obtained from NADC, Johnsville. As mentioned in the section on experimental equipment, those hydrophones in sonobuoys designated for measurements at depths greater than 95 feet had to be replaced by AN/SSQ-41 hydrophones for which hydrophone/preamplifier sensitivities were not available. This meant that a procedure for obtaining hydrophone/preamplifier sensitivity was required. An Underwater Sound Reference Laboratory G-19 Calibrator was utilized for this calibration. This device employs an open ended vertical cylindrical water column with an electrmagnetic driver mounted in the base. A comparison technique was used in which an AN/SSQ-57 calibrated sonobuoy hydrophone of known sensitivity was located in the calibrator alongside and at the same depth as the hydrophone to be calibrated. SPL at hydrophone depth was determined using the reference hydrophone by means of the following expression.

$$SPL = VL - G - SL$$

where VL = Voltage level at the output of the audio amplifier in dB

G = Gain of the audio amplifier in dB

SL = Sensitivity of the hydrophone in dB (re 1 volt/μbar)

Then the sensitivity of the unknown hydrophone was determined using the above expression where SPL was known, VL of the sonobuoy with the unknown hydrophone was observed and gain was known. Since the sensitivity of the hydrophone was known to be flat for the frequency range of interest, 30-1000 Hz, the calibration procedure was carried out at one frequency only within this range (specifically 440 Hz).

The block diagram in Fig. A-1 shows the equipment arrangement for this calibration procedure.

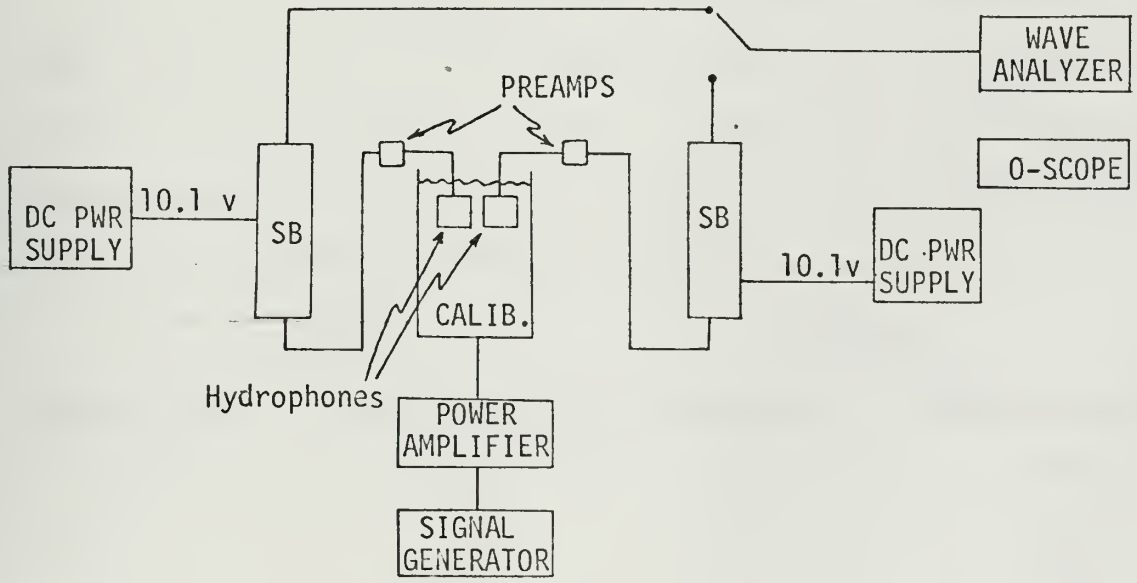

Fig. A-1

BLOCK DIAGRAM FOR HYDROPHONE CALIBRATION

The use of a DC power supply in lieu of the salt water actuated battery contained within the sonobuoy was made possible by means of a 2 conductor cable fitted with a 9 pin connector which was inserted in the test plug at the top of the sonobuoy. The power supply was connected in this way to pins 3 and 1 of the test plug. Pins 8 and 9 were shorted together in the connector in order to maintain electrical contact between the hydrophone/preamplifier line and the input to the audio amplifier.

The Gain of each buoy at 440 Hz was determined by injecting a sinusoidal signal into the input of the audio amplifier and measuring the output. To facilitate this, a second 4 conductor cable fitted with a 9 pin connector was inserted in the test plug at the top of the sonobuoy. Two of the conductors provided DC power (pins 3 and 1); the other two provided the AC input signal. By inserting the input signal across pins 9 and 1 the signal was introduced at the input of the audio amplifier.

As a check on the system, several hydrophones of known sensitivity level were calibrated. In all cases the sensitivity obtained was within 0.5 dB of the value provided by NADC. A compilation of hydrophone sensitivity levels in dB (re 1 volt/μbar) either provided by NADC or obtained by the above procedure is shown in Fig. A-2.

FLIPEX I		FLIPEX II	
Sonobuoy Ser.	Sensitivity Level	Sonobuoy Ser.	Sensitivity Level
6	-71.0	16	-73.0
5	-72.0	7	-71.5
2	-82.9	10	-67.1
14	-71.5	14	-71.5
12	-72.0	31	-73.0
30	-84.1	6	-68.0

Fig. A-2
COMPILATION OF HYDROPHONE SENSITIVITY LEVELS

3. AUDIO AMPLIFIER FREQUENCY RESPONSE

Frequency response data for the hydrophone/preamplifier/audio amplifier combination in each sonobuoy were provided by NADC. It was given in dB relative to the gain at a reference frequency of 440 Hz. The 4 conductor test cable described in the last paragraph was used with the 9 pin sonobuoy test plug to verify this data by inserting a signal tone at the input of the audio amplifier and reading the output. The block diagram in Fig. A-3 shows the equipment arrangement for carrying out this procedure.

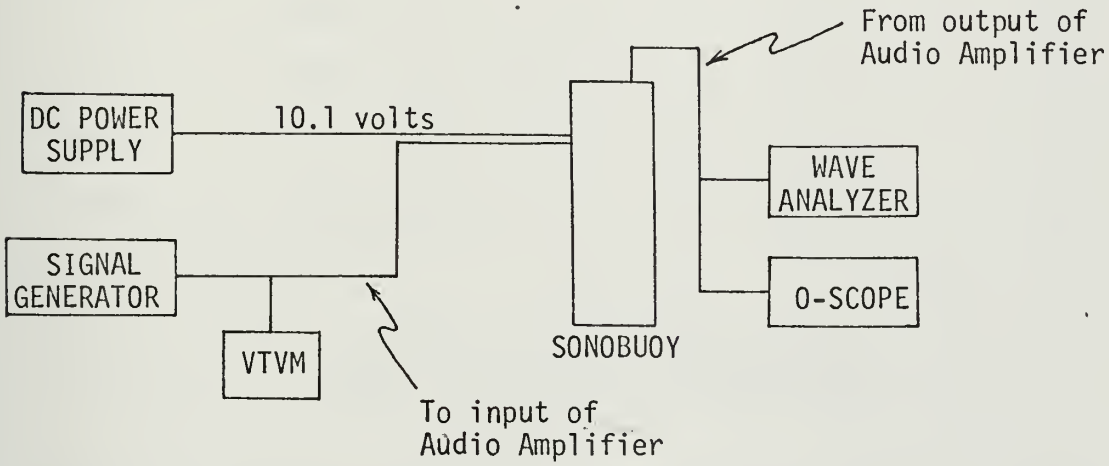

Fig. A-3
BLOCK DIAGRAM FOR VERIFYING FREQUENCY
RESPONSE OF SONOBUOY AUDIO AMPLIFIERS

A wave analyzer with a bandwidth of 10 Hz was utilized because of the poor signal to noise ratio of the sonobuoy output at low frequencies (below 100 Hz).

A compilation of audio amplifier frequency response data referenced to the gain in dB at 440 Hz is provided below for each sonobuoy used in FLIPEX I and FLIPEX II.

Sonobuoy Ser.	Frequency (Hz) 30	50	100	200	300	440	500	1K
2	-17.8	-14.6	-10.0	-5.7	-3.0	0	0.9	6.3
5	-17.5	-14.5	-9.6	-5.4	-2.6	0	1.0	5.9
6	-18.7	-15.5	-10.4	-5.8	-3.0	0	0.8	6.0
7	-17.1	-14.1	-9.3	-5.4	-2.7	0	0.9	5.7
10	-18.2	-15.0	-10.0	-6.0	-3.0	0	1.0	6.7
12	-17.3	-14.0	-9.7	-5.2	-2.7	0	1.0	5.9
14	-17.5	-14.4	-9.5	-5.5	-3.0	0	0.8	6.1
16	-19.0	-15.5	-10.4	-6.0	-3.0	0	1.0	6.4
30	-17.5	-14.3	-9.6	-5.6	-2.8	0	1.0	6.6
31	-16.2	-13.4	-8.9	-5.4	-3.6	0	-0.1	5.7

Fig. A-4
COMPILATION OF SONOBUOY AUDIO
AMPLIFIER FREQUENCY RESPONSE DATA

Agreement of the above data with that provided by NADC was within ±1.0 dB. Note that in the equipment arrangement for obtaining these results, the output of the sonobuoy was loaded with essentially an infinite impedance. During the experiments at sea, loading was approximately 1800 ohms. However variation in electrical load on the sonobuoy was observed not to vary the relative frequency response even though absolute gains were of course effected. Hence the above results were considered valid.

4. LINE FREQUENCY RESPONSE

Since the two transformers used at either end of each line had a non-flat frequency response, it was essential to obtain frequency response data for each line. The gain of each line was obtained for the same

frequencies used in obtaining audio amplifier response. The equipment arrangement simply involved a signal generator providing a signal at the sonobuoy end of the line with two VTVM's reading voltage levels at either end. A compilation of line frequency response data referred to the gain in dB at 440 Hz is provided in Fig. A-5 below.

	Frequency (Hz)							
	30	50	100	200	300	440	500	1K
CLUSTER I								
Line 1	-1.6	-0.8	-0.3	-0.1	0	0	0	0.1
Line 2	-1.5	-0.8	-0.3	-0.1	0	0	0	0.1
Line 3	-1.5	-0.9	-0.3	-0.1	0	0	0	0.1
CLUSTER II								
Line 1	-1.8	-0.9	-0.3	0	0	0	0.1	0.2
Line 2	-1.5	-0.8	-0.2	0	0	0	0.1	0.2
Line 3	-1.6	-0.9	-0.3	-0.1	-0.1	0	0	0.1

Fig. A-5
COMPILATION OF SIGNAL LINE
FREQUENCY RESPONSE DATA

5. TAPE RECORDER CALIBRATION

As mentioned in the section on system design and construction, a 100 K resistor was placed in series with the tape recorder input so that changes in the input impedance of the tape recorder (which result when adjusting tape recorder input gain) would not appreciably change the loading of the sonobuoy and signal line. The arrangement was as shown in Fig. A-6. Calibration of the Precision Instrument Tape Recorder Model PI-6200 used in the experiment involved the setting of the input gain adjustment such that an input signal of some level would be recorded on tape as 1.0 volt

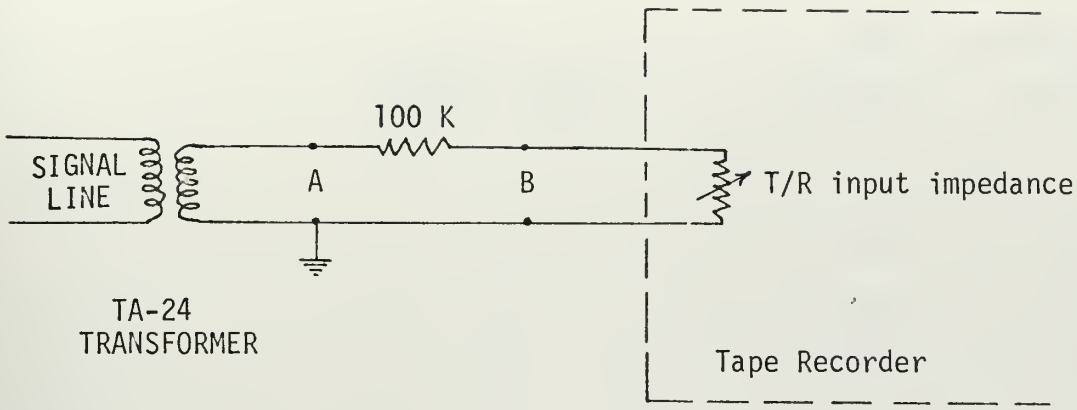

. Fig. A-6
SCHEMATIC OF TAPE RECORDER INPUT CIRCUITRY

which is the distortion free limit of the tape recorder. The input signal usually selected for this calibration, 15 dB (re 0.775 volt), was larger than the largest signal levels anticipated during the experiment. Because of the voltage dividing action of the 100 K resistor and the tape recorder input impedance, an adjustment of the input gain changed the voltage attenuation from point A to point B. It was necessary that this attenuation be measured. To permit this, BNC connectors were installed at points A and B in an input patch panel. Once each channel of the tape recorder was calibrated to its 15 dB input level, the voltage levels in dB at points A and B were read and the attenuation determined. A compilation of input attenuations recorded for both FLIPEX I and II is shown in Fig. A-7.

6. SYSTEM GAIN

It was essential that the gain for the entire system (i.e., sonobuoy audio amplifier and line) be obtained just before the experiment with the sonobuoys and lines matched up and the lines properly loaded with the tape recorder. This was done using a 440 Hz tone introduced at the input

	Tape Recorder Channel Number	INPUT ATTENUATION FLIPEX I	FLIPEX II
CLUSTER I			
Line 1	1	10.5	10.3
Line 2	3	10.5	10.2
Line 3	5	10.9	10.4
CLUSTER II			
Line 1	2	10.6	10.8
Line 2	4	11.0	10.6
Line 3	6	10.7	10.3

Fig. A-7
COMPILATION OF TAPE RECORDER INPUT ATTENUATIONS

of the audio amplifier using the test plug. (A 10.1 volt external DC voltage was also applied to the test plug as discussed earlier.) The output of the line (point A in the schematic of Fig. A-6) was recorded. Tape recorder calibration was accomplished before these readings so that line loading would be correct. A compilation of system gains (relative to an arbitrary level in dB) obtained in this way is shown in Fig. A-8. Note that the assignment of sonobuoys by serial number to specific lines may be determined in this compilation. The absolute system gains are on file with Dr. H. Medwin, Physics Department, Naval Postgraduate School.

7. SYSTEM CALIBRATION CURVES

It was desired that a plot be obtained which would enable the experimenter to convert voltage level in dB on the data tapes to sound pressure

	FLIPEX I		FLIPEX II	
	Sonobuoy Ser. No.	System Gain	Sonobuoy Ser. No.	System Gain
CLUSTER I				
Line 1	6	10.2	16	12.0
Line 2	5	10.8	7	12.4
Line 3	2	10.3	10	14.4
CLUSTER II				
Line 1	14	10.3	14	11.6
Line 2	12	7.5	31	13.1
Line 3	30	11.6	6	10.6

Fig. A-8
COMPILATION OF SONOBUOY/LINE SYSTEM GAINS

level at the sonobuoy hydrophone. All data presented in the first six sections of this appendix were used to obtain such plots.

The following sample calculation for sonobuoy #16 used during FLIPEX II shows how these plots were obtained.

a) Sonobuoy #16 was connected to Cluster I, line 1, which provided input to tape recorder channel 1.

b) For channel 1 of the T/R, 15 dB (re 0.775 v) input corresponded to 1.05 volt or 0.1 dB (re 1.0 v) on tape. Hence 14.9 dB (re 0.775 v) corresponded to 0 dB (re 1 v) on tape.

c) Input attenuation = 10.3 dB. Hence an output level of 14.9 + 10.3 dB = 25.2 dB (re 0.775 v) from the signal line corresponded to 0 dB on tape.

d) Now, for 440 Hz, this level of 25.2 dB out of the signal line is converted to SPL (relative to an arbitrary level in dB) at the hydrophone:

$$SPL = VL - (SL + G) - 2.2$$

$$= 25.2 - (-73.0 + 12.0) - 2.2$$

$$= 84.0 \text{ dB (re 1 } \mu\text{bar)}$$

where G is the relative system gain measured just prior to the experiment.

So 0 dB VL (re 1.0 volt) at 440 Hz may be converted to 84.0 dB (re 1 μbar) SPL.

e) What remains to be done is to determine this conversion for other frequencies in the range of interest. This was done by combining the frequency responses of the sonobuoy audio amplifier and the appropriate line with the gain at 440 Hz as a reference. This relative system response was then applied to the 440 Hz conversion factor obtained above to determine the conversion factors for any frequency. The table below summarizes this calculation:

	Frequency (Hz)							
	30	50	100	200	300	440	500	1K
Line resp.	-1.6	-0.8	-0.3	-0.1	0	0	0	0.1
Audio amp. resp.	-19.0	-15.5	-10.4	-6.0	-3.0	0	1.0	6.4
System response	-20.6	-16.3	-10.7	-6.1	-3.0	0	1.0	6.5
Conversion factor	104.6	100.3	94.7	90.1	87.0	84.0	83.0	77.5

The conversion factor is the relative SPL in dB (re 1 μbar) corresponding to 1.0 volt on tape. For each sonobuoy these conversion factors were plotted for both FLIPEX I and II. These plots are shown in Figs. A-9 through A-20.

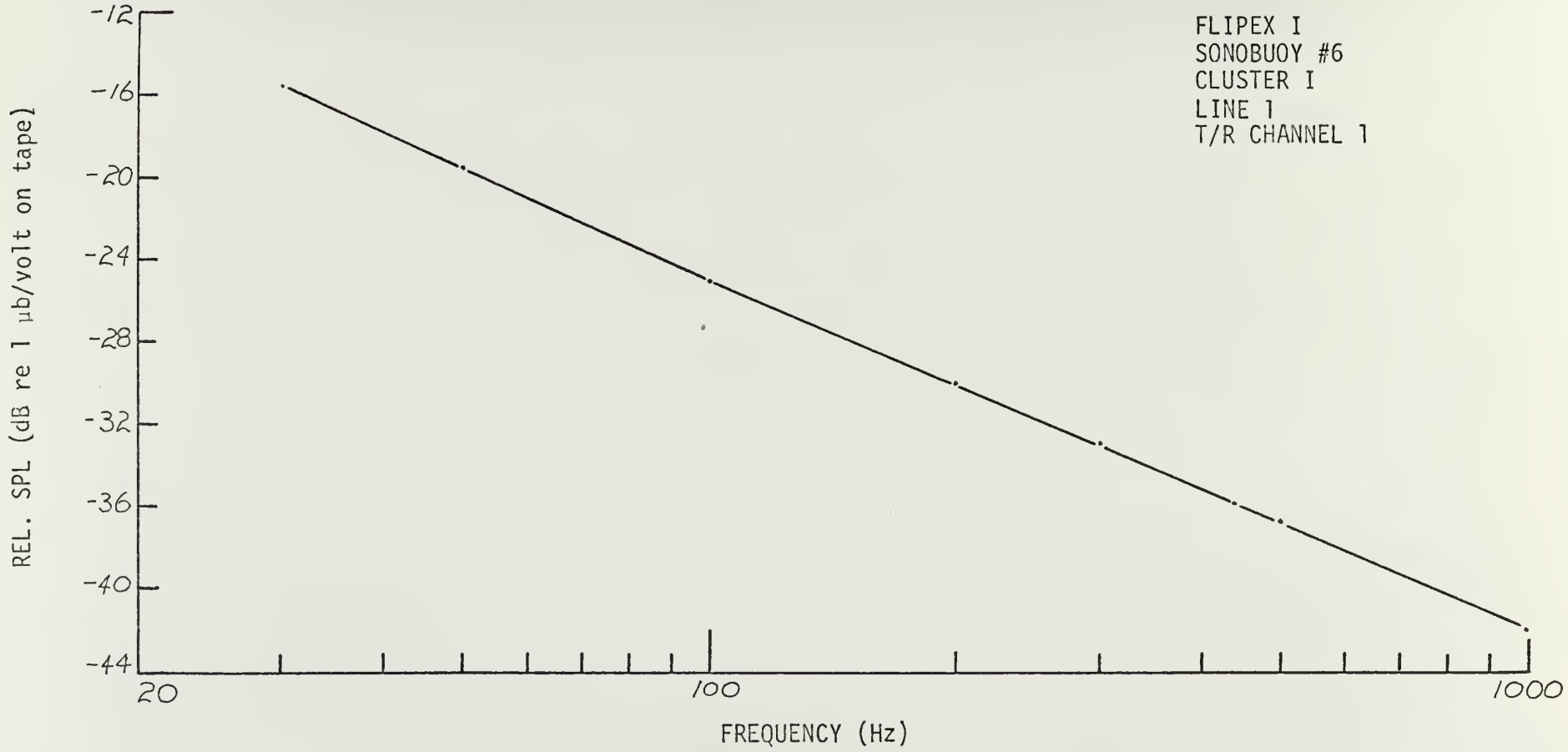

Fig. A-9

CALIBRATION CONVERSION CURVE FOR SONOBUOY #6, FLIPEX I

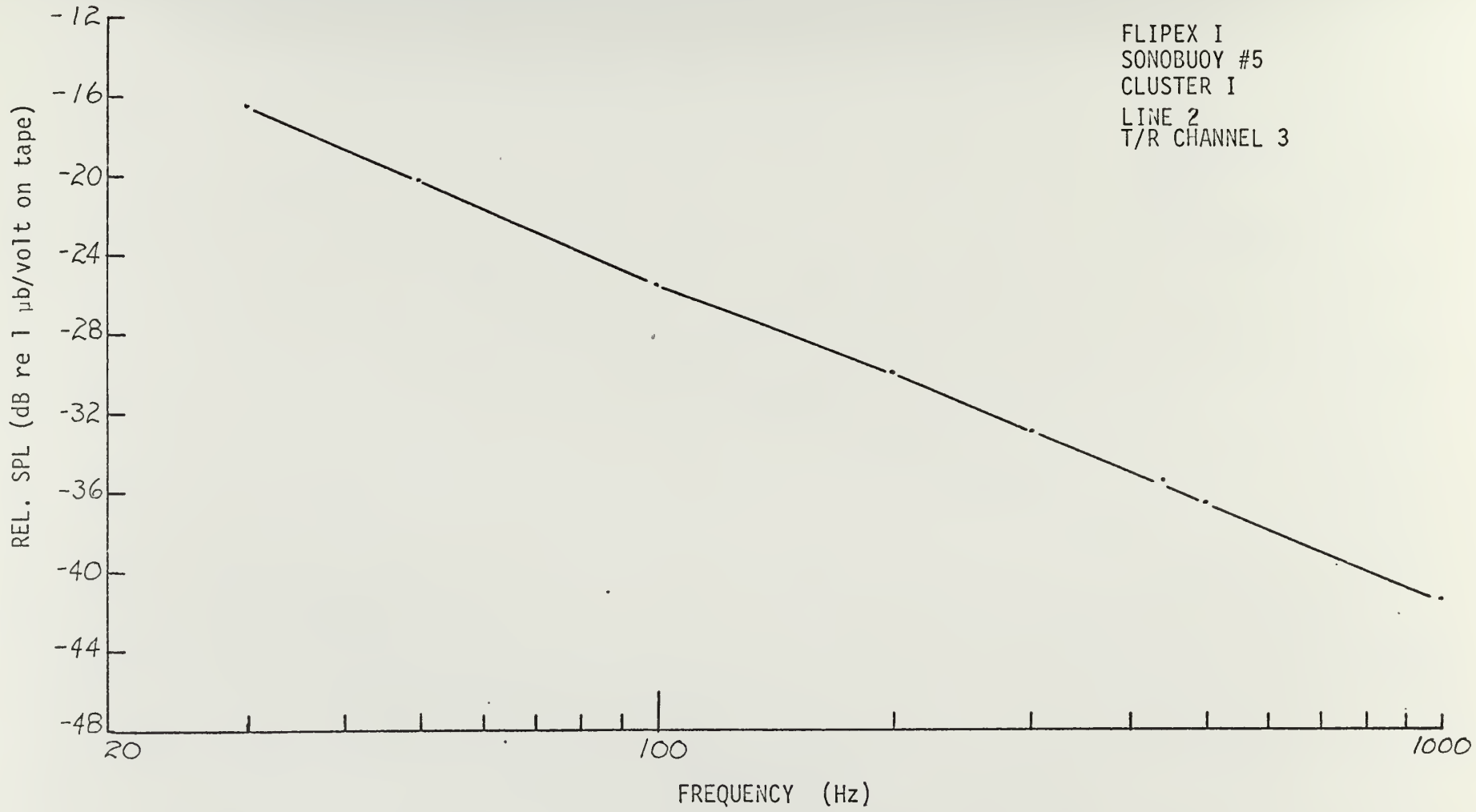

Fig. A-10

CALIBRATION CONVERSION CURVE FOR SONOBUOY #5, FLIPEX I

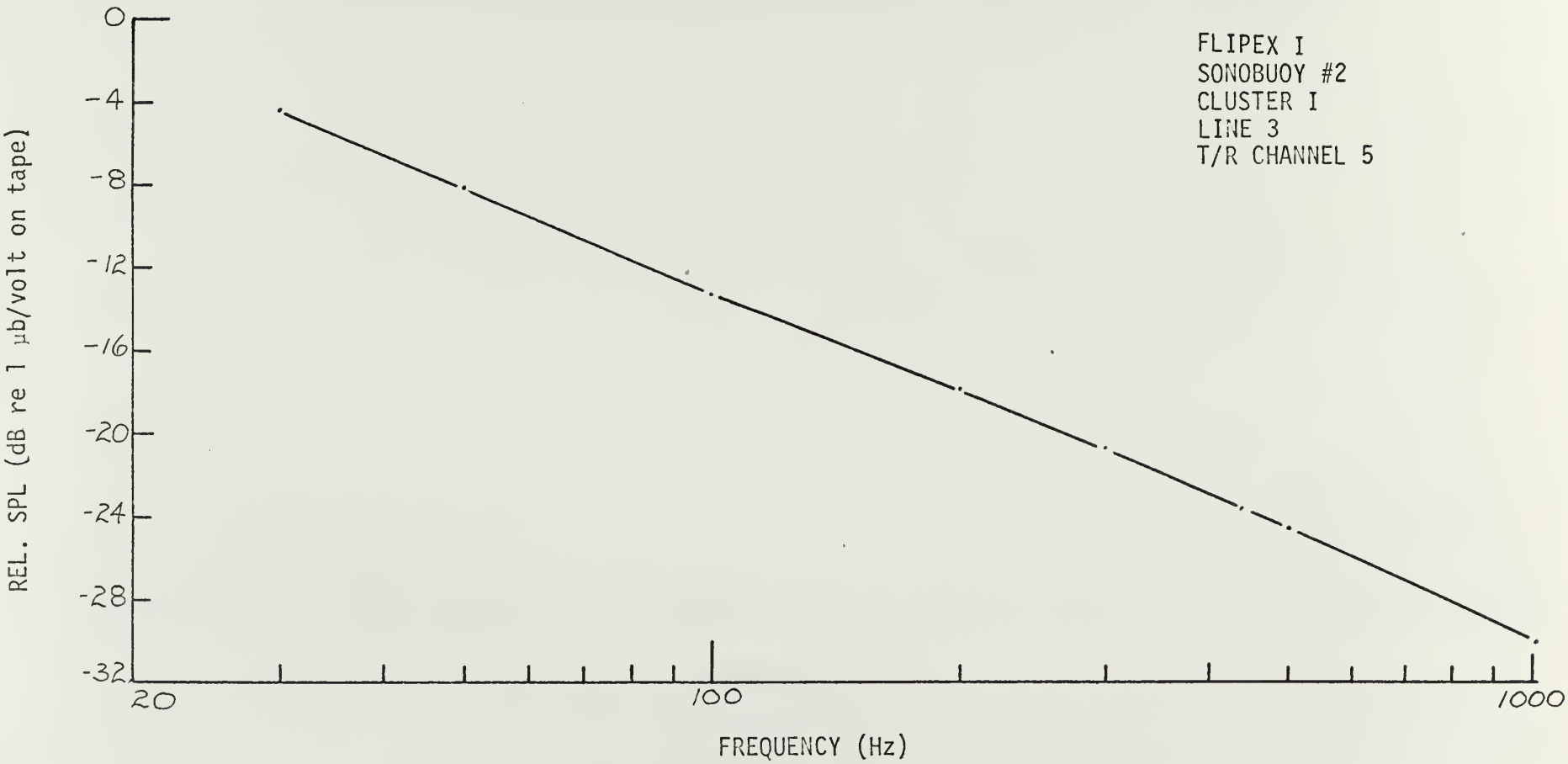

Fig. A-11

CALIBRATION CONVERSION CURVE FOR SONOBUOY #2, FLIPEX I

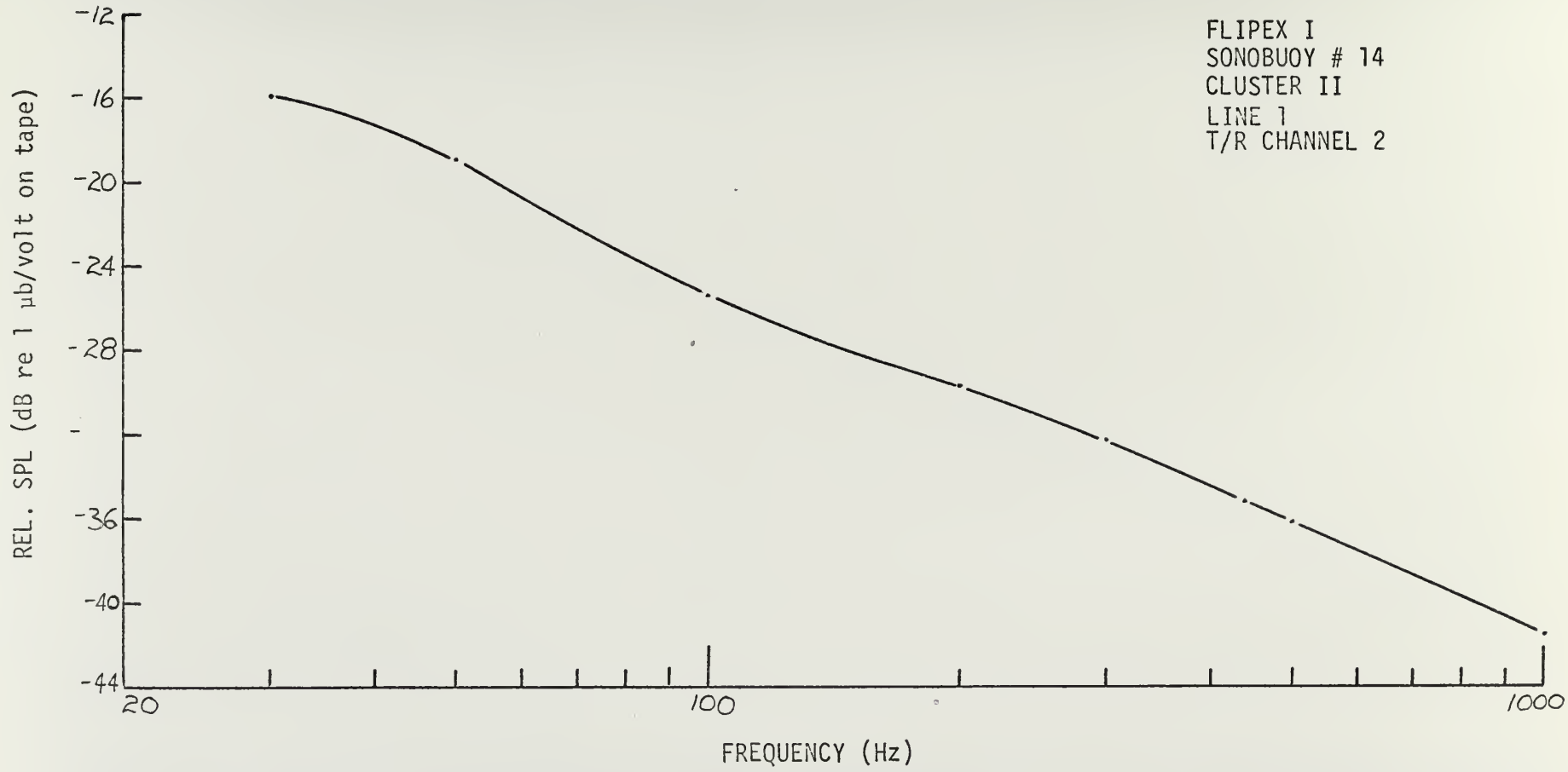

Fig. A-12

CALIBRATION CONVERSION CURVE FOR SONOBUOY # 14, FLIPEX I

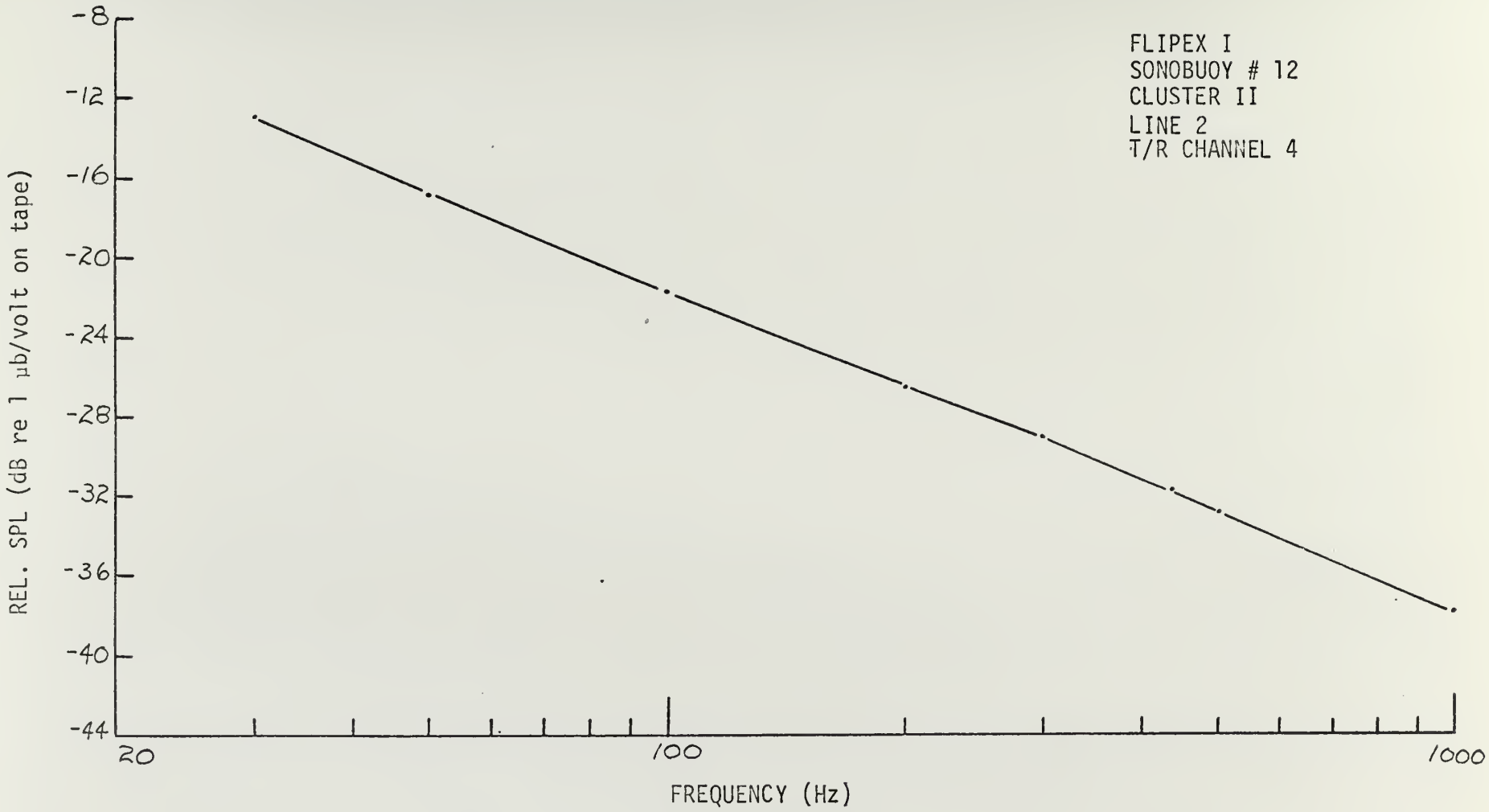

Fig. A-13

CALIBRATION CONVERSION CURVE FOR SONOBUOY #12, FLIPEX I

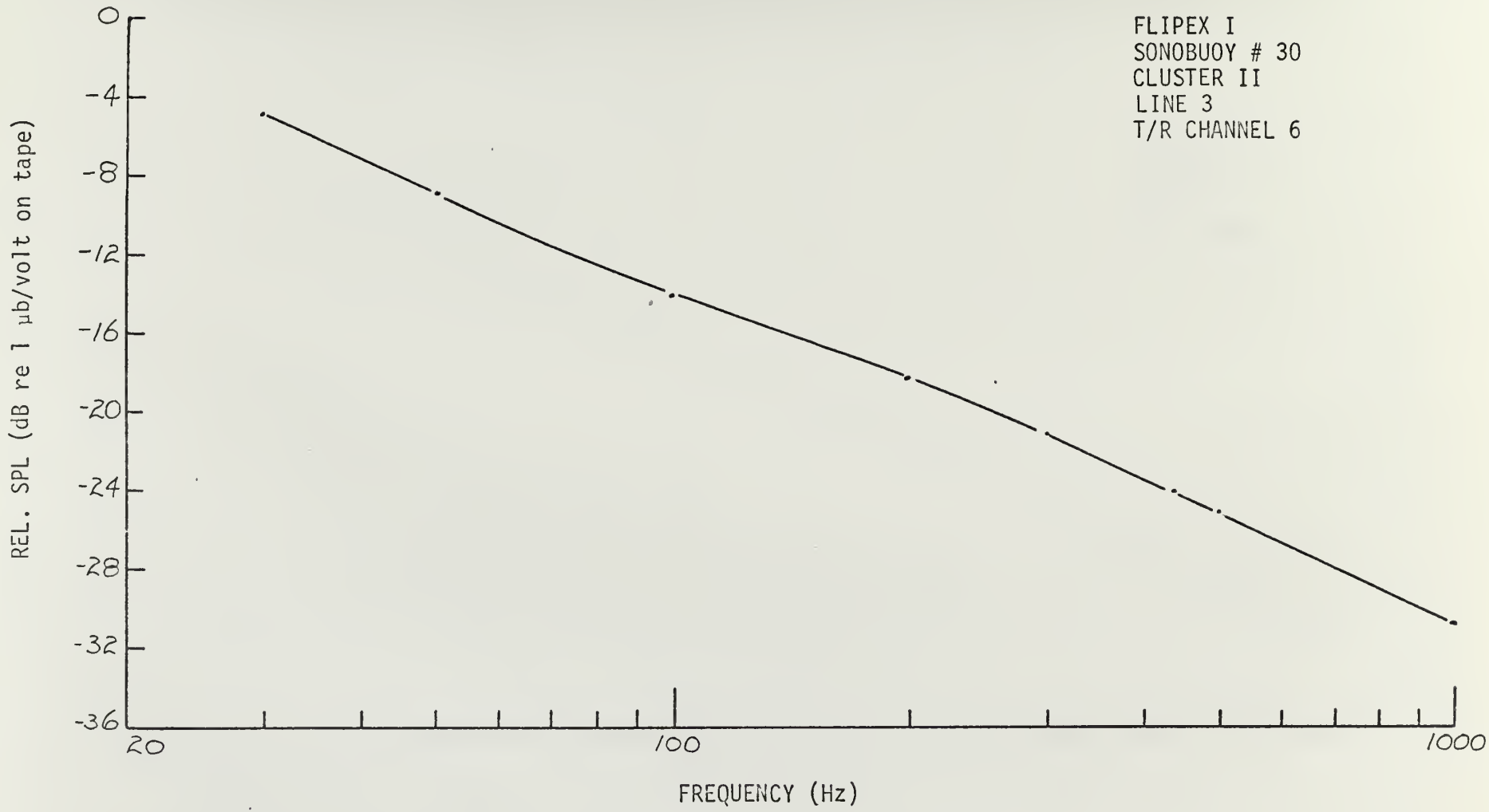

Fig. A-14

CALIBRATION CONVERSION CURVE FOR SONOBUOY #30, FLIPEX I

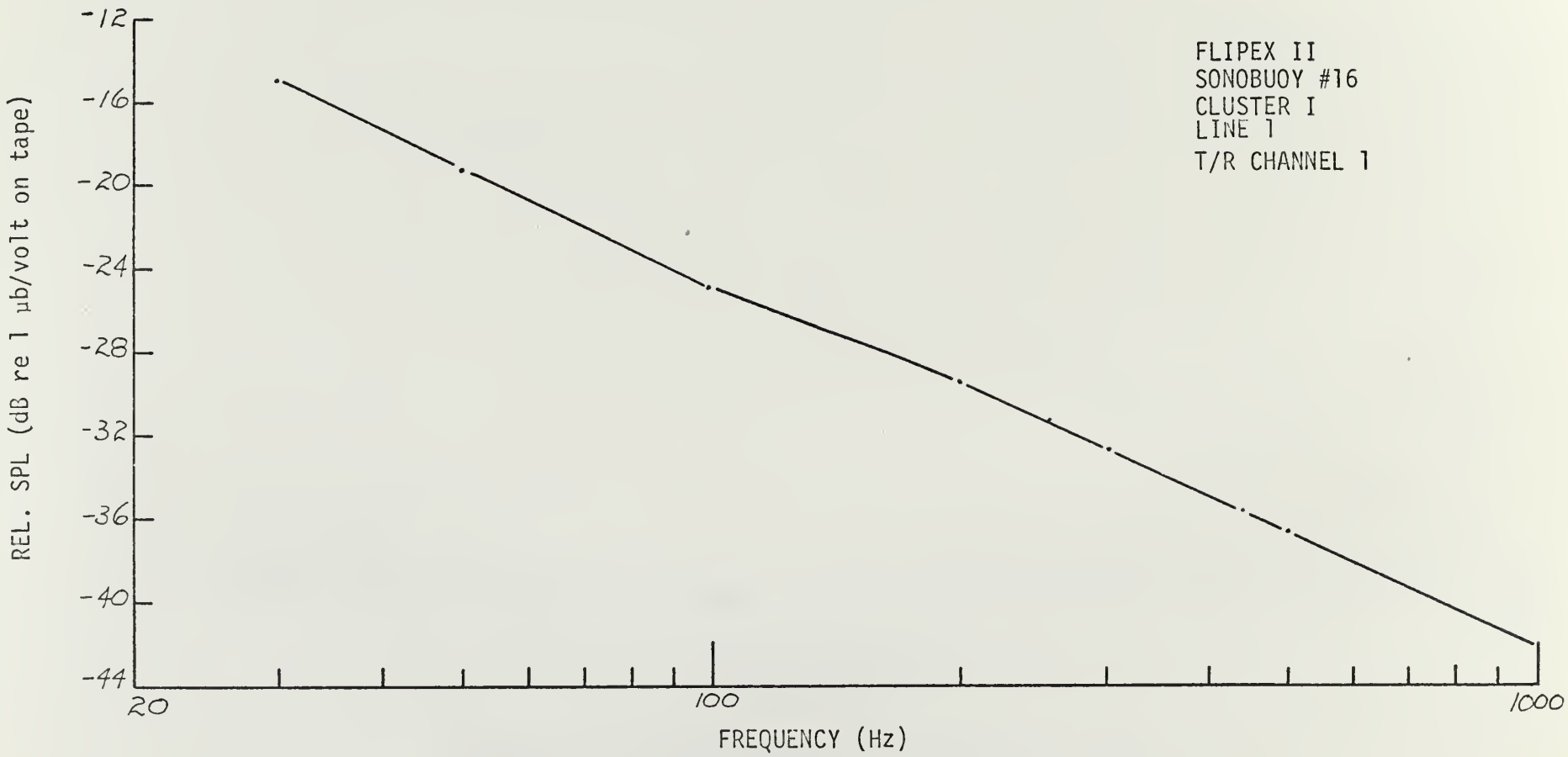

Fig. A-15

CALIBRATION CONVERSION CURVE FOR SONOBUOY #16, FLIPEX II

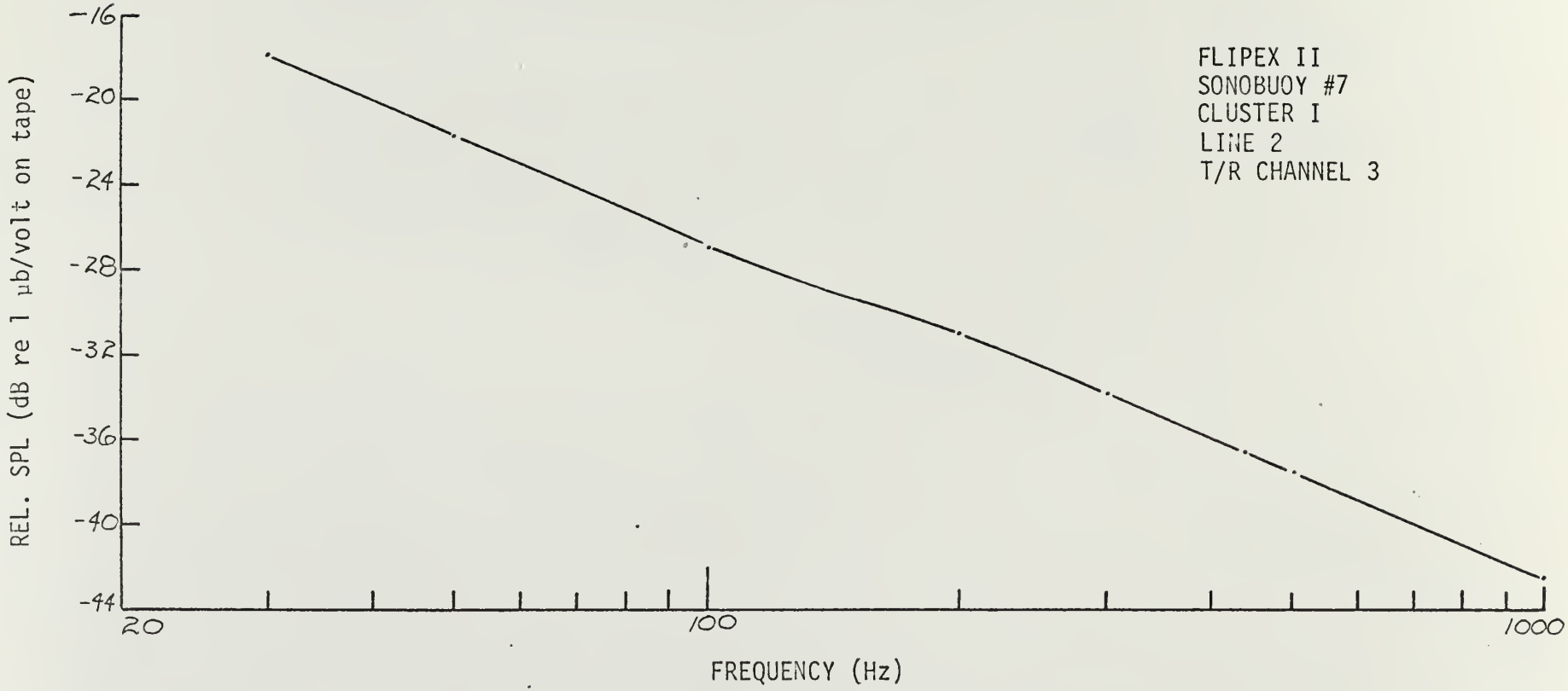

Fig. A-16

CALIBRATION CONVERSION CURVE FOR SONOBUOY #7, FLIPEX II

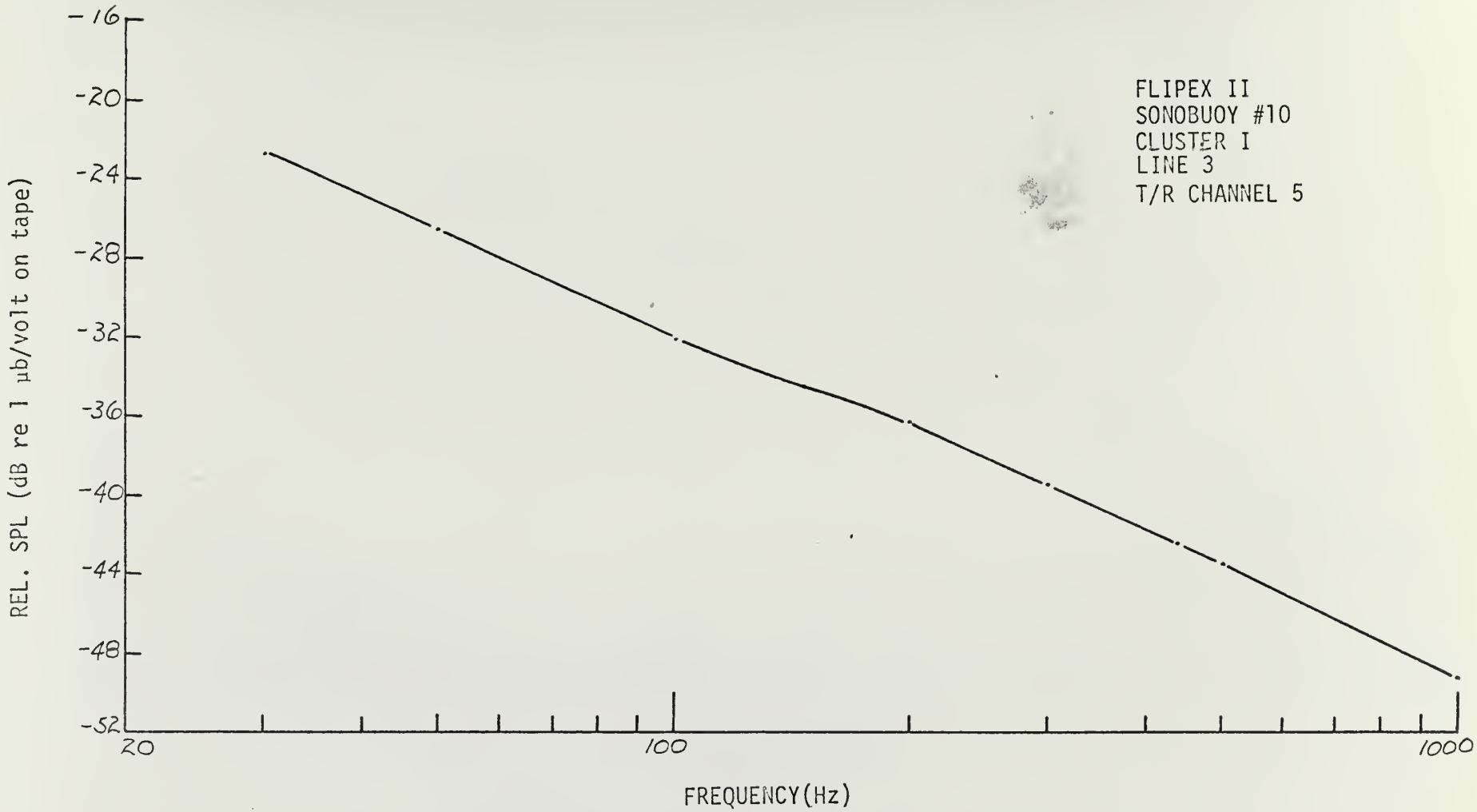

Fig. A-17

CALIBRATION CONVERSION CURVE FOR SONOBUOY #10, FLIPEX II

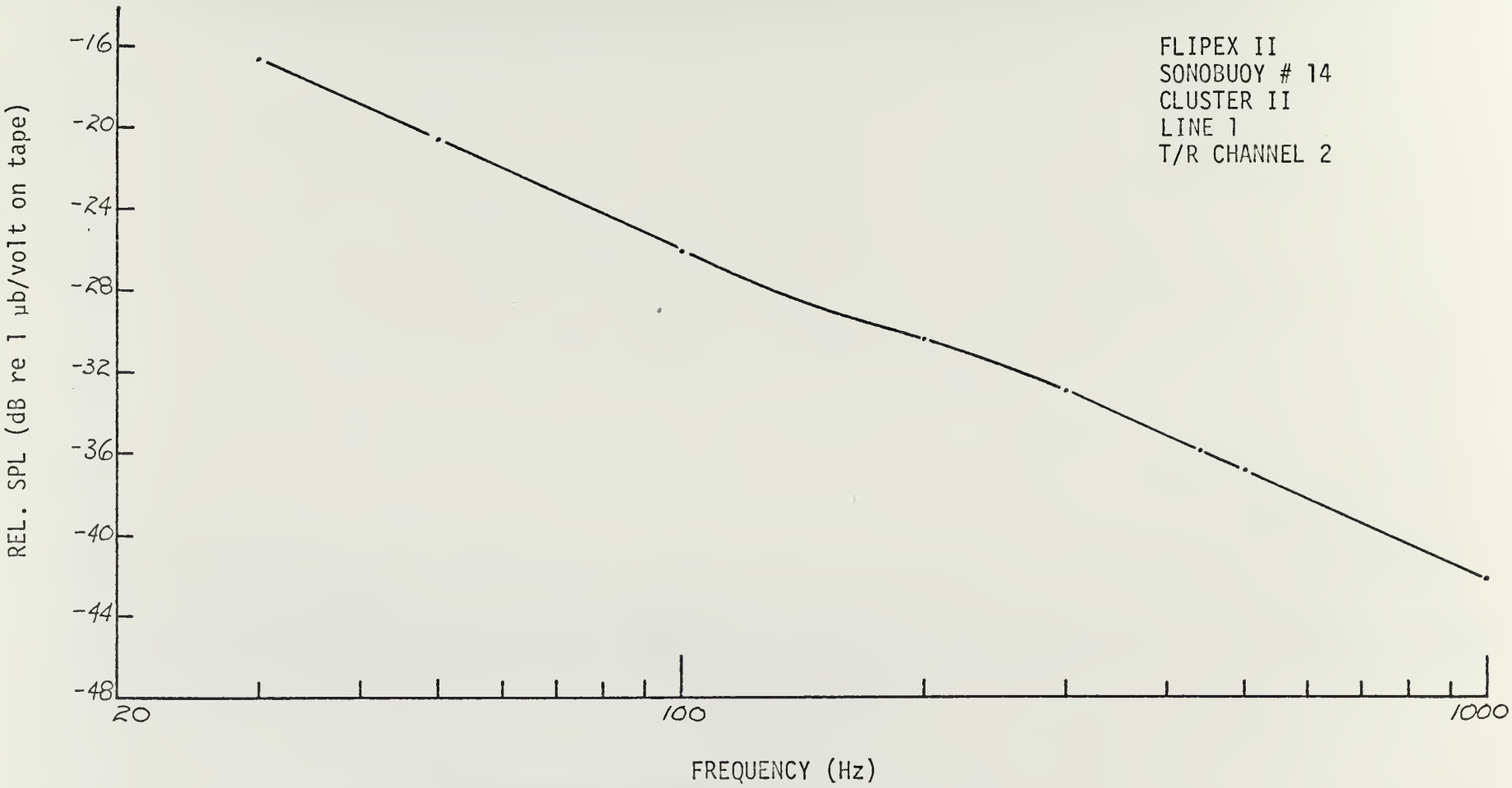

Fig. A-18

CALIBRATION CONVERSION CURVE FOR SONOBUOY #14, FLIPEX II

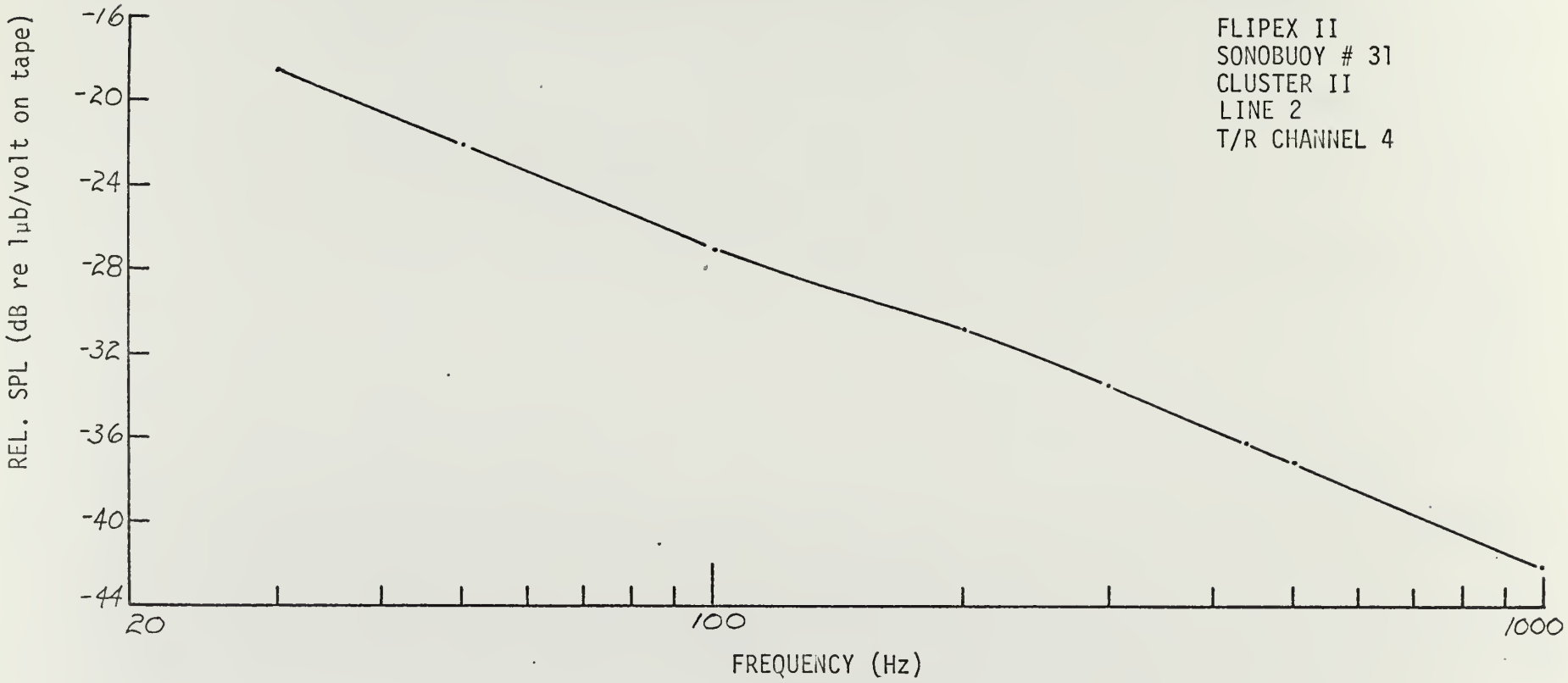

Fig. A-19

CALIBRATION CONVERSION CURVE FOR SONOBUOY # 31, FLIPEX II

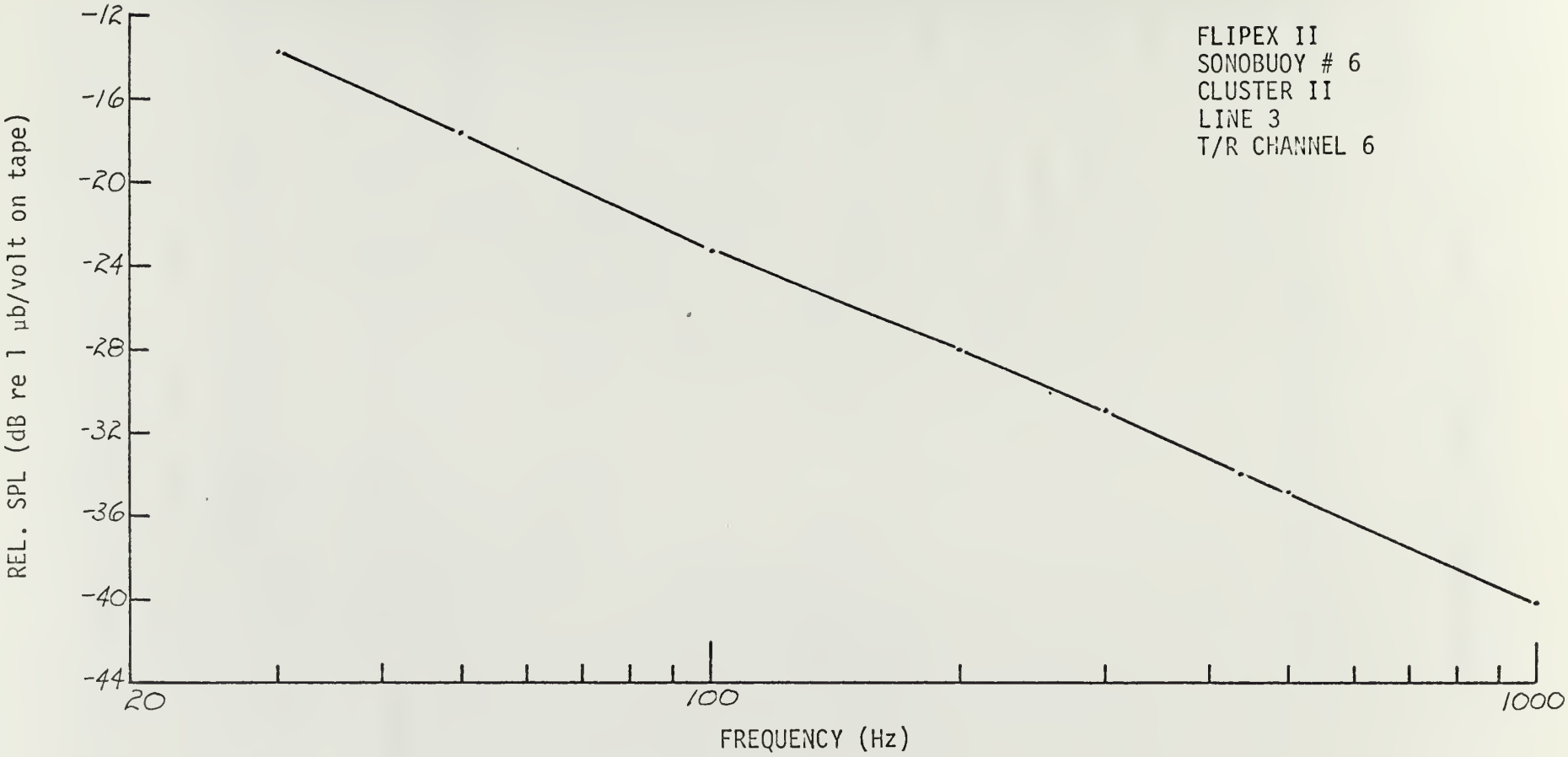

Fig. A-20

CALIBRATION CONVERSION CURVE FOR SONOBUOY #6, FLIPEX II

APPENDIX B EXPERIMENT DESCRIPTIONS

EXPERIMENT I

Purpose: Obtain crosswind[1] data at 150 ft altitude

Date/Time: 28 May AM

Helo Altitude: 150 ft.

Type of run: pass

Number of passes: 18

Position:[2] Cluster II

Cluster separation: 80 ft.

Remarks:

i. Tape recorder calibration[3] in dB (re 0.775 v):

	Passes 1-5	Passes 6-18
Ch 2,4	20	25
Ch 1,3,5,6	10	15

ii. Pass 13 aborted.

iii. Helo speed 45 kts. for passes 1-3
30 kts. for passes 4-18

EXPERIMENT 2

Purpose: Obtain upwind/downwind[1] data at 150 ft. altitude

---

[1] "Crosswind" and "upwind/downwind" refers to helo heading. Hereafter assume crosswind if not otherwise stated.

[2] "Position" refers to point overflown by helo.

[3] Tape recorder calibration refers to voltage level input to tape recorder corresponding to 1 volt output.

Date/Time: 28 May AM

Helo Altitude: 150 ft.

Type of run: pass (30 kt.)

Number of passes: 7

Position: Clusters I and II (almost together)

Cluster separation: 80 ft.

Remarks:

i. Tape recorder calibration: 15 dB for all channels, all passes.

ii. Kelp cutter ship in vicinity of FLIP during experiment.

EXPERIMENT 3

Purpose: Obtain data at 750 ft. altitude, 600 ft. cluster separation.

Date/Time: 29 May AM

Helo altitude: 750 ft.

Type of run: hover

Duration of hover: approximately 10 minutes

Position of hover: Cluster II

Cluster separation: 600 ft.

Remarks:

i. Tape recorder calibration: 15 dB all channels.

ii. 2 inch surface microphone not functioning for this and all succeeding 29 May experiments.

EXPERIMENT 4

Purpose: Obtain data at 150 ft. altitude, 600 ft. cluster separation.

Date/Time: 29 May AM

Helo altitude: 150 ft.

Type of run: pass (15 kt.)

Number of passes: 9

Position: Cluster II

Cluster separation: 600 ft.

Remarks:

i. Tape recorder calibration: 15 dB all channels.

EXPERIMENT 5

Purpose: Obtain data at 150 ft. altitude, 300 ft. cluster separation.

Date/Time: 29 May AM

Helo altitude: 150 ft.

Type of run: pass (15 kt.)

Number of passes: 9

Position: Cluster II

Cluster separation: 300 ft.

Remarks:

i. Tape recorder calibration: 15 dB all channels.

EXPERIMENT 6

Purpose: Obtain data at 150 ft. altitude, clusters together.

Date/Time: 29 May AM

Helo altitude: 150 ft.

Type of run: pass (15 kt.)

Number of passes: 3

Position: Clusters I and II

Cluster separation: together

Remarks:

i. Tape recorder calibration 15 dB all channels.

EXPERIMENT 7

Purpose: Obtain data for 40 foot altitude hover.

Date/Time: 17 August 1446-1456T.

Helo Altitude: 40 ft.

Type of run: hover

Duration of hover: 10 minutes

Position: sidestepped 200 ft. from clusters in crosswind direction

Cluster separation: together

Remarks:

i. Tape recorder calibration 15 dB all channels.

ii. Surface microphone not on hand. Sonobuoy 14 hydrophone at 10 ft. depth.

EXPERIMENT 8

Purpose: Obtain further data for 40 foot altitude hover

Date/Time: 17 August 1458-1508T

Helo Altitude: 40 ft.

Type of run: hover

Duration of hover: 10 minutes

Position: sidestepped 620 ft. from clusters in crosswind direction.

Cluster separation: together

Remarks:

i. Tape recorder calibration 15 dB all channels.

ii. Surface microphone not on hand. Sonobuoy #14 hydrophone at 10 ft. depth.

EXPERIMENT 9

Purpose: Obtain data at 750 ft. altitude.

Date/Time: 17 August 1607-1618T.

Helo Altitude: 750 ft.

Type of run: hover

Duration of hover: 11 minutes

Position: sidestepped 340 ft. from clusters in crosswind direction.

Cluster separation: together

Remarks:

i. Tape recorder calibration 15 dB all channels.

ii. Sonobuoy #14 hydrophone placed in kiddy pool to serve as surface microphone. Continued to so serve throughout remainder of experiments.

iii. Hover sidestepped to facilitate helo position keeping with respect to kiddy pool.

EXPERIMENT 10

Purpose: Obtain data at 750 ft. altitude with helo passing overhead clusters.

Date/Time: 17 August PM

Helo Altitude: 750 ft.

Type of run: pass (5 kt.)

Number of passes: 4

Position: Overhead both clusters

Cluster separation: together

Remarks:

i. Tape recorder calibration 15 dB all channels.

ii. Sonobuoy 31 (100 ft. depth) failed during this experiment.

EXPERIMENT 11

Purpose: Obtain data for 600 ft. altitude hover for very calm sea surface which existed.

Date/Time: 18 August 0832T

Helo Altitude: 600 ft.

Type of Run: hover

Duration of hover: 4 minutes (See Remark ii)

Position: Varied between Clusters I and II

Cluster separation: 150 ft.

Remarks:

i. Tape recorder calibration 15 dB all channels.

ii. Initial position which was held for approximately 35 sec. was over Cluster I.

iii. Helo had difficulty maintaining position.

EXPERIMENT 12

Purpose: Obtain data at 150 ft. altitude.

Date/Time: 18 August 0836T.

Helo Altitude: 150 ft.

Type of run: pass (5 kt.)

Number of passes: 2

Position: Cluster II

Cluster separation: 150 ft.

Remarks:

i. Tape recorder calibration 15 dB all channels for first pass. Changed surface microphone channel (ch. 4) to 25 dB for second pass.

ii. Clusters aligned crosswind. Helo heading perpendicular to cluster line.

EXPERIMENT 13

Purpose: Determine if surface microphone sonobuoy limiting occurred for 600 ft. altitude pass.

Date/Time: 18 August 0901T

Helo Altitude: 600 ft.

Type of run: pass (5 kt.)

Number of passes: 1

Position: Cluster II

Cluster separation: 150 ft.

Remarks:

i. Tape recorder calibration: Ch. 4 25 dB
Other channels 15 dB

ii. Clusters still aligned crosswind. Helo heading perpendicular to cluster line.

EXPERIMENT 14

Purpose: Increase distance of source from surface microphone so as to eliminate sonobuoy limiting.

Date/Time: 18 August 0910-0940T

Helo Altitude: 600 ft.

Type of run: pass (5 kt.)

Number of passes: 11

Position: Approximately 100 yards outboard Cluster II (See Remark ii)

Cluster separation: 150 ft.

Remarks:

i. Tape recorder calibration:

	Passes 1-7	Passes 8-12
Ch. 4	25 dB	15 dB
Other channels	15 dB	15 dB

ii. Helo position not measured. 100 yard distance from Cluster II was pilot's estimate.

iii. Limiting very slight.

iv. Clusters still aligned crosswind. Helo heading perpendicular to cluster line.

EXPERIMENT 15

Purpose: Continuation of Experiment 14 at 300 ft. altitude due to low flying aircraft in area.

Date/Time: 18 August 0945-1010T

Helo altitude: 300 ft.

Type of run: pass (5 kt.)

Number of passes: 9

Position: Approximately 100 yards outboard Cluster II. (see Remark ii)

Cluster separation: 150 ft.

Remarks:

i. Tape recorder calibration 15 dB all channels.

ii. Helo position not measured. 100 yard distance from Cluster II was pilot's estimate.

iii. FLIP orienter motors energized.

EXPERIMENT 16

Purpose: Obtain 300 ft. altitude data with aircraft passing over Cluster I

Date/Time: 18 August 1244-1305T

Helo altitude: 300 ft.

Type of run: pass (5 kt.)

Number of passes: 12

Position: Cluster I

Cluster separation: 150 ft.

Remarks:

i. Tape recorder calibration, 15 dB all channels.

EXPERIMENT 17

Purpose: Obtain 600 ft. altitude data with aircraft passing over Cluster I.

Date/Time: 18 August 1305-1325T

Helo altitude: 600 ft.

Type of run: pass (5 kt.)

Number of passes: 7

Position: Cluster I

Cluster separation: 150 ft.

Remarks:

i. Tape recorder calibration: 15 dB all channels

ii. Passes 18 and 19 best with respect to position over Cluster I.

EXPERIMENT 18

Purpose: Increase distance of source from surface microphone so as to eliminate sonobuoy limiting.

Date/Time: 18 August 1334-1413T

Helo altitude: 300 ft.

Type of run: pass (5 kt.)

Number of passes: 12

Position: Over smoke float which was initially positioned outboard of Cluster II

Cluster separation: 150 ft.

Remarks:

i. Tape recorder calibration: 15 dB all channels.

ii. Smoke float distance from FLIP determined using bubble sextant readings. Times of sextant readings and helo passes recorded.

EXPERIMENT 19

Purpose: Obtain record of helicopter noise with continuously decreasing grazing angles.

Date/Time: 18 August 1430-1443T

Helo altitude: 40 ft.

Type of run: modified hover

Duration of hover: 13 minutes

Position: Over smoke float which was initially positioned outboard of Cluster II.

Cluster separation: 150 ft.

Remarks:

i. Tape recorder calibration: 15 dB all channels

ii. Helo remained over smoke float throughout experiment. Smoke float distance from FLIP determined using bubble sextant readings. Times of sextant readings recorded.

EXPERIMENT 20

Purpose: Obtain 300 ft. altitude data with helicopter making alternate passes over Clusters I and II.

Date/Time: 18 August 1445-1525T

Helo altitude: 300 ft.

Type of run: pass (5 kt.)

Number of passes: 16

Position: Clusters I and II alternately

Cluster separation: 150 ft.

Remarks:

i. Tape recorder calibration: 15 dB all channels.

APPENDIX C BATHYTHERMOGRAPH DATA

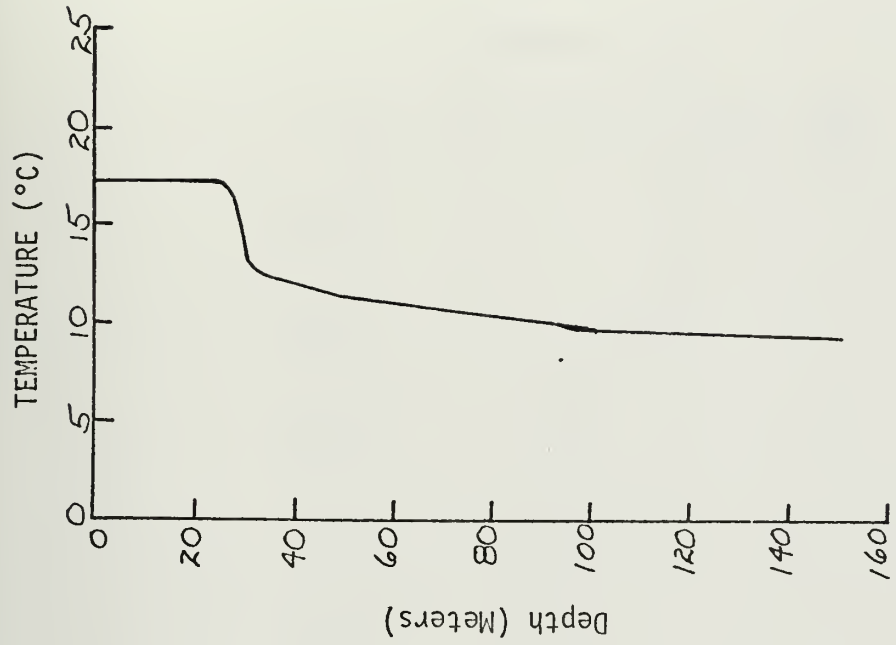

Fig. C-2

BT DATA
281735T May 1970

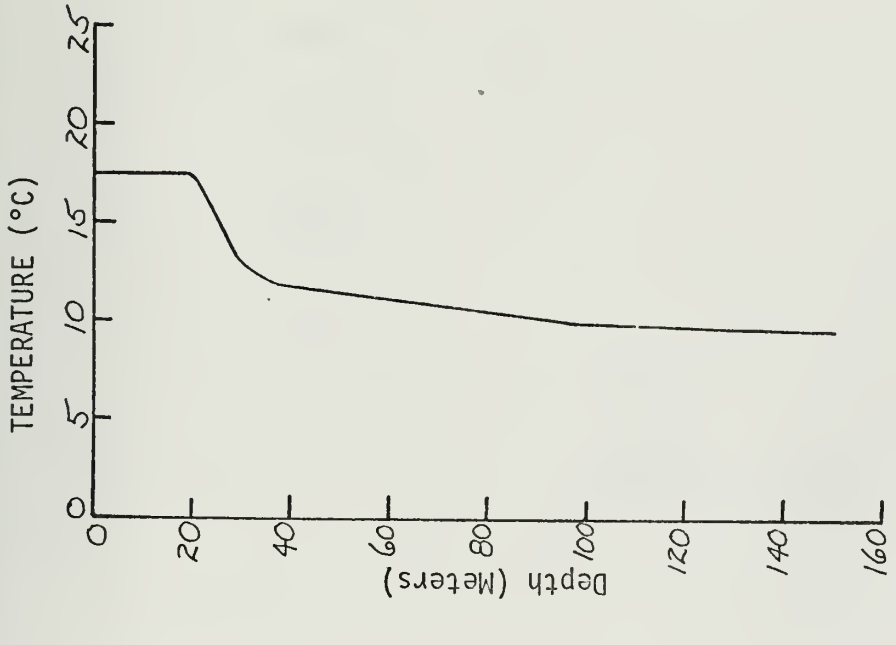

Fig. C-1

BT DATA
281515T May 1970

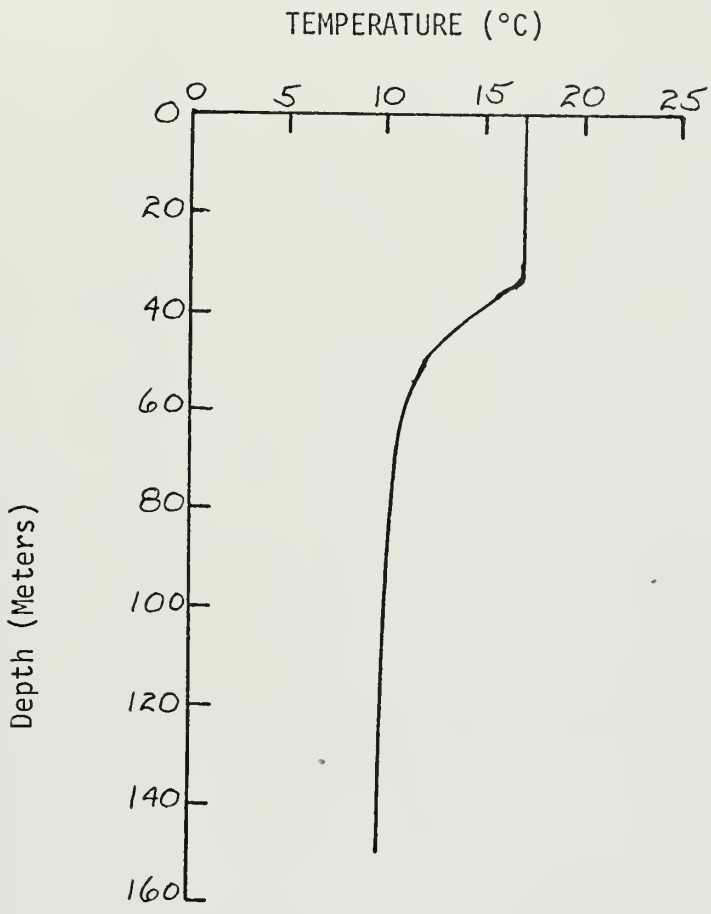

Fig. C-3

BT DATA
291000T May 1970

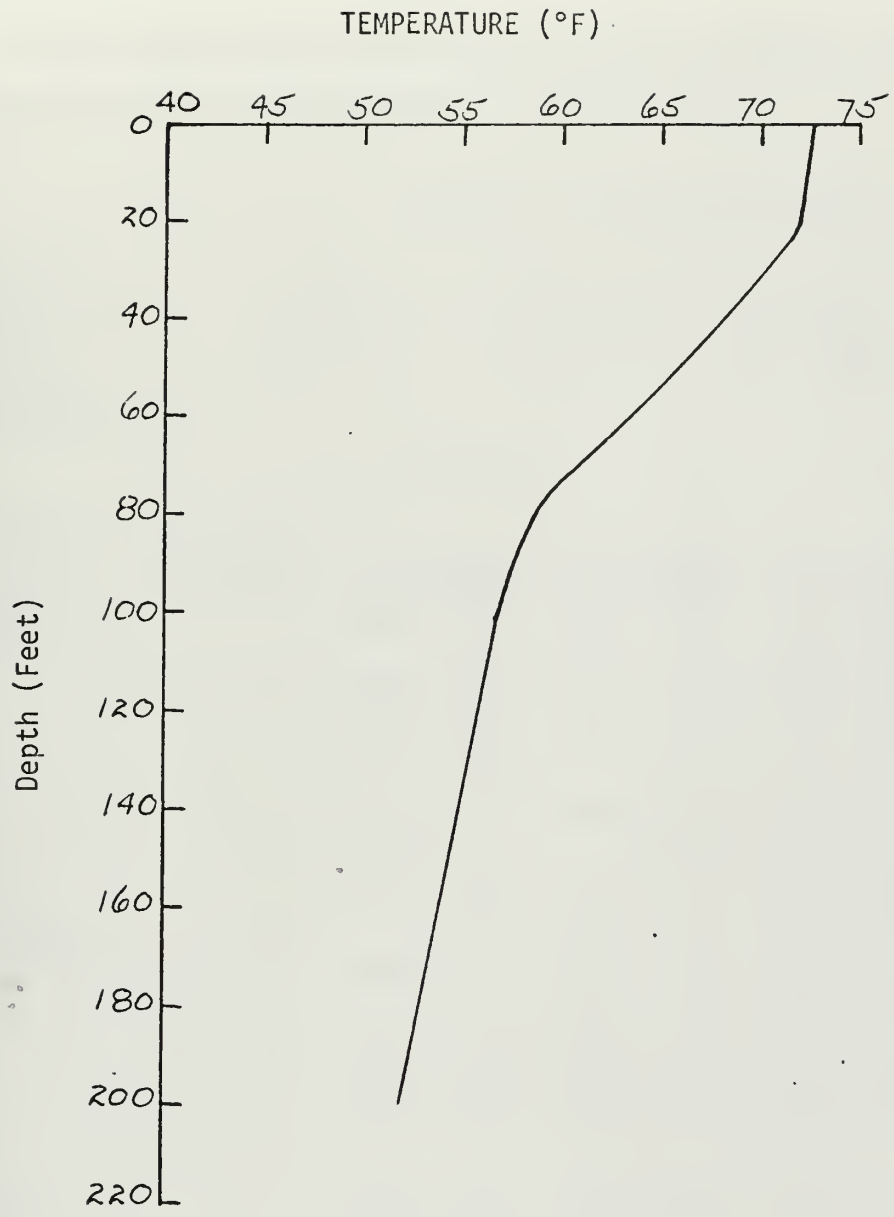

Fig. C-4

BT DATA
172130T Aug. 1970

APPENDIX D MEAN SQUARE SURFACE WAVE HEIGHTS

Mean square surface wave heights in m^2 for FLIPEX I and II are compiled below for various ranges of wave period, T.

FLIPEX I (Vibrotron data only)

Date/Time of Data	T < 20 sec.	T < 10 sec.	T < 5 sec.	T < 3 sec.
29 May 1034-1052T 1034-1052T	2.75×10^{-2}	1.44×10^{-2}	2.23×10^{-3}	3.67×10^{-4}

FLIPEX II

Date/Time of Data	Wave Probe Desig.	T < 20 sec.	T < 10 sec.	T < 5 sec.	T < 3 sec.
17 Aug 1729-1827T	A	2.63×10^{-2}	1.55×10^{-2}	1.05×10^{-2}	4.58×10^{-3}
	B	2.36×10^{-2}	1.41×10^{-2}	9.58×10^{-3}	4.34×10^{-3}
	C	2.49×10^{-2}	1.56×10^{-2}	1.10×10^{-2}	5.13×10^{-3}
	D	2.11×10^{-2}	1.37×10^{-2}	9.97×10^{-3}	3.77×10^{-3}
17 Aug 1827-2038T	A	2.32×10^{-2}	1.32×10^{-2}	9.59×10^{-3}	3.23×10^{-3}
	B	2.20×10^{-2}	1.25×10^{-2}	9.09×10^{-3}	3.00×10^{-3}
	C	2.40×10^{-2}	1.46×10^{-2}	1.14×10^{-2}	3.47×10^{-3}
	D	1.99×10^{-2}	1.24×10^{-2}	9.52×10^{-3}	2.86×10^{-3}
18 Aug 1000-1216T	A	1.86×10^{-2}	1.16×10^{-2}	7.18×10^{-3}	2.20×10^{-3}
	B	1.71×10^{-2}	1.03×10^{-2}	6.13×10^{-3}	2.01×10^{-3}
	C	2.00×10^{-2}	1.16×10^{-2}	7.02×10^{-3}	2.22×10^{-3}
	D	1.78×10^{-2}	1.04×10^{-2}	6.51×10^{-3}	2.11×10^{-3}
18 Aug 1230-1343T	A	2.06×10^{-2}	9.74×10^{-3}	5.99×10^{-3}	2.16×10^{-3}
	B	1.95×10^{-2}	9.17×10^{-3}	5.54×10^{-3}	1.93×10^{-3}
	C	2.29×10^{-2}	1.01×10^{-2}	5.84×10^{-3}	2.12×10^{-3}
	D	2.08×10^{-2}	9.35×10^{-3}	5.82×10^{-3}	2.17×10^{-3}

APPENDIX E A TEST FOR THE VALIDITY OF THE KIRCHHOFF APPROXIMATION

It is shown by Beckmann in Chapter 5 of Ref. 8 that for the Kirchhoff Approximation to apply, $L >> \lambda$,

Where: L is the correlation distance for which the surface correlation function, as approximated by the Gaussian form $C(\ell) = e^{-\ell^2/L^2}$ falls to $1/e$ of $C(0)$.

λ is the acoustic wavelength.

It is further shown by Beckmann in Appendix D of Ref. 8 that, for a surface with a Gaussian distribution of heights and having a Gaussian correlation function, the mean square surface slope, Σ, is related to the correlation distance, L, and the mean square surface height, σ, by the following expression:

$$\Sigma^2 = \frac{2\sigma^2}{L^2}$$

σ^2 was measured during the experiment. Σ^2 may be estimated from wind speed using the Cox and Munk equation:

$$\left(\begin{matrix}\text{RMS SEC}\\ \text{WAVE}\\ \text{SLOPE}\end{matrix}\right)^2 = \Sigma^2 = 0.003 + 5.12 \times 10^{-3} W$$

where W is wind speed in m/sec.

L can then be determined and the criterion $L >> \lambda$ tested for applicability of the Kirchhoff approximation.

In order to determine that region of roughness, R, for which $L/\lambda < 1$, the value of R for which $\lambda = L$ was calculated for each ocean surface encountered during the experiments. λ in water was used as a worst case.

The results of this calculation are compiled below:

Expt. Nr.	Wind Speed in m/sec	Σ^2	$\sigma^2(m^2)$	L(m)	Freq. for λ=L	R for λ=L
11	2.54	1.6×10^{-2}	1.78×10^{-2}	1.49	1000 Hz	3.55
16,17	4.56	2.6×10^{-2}	2.1×10^{-2}	1.25	1200 Hz	6.05

APPENDIX F RELATIVE HELICOPTER NOISE SPECTRA

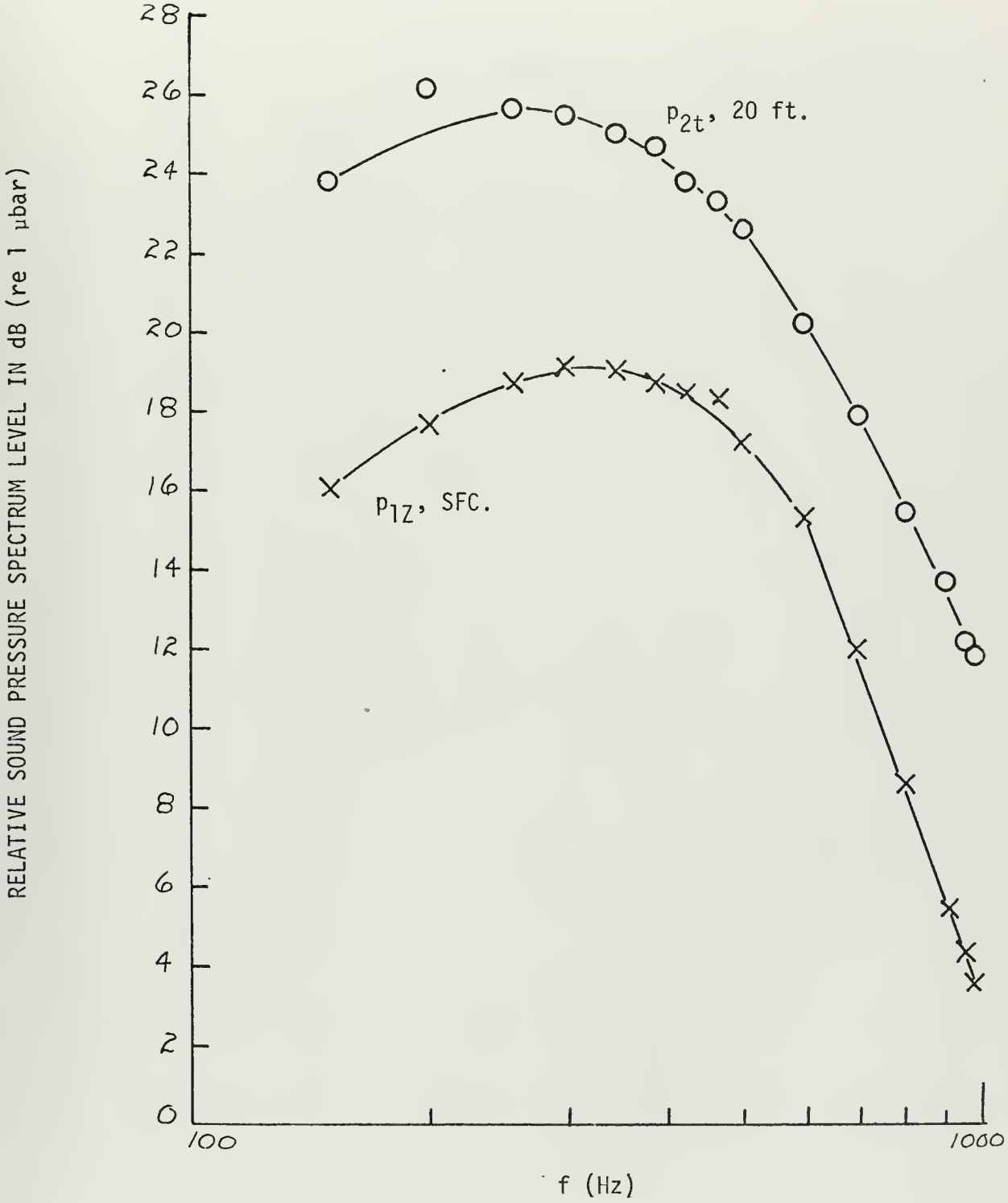

Fig. F-1

EXPT. 11. 600 FT. HOVER RELATIVE SPECTRA FOR SFC MIC. AND 20 FT. HYDROPHONE.

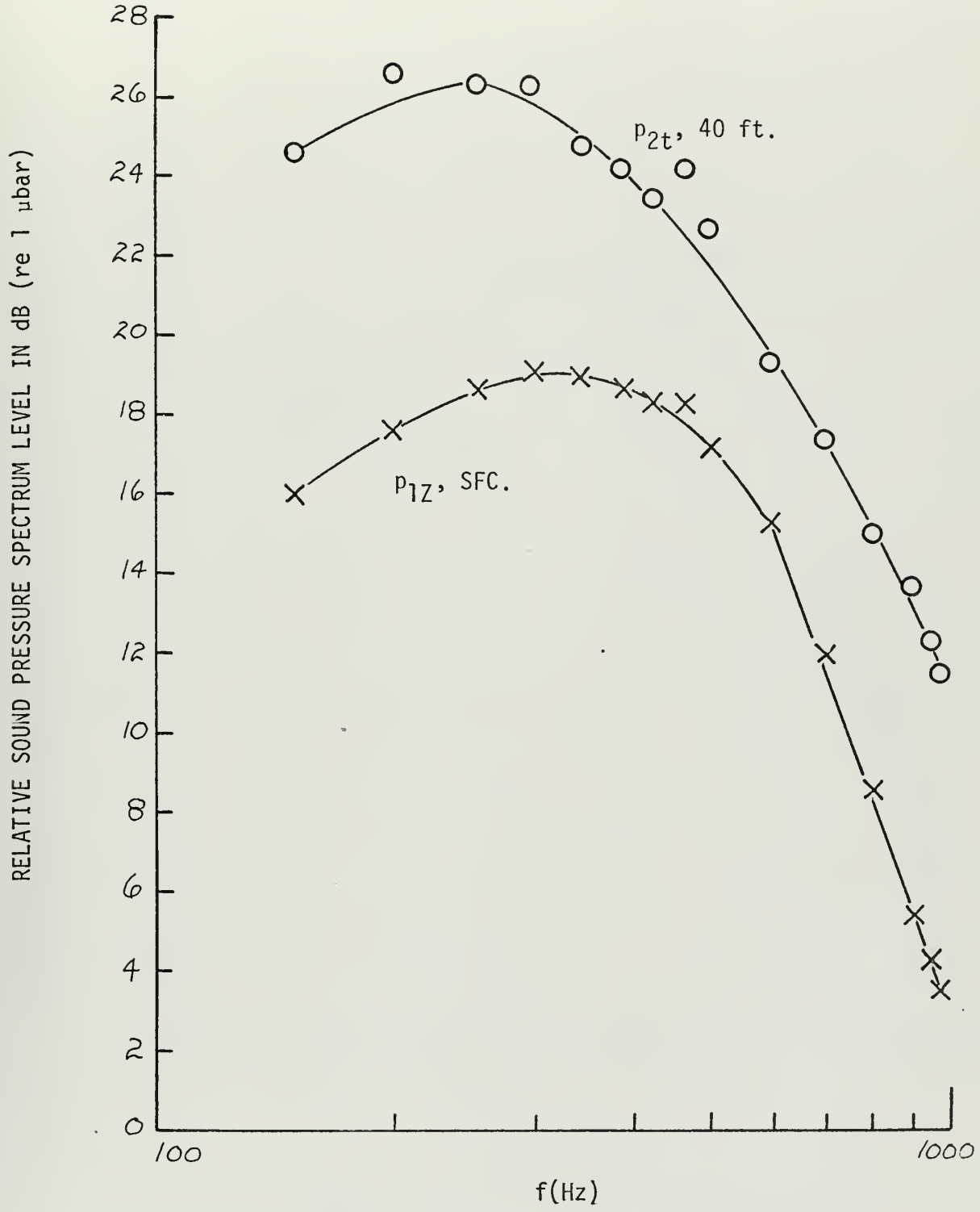

Fig. F-2

EXPT. 11 600 FT. HOVER RELATIVE SPECTRA FOR SFC. MIC. AND 40 FT. HYDROPHONE

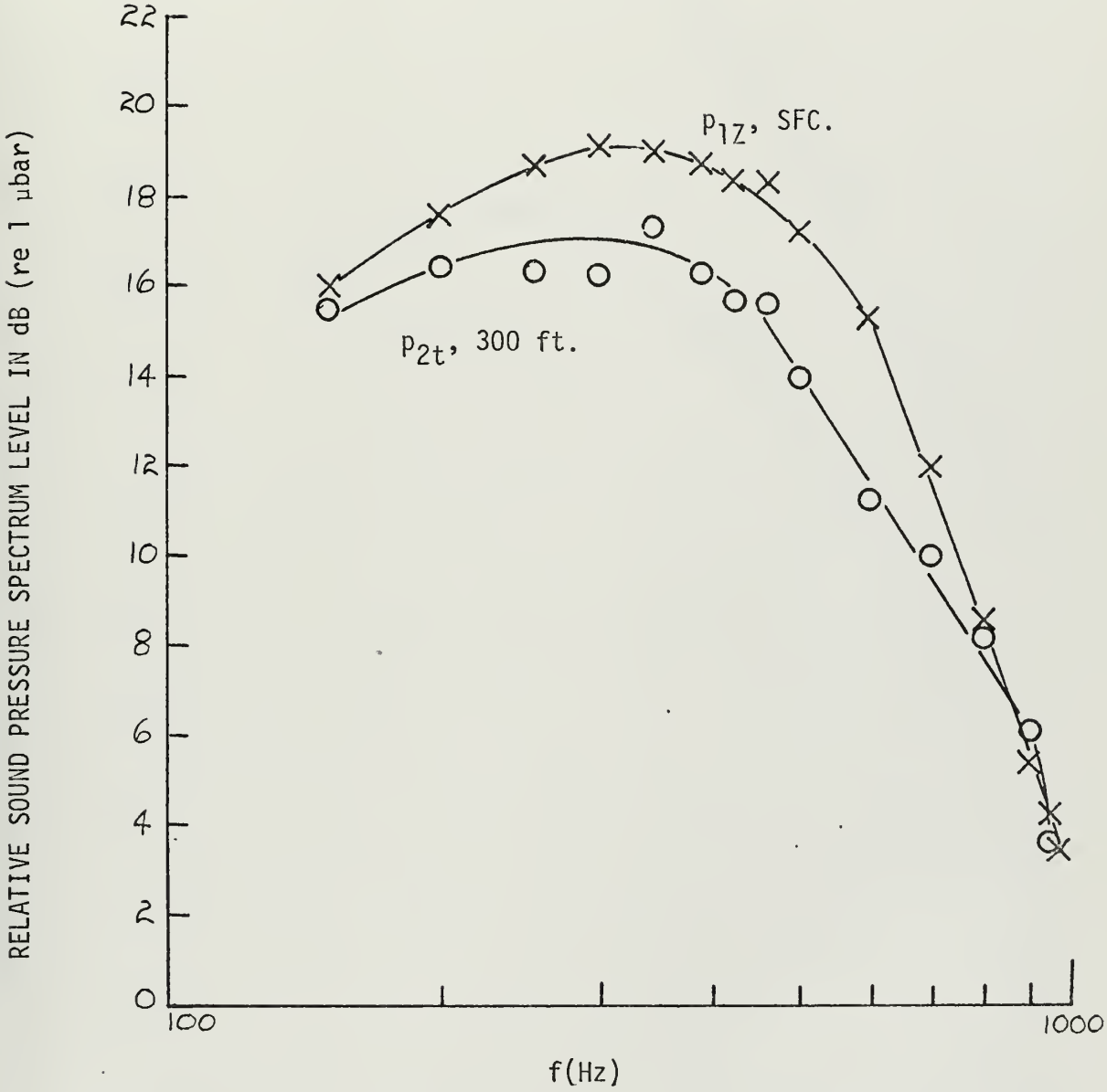

Fig. F-3

EXPT. 11 600 FT. HOVER RELATIVE SPECTRA FOR SFC. MIC. AND 300 FT. HYDROPHONE

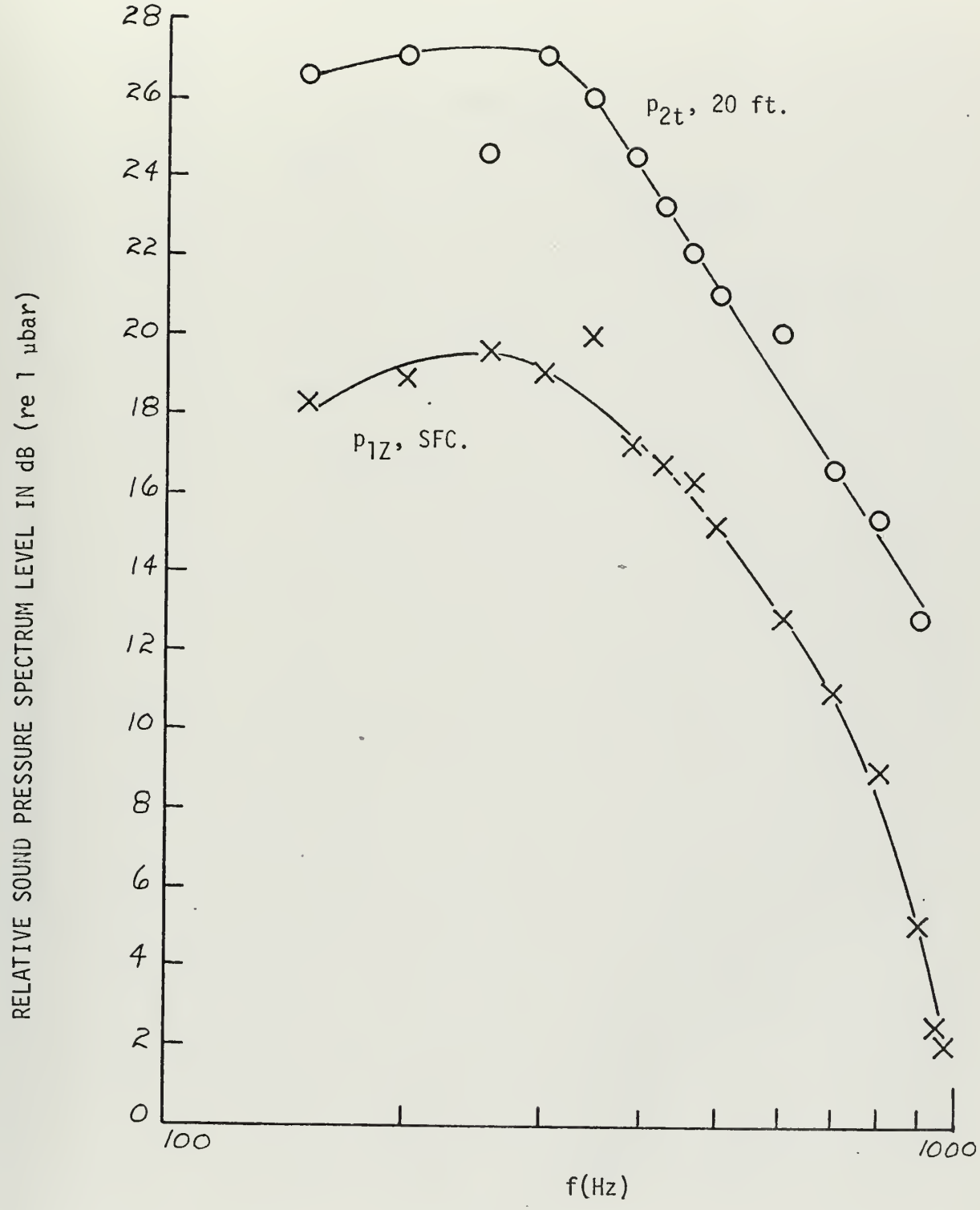

Fig. F-4

EXPT. 16 300 FT. PASS RELATIVE SPECTRA FOR SFC. MIC. AND 20 FT. HYDROPHONE

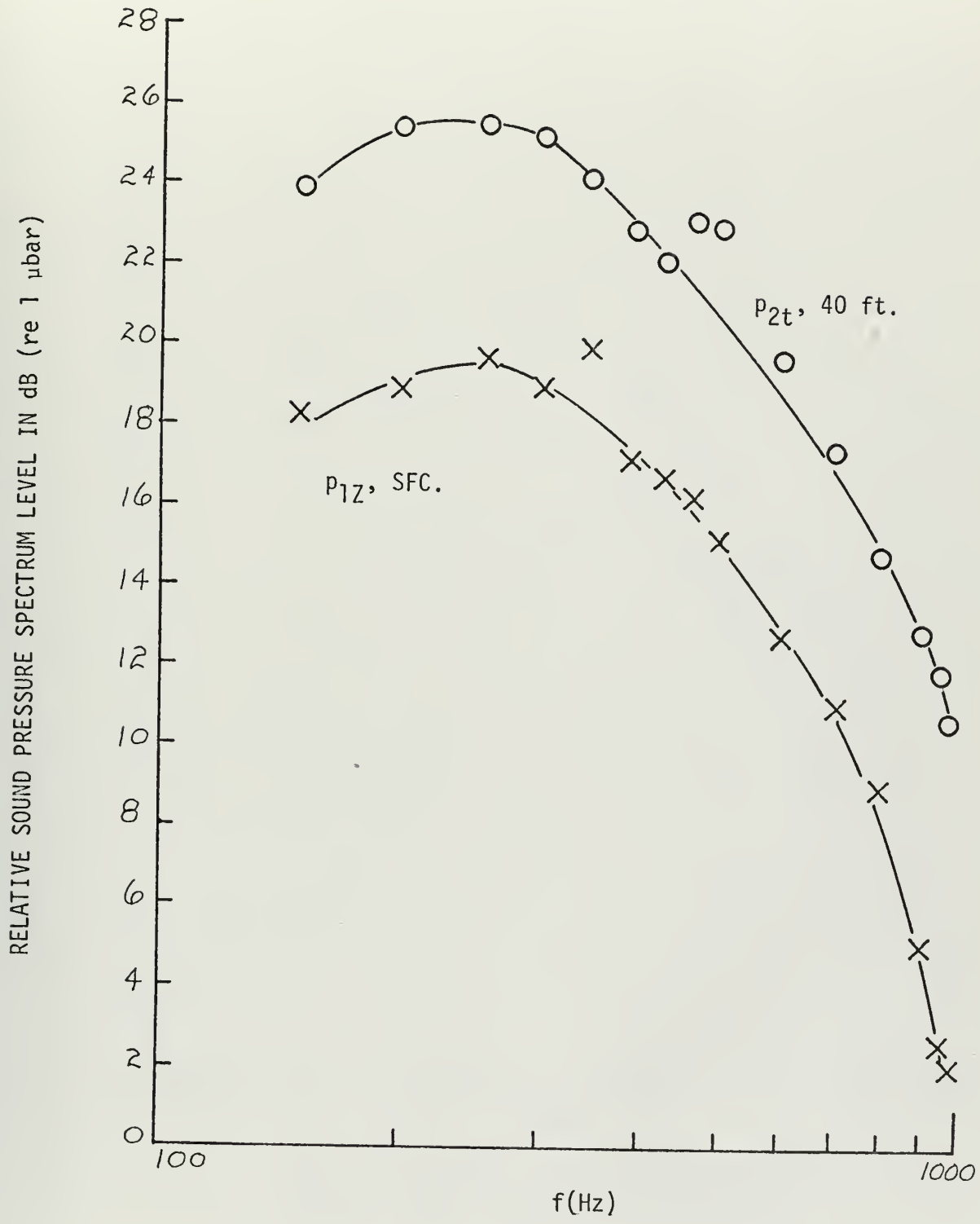

Fig. F-5

EXPT. 16 300 FT. PASS RELATIVE SPECTRA FOR SFC. MIC AND 40 FT. HYDROPHONE.

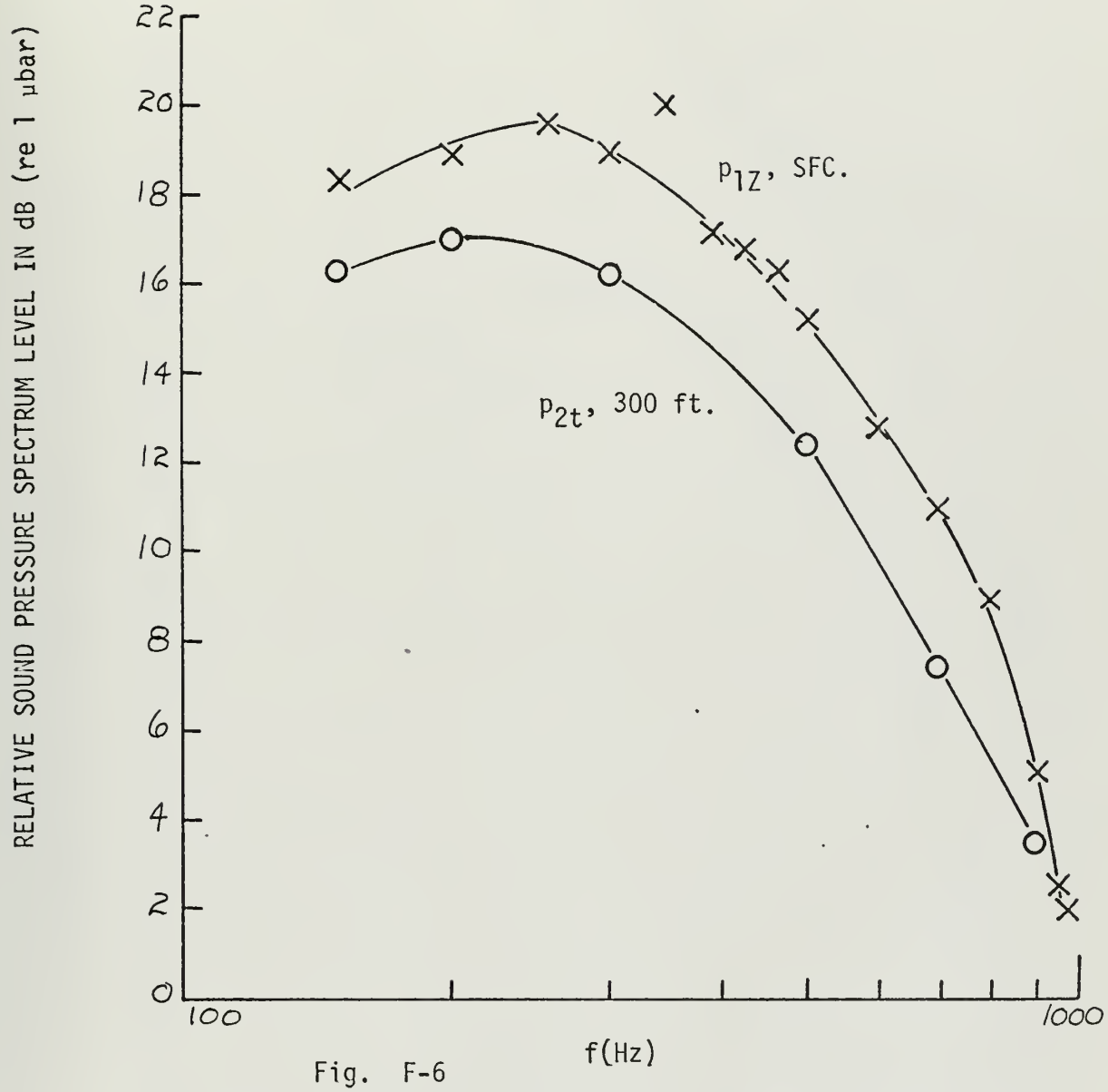

Fig. F-6

EXPT. 16 300 FT. PASS RELATIVE SPECTRA FOR SFC. MIC. AND 300 FT. HYDROPHONE

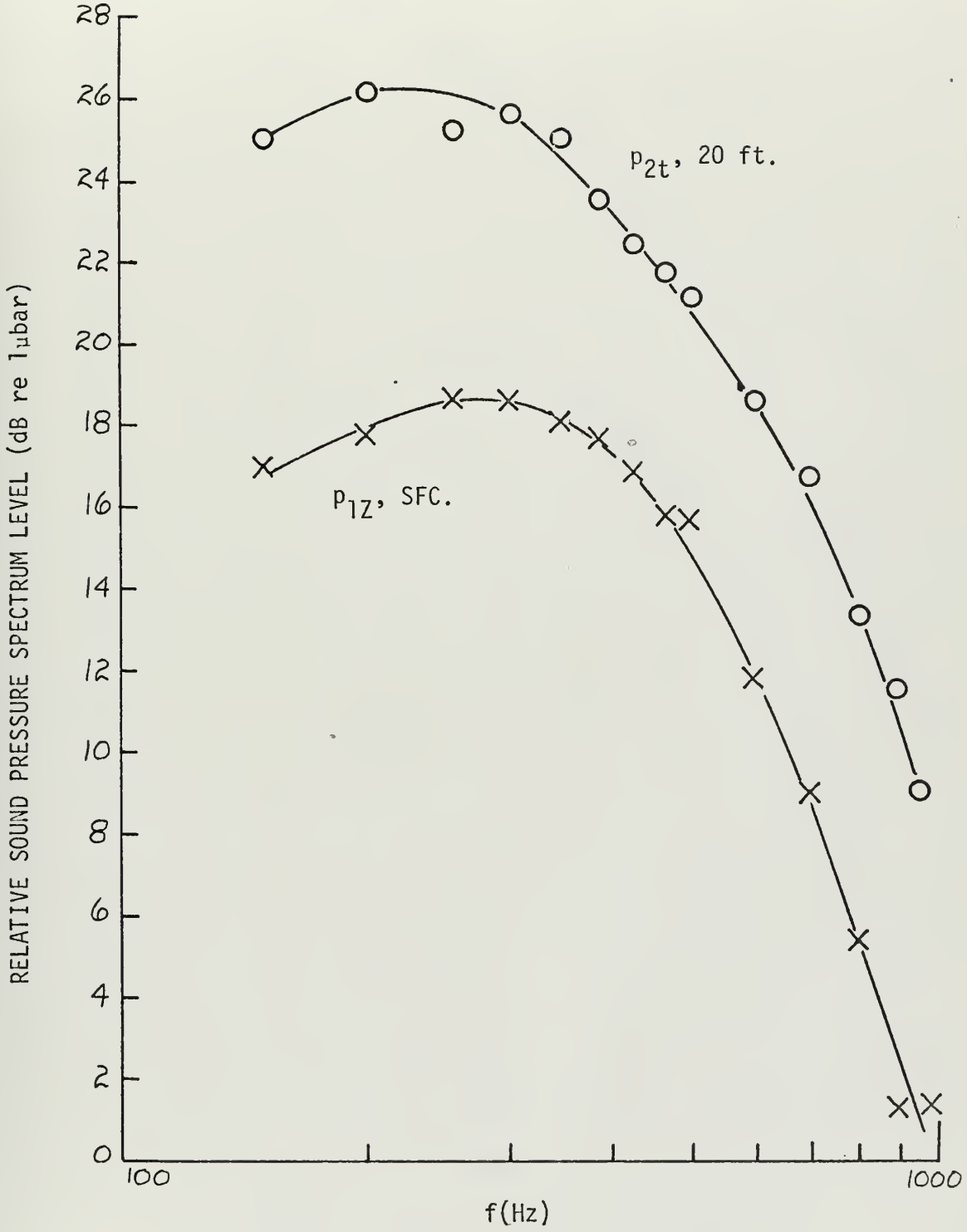

Fig. F-7

EXPT. 17 600 FT. PASS RELATIVE SPECTRA FOR SFC. MIC. AND 20 FT. HYDROPHONE

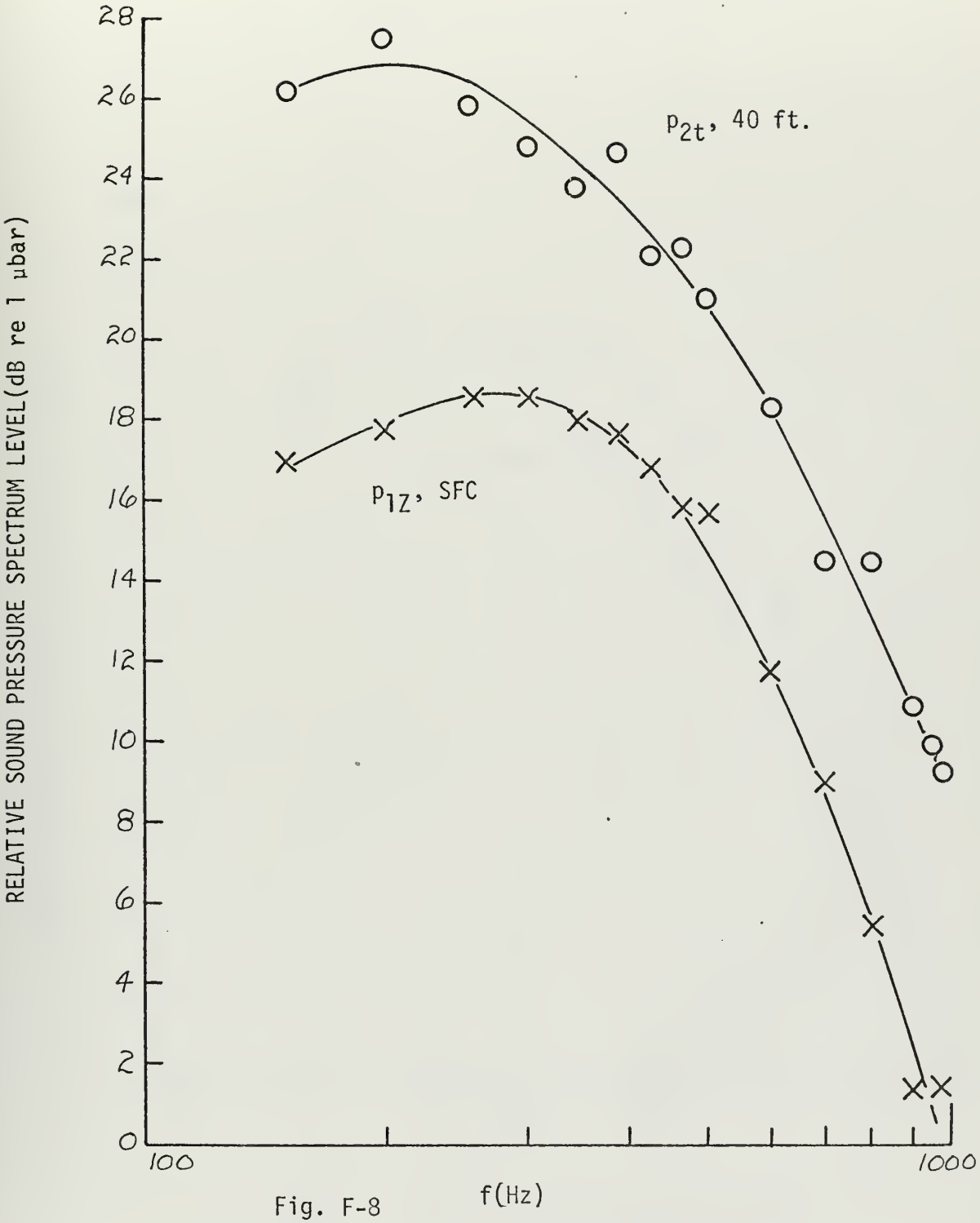

Fig. F-8

EXPT. 17 600 FT. PASS RELATIVE SPECTRA FOR SFC. MIC. AND 40 FT. HYDROPHONE.

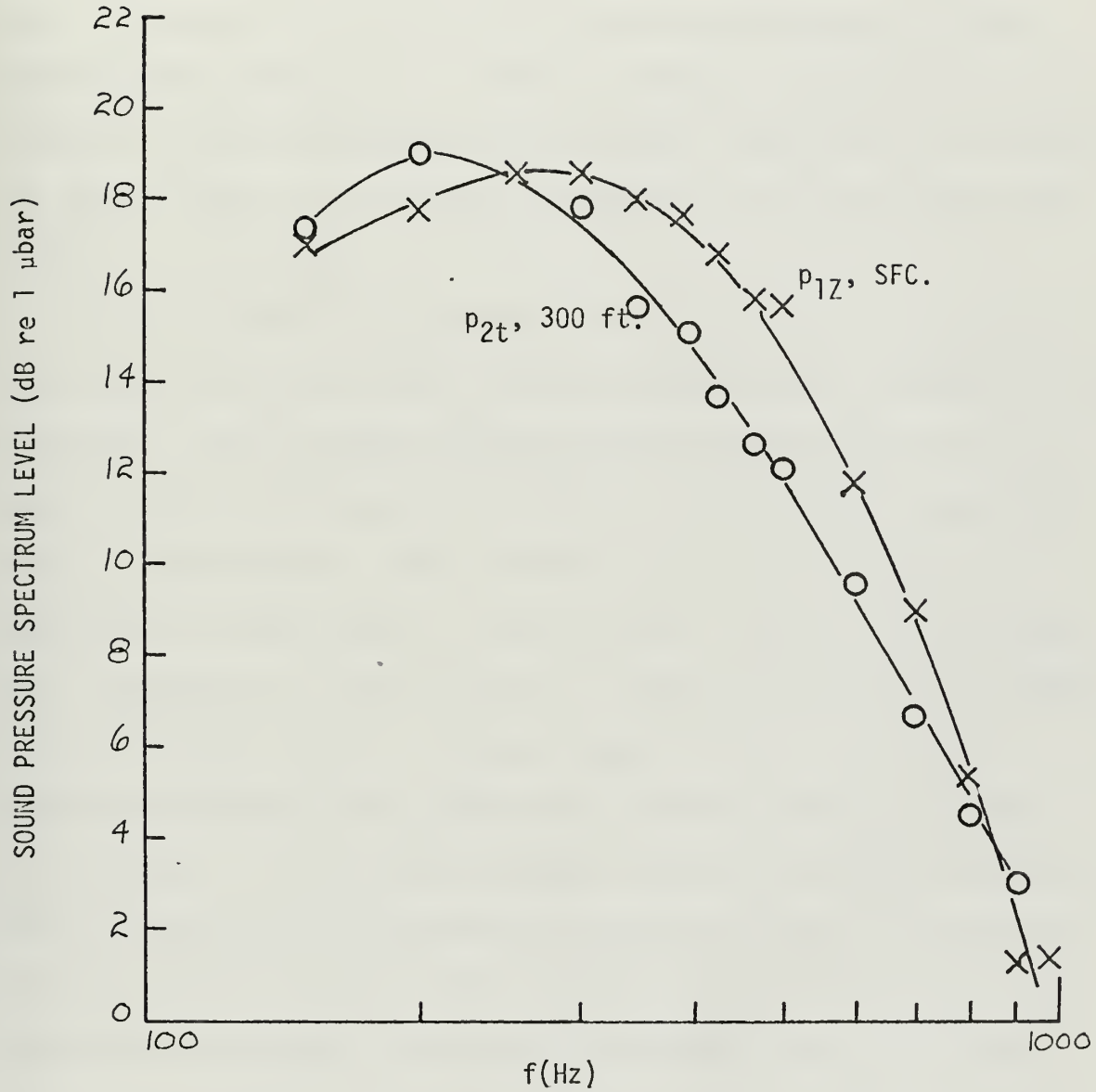

Fig. F-9

EXPT. 17 600 FT. PASS RELATIVE SPECTRA FOR SFC. MIC. AND 300 FT. HYDROPHONE

APPENDIX G LIMITING EXPERIMENT

During FLIPEX II, some distortion, due to sonobuoy limiting, was observed in the signals from the surface microphone and the 20 and 40 foot hydrophones (but not for the 300 foot hydrophone) when the helicopter passed overhead at an altitude of 300 feet. Limiting was slightly reduced but not eliminated when the helicopter passed over at an altitude of 600 feet which was the maximum altitude that the cloud ceiling would permit.

In order to determine the effect of this limiting on the spectrum of the recorded helicopter noise, a limiting experiment was conducted in the laboratory. The experiment involved introducing helicopter noise at various levels to the input of a sonobuoy. The levels were controlled using a step attenuator. The amplified output of the sonobuoy was observed on an oscilloscope. Input attenuator settings were determined that corresponded to various degrees of limiting evidenced in the appearance of the output signal. Sonobuoy outputs for the various input attenuation settings were analyzed using the method described in Part C of Section V. In order that the noise introduced to the sonobuoy have the same spectrum as that recorded in the ocean a means of compensating for the frequency response of the sonobuoy audio amplifier/signal line combination was required. This was accomplished by means of a General Radio Type 1925 multifilter which permitted individual setting of attenuators associated with a bank of 1/3 octave filters. Initially the plan was to introduce the signal to the sonobuoy hydrophone using the USNRL G-19 Calibrator described in Appendix A. However the introduction of a sinusoidal signal first at the hydrophone through the calibrator and then

at the input of the audio amplifier showed that the onset of limiting occurred with the same output voltage level in both cases. This test was repeated with the same results using several frequencies representing the range of interest in the analysis. From this it was concluded that limiting occurred in the audio amplifier and not in the preamplifier. Accordingly it was decided to introduce the signal at the input of the audio amplifier. In the case of each sonobuoy tested, the input signal to the multifilter was the signal recorded at sea from that sonobuoy's hydrophone. The equipment arrangement for the experiment is shown in Fig. G-1.

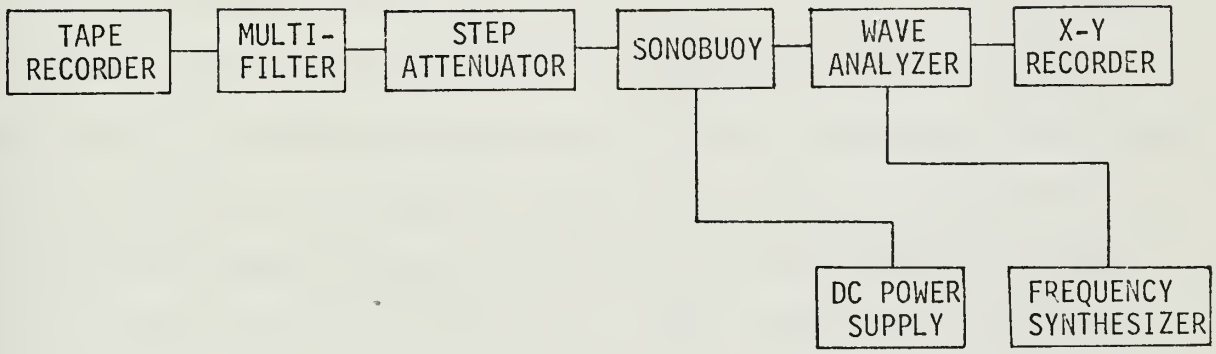

Fig. G-1
BLOCK DIAGRAM FOR LIMITING EXPERIMENT

The short hover in Experiment 11 was selected for providing the input to the sonobuoys for the experiment. For each sonobuoy, a plot of helicopter signal was made for each of four frequencies at each of four attenuator settings. The four frequencies were 150, 300, 500 and 700 Hz. The attenuator settings varied from sonobuoy to sonobuoy and corresponded to

the following qualitative descriptions of limiting extent:

Attenuator Setting	Limiting Description
#1	onset of limiting
#2	slight limiting
#3	bad limiting
#4	solid limiting

Using the known gain of the sonobuoy (loaded with the wave analyzer) for each frequency and the sensitivity of its hydrophone, output voltage level for each frequency for attenuation corresponding to the onset of limiting was converted to equivalent SPL (dB re 1 μbar) at the hydrophone. Also computed was the increase in VL for attenuation settings #2, #3, and #4 over VL at attenuation settings #1 for each frequency. The increase in VL was observed to be frequency independent. The compilation in Fig. G-2 shows the average increase in VL, $\Delta VL_{avg.}$, for attenuation settings #2, #3, and #4 over VL at attenuator #1. Also, attenuator settings #2, #3, and #4 relative to attenuator setting #1 are shown. From the relative attenuator settings and $\Delta VL_{avg.}$, a limiting correction was obtained. SPL (dB re 1 μbar), relative to an arbitrary level in dB, and corresponding to onset of limiting, is shown. The absolute SPL's corresponding to onset of limiting are on file with Dr. H. Medwin, Physics Department, Naval Postgraduate School.

The limiting corrections compiled in Fig. G-2 were plotted against $\Delta VL_{avg.}$ for each sonobuoy. These plots are shown in Fig. G-3. By comparing the experimental SPL's with those shown in Fig. G-2 for the onset of limiting and entering the plots in Fig. G-3 with the differences obtained, correction factors for each sonobuoy were obtained.

Sonobuoy Nr.	Relative Attenuator Setting (dB)	$\Delta VL_{avg.}$ (dB)	Limiting Correction (dB)	Freq. (Hz)	Onset of Limiting Rel. SPL (dB re 1 μbar)
14	0	0	0	150	25.4
	-3	1.9	1.1	300	26.2
	-6	4.4	1.6	500	24.9
	-9	6.9	2.1	700	19.0
16	0	0	0	150	24.2
	-3	1.9	1.1	300	25.9
	-6	3.7	2.3	500	21.5
	-9	6.1	2.9	700	15.8
7	0	0	0	150	25.7
	-3	2.3	0.7	300	26.5
	-6	3.8	2.2	500	21.2
	-9	5.6	3.4	700	17.1

Fig. G-2
COMPILATION OF LIMITING EXPERIMENT RESULTS

Correction factors obtained for each sonobuoy were:

Sonobuoy #14 (surface microphone): 1.5 dB

Sonobuoy #16 (20 ft. hydrophone): 2.8 dB

Sonobuoy # 7 (40 ft. hydrophone): 2.8 dB

There was no measurable difference between the correction factor for 300 foot altitude and that for 600 feet. These corrections were applied in obtaining the relative spectra shown in Appendix F.

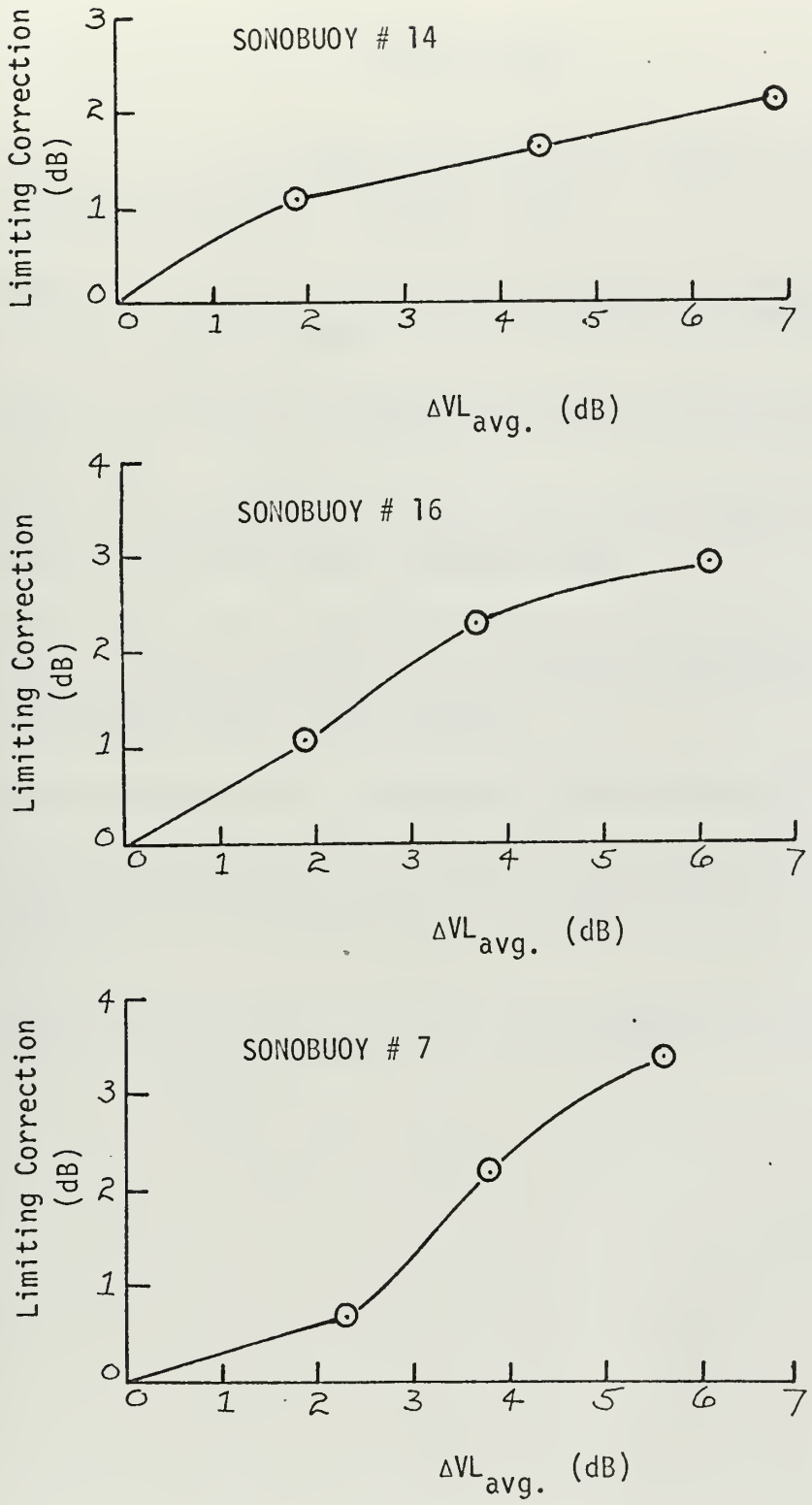

Fig. G-3
CURVES FOR LIMITING CORRECTION FACTOR

BIBLIOGRAPHY

1. Hagy, J. D., Jr., Transmission of Sound Through a Randomly Rough Interface, Electrical Engineer's Thesis, Naval Postgraduate School, Monterey, California, September 1970.

2. Medwin, H., "Specular Scatter of Underwater Sound From a Wind Driven Surface," Journal of the Acoustical Society of America, v. 41, p. 1485-1495, June 1967.

3. NAVAIR 16-30SSQ57-1, Handbook Operating Instructions Sonobuoy AN/SSQ-57, 1 November 1967.

4. Wenz, G. M., "Acoustic Ambient Noise in the Ocean: Spectra and Sources," Journal of the Acoustical Society of America, v. 34, Number 12, p. 1936-1956, December 1962.

5. Pennsylvania State University Institute for Science & Engineering Report Serial NOw65-0123-d-19, Underwater Sound Signatures of Flight Vehicles (U) A Literature Survey, by W. L. Baker and J. A. Macaluso, 15 October, 1967. (CONFIDENTIAL)

6. General Radio Company, Handbook of Noise Measurement, 6th ed., 1967.

7. Naval Postgraduate School Report Serial NPS-58DW9071A, Digital Analysis of Turbulence Data on the IBM 360/67 at the Naval Postgraduate School, by J. R. Wilson, N. E. J. Boston, and W. W. Denner, July, 1969.

8. Beckmann, P. and Spizzichino, A., The Scattering of Electromagnetic Waves from Rough Surfaces, Macmillan, 1963.

INITIAL DISTRIBUTION LIST

		No. Copies
1.	Defense Documentation Center Cameron Station Alexandria, Virginia 22314	2
2.	Library, Code 0212 Naval Postgraduate School Monterey, California 93940	2
3.	Professor Herman Medwin Code 61Md Department of Physics Naval Postgraduate School Monterey, California 93940	10
4.	Manager, ASW Systems Project Office Navy Department Washington, D. C. 20360 (Attn: Director of Aircraft Systems Group, Code ASW21)	2
5.	Commander, Naval Ordnance Systems Command Department of the Navy Washington, D. C. 20360	1
6.	Dr. John C. Johnson, Director Ordnance Research Laboratory Pennsylvania State University Box 30, State College, Pennsylvania 16801	1
7.	Mr. J. A. Macaluso Ordnance Research Laboratory Pennsylvania State University Box 30, State College, Pennsylvania 16801	1
8.	Dr. Fred Spiess, Director Marine Physical Laboratory Scripps Institution of Oceanography University of California San Diego, California 92152	1
9.	Lt. James D. Hagy FAIRKEF U. S. Naval Station, Keflavik FPO, New York 09571	1
10.	Lcdr. Raymond A. Helbig Naval Inshore Operations Training Center Mare Island, Vallejo, California 94592	1

11. Mr. William Smith 1
Department of Physics
Naval Postgraduate School
Monterey, California 93940

Security Classification

DOCUMENT CONTROL DATA - R & D

(Security classification of title, body of abstract and indexing annotation must be entered when the overall report is classified)

1 ORIGINATING ACTIVITY (Corporate author)

Naval Postgraduate School
Monterey, California 93940

2a. REPORT SECURITY CLASSIFICATION

Unclassified

2b. GROUP

3 REPORT TITLE

The Effects of Ocean Surface Roughness on the Transmission of Sound from an Airborne Source

4. DESCRIPTIVE NOTES (Type of report and inclusive dates)

Master's Thesis; December 1970

5. AUTHOR(S) (First name, middle initial, last name)

Raymond Allan Helbig

6. REPORT DATE	7a. TOTAL NO. OF PAGES	7b. NO. OF REFS
December 1970	120	8

8a. CONTRACT OR GRANT NO.	9a. ORIGINATOR'S REPORT NUMBER(S)
b. PROJECT NO.	
c.	9b. OTHER REPORT NO(S) (Any other numbers that may be assigned this report)
d.	

10 DISTRIBUTION STATEMENT

This document has been approved for public release and sale; its distribution is unlimited.

11. SUPPLEMENTARY NOTES	12. SPONSORING MILITARY ACTIVITY
	Naval Postgraduate School Monterey, California 93940

13. ABSTRACT

Using the research platform "FLIP", experiments were conducted to determine the effect of measured ocean surface roughness on transmission of sound from an airborne source into the sea. Signal noise both at the air-water interface and at points in the underwater sound field were recorded using modified AN/SSQ-57 sonobuoys. Ocean wave spectra and rms wave height, σ, were determined from simultaneous recordings of ocean surface wave height variations. The results of analog data analysis compared well with theory developed by Hagy and Medwin: for $R < 1$, perpendicular incidence transmission loss increased approximately as $10 \log_{10} e^{R}$ where $R = k_2^2 \sigma^2 (c_2/c_1 \cos \theta_1 - \cos \theta_2)^2$ (Subscript 2 refers to propagation constant, speed, and angle of transmission in water; subscript 1 in air). For $1 < R < 4$ the transmission loss decreased with increasing roughness, presumably due to off-axis incoherent contributions.

DD FORM 1 NOV 65 1473 (PAGE 1)

S/N 0101-807-6811

Security Classification

A-31408

14 KEY WORDS	LINK A		LINK B		LINK C	
	ROLE	WT	ROLE	WT	ROLE	WT
Sound transmission						
Ocean surface roughness						
Air-sea interface						
Underwater sound						
Helicopter sound field						
Transmission loss						

DD FORM 1 NOV 65 1473 (BACK)

S/N 0101-807-6821